Validation of PLAXIS Embedded Piles

For Lateral Loading

Master of Science Thesis

T.P.T. Dao

April 2011

Delft University of Technology

Faculty of Civil Engineering and Geosciences

Section of Geo-Engineering

Plaxis bv

Research Department

Validation of PLAXIS Embedded Piles

For Lateral Loading

T.P.T. Dao

Student no. 4040546

Delft University of Technology

Faculty of Civil Engineering and Geosciences

Section of Geo-Engineering

Plaxis bv

Research Department

Graduation Committee:

Prof. Ir. A.F. van Tol	TU Delft (section Geo-Engineering) & Deltares
Dr. Ir. R.B.J. Brinkgreve	TU Delft (section Geo-Engineering) & Plaxis bv
Dr. Ir. K.J. Bakker	TU Delft (section Hydraulic Engineering)
Ir. F.A.J.M. Mathijssen	TU Delft (section Geo-Engineering) & Hydronamic bv
Ing. H.J. Everts	TU Delft (section Geo-Engineering) & ABT

PREFACE

This thesis is the final part of the study program to obtain the degree Master of Science at Delft University of Technology. The research described in this thesis has been executed in collaboration between the Research Department of Plaxis bv and the Geo-Engineering Department of the university.

Although this thesis is in principal an individual project, I would not have been able to complete this thesis without the "external" support of a number of people whom I like to thank here.

First of all, I am profoundly indebted to Dr. Ir. Ronald Brinkgreve who provided sincere guidance, advice, criticism and encouragement in every stage of my research process. In addition to his dedicated supervision, his critical reading and suggestions helped me to improve the coherence between contributing parts of the report as well as the quality of the report.

I would like to express my grateful gratitude and sincere thanks to Prof. Ir. A.F. van Tol, Dr. Ir. K.J. Bakker, Ing. H.J. Everts and Ir. F.A.J.M Mathijssen, who have invested a lot of time for valuable comments and simulating discussions. I really enjoyed their friendly supervision.

I would like to thank Plaxis bv for offering me the opportunity to join in professional and pleasant working environment. A word of special thanks goes to Dr. Ir. Paul Bonnier and to all colleagues at Plaxis bv for their warm and continuous help.

My two-year study was financially supported by Can Tho 150 Project under Vietnamese government fund. This support is gratefully acknowledged.

Last but not least, I wish to thank my parents for their support and advice throughout the many years of study I enjoyed.

Delft, 21 April 2011
T.P.T. Dao

SUMMARY

In recent years, the embedded pile model has been successfully implemented in PLAXIS 3D. The embedded pile consists of beam elements connecting to the surrounding soil by means of special interfaces (skin interface and foot interface). Although the embedded pile doesn't take into account volume, a particular *elastic region* around the pile whose dimension is equivalent to the pile diameter is assumed in which plastic behavior is neglected. This makes the embedded pile almost behave like the volume pile. Therefore, it may be said that the embedded pile model is considered as a 'simplified' model of the volume pile.

Although the embedded pile is a relatively new feature, it has been validated by comparisons with the volume pile as well as with measurements from real tests. The finding shows that the embedded pile is not only in good agreement with the volume pile, but also able to resemble the real pile behavior. However these validations are only considered in terms of axial loading (compression loading and tension loading). Therefore it's questionable whether the embedded pile also shows a good performance in the situation of being subjected to lateral loading. In order to answer this question, this thesis is aimed to give a validation of the embedded pile for lateral loading caused by external forces as well as soil movements in embankment applications. This validation is firstly made in PLAXIS imaginary models (a 'simplified' model as considered in Chapter 3 and 'advanced' models as considered in Chapter 4) and then in a PLAXIS model of a real case study as considered in Chapter 5.

- The 'simplified' model simulates a 'short' embedded pile which is moved laterally into soils. Some aspects are required: investigation of the surrounding soil and the pile-soil interaction as well as comparison with the volume pile. The evaluation of *an imaginary elastic region* around the embedded pile is firstly considered. It will be shown that the soil is fully elastic inside this region as expected. Besides the pile-soil contact at the back of the *shaft surface of the elastic region* is restored. This is because the function of '*tension cut-off*' is deselected that enables the soil to sustain tensile stresses. In addition to the soil inside the elastic region, the soil outside is also evaluated. The finding is that the stress-strain distributions around the elastic region in the embedded pile model comply with the trend as generally observed in practical application. A comparison with the volume pile in the same test geometries is made in order to take the condition of the pile-soil interaction in which the embedded pile model gives a good prediction into account. Besides a discussion of the embedded pile model in a realistic application is also given to see how good the embedded model is in modeling the laterally loaded pile.

- In the 'advanced' models, the laterally loaded embedded pile is considered with both causes of external forces and soil movements in embankment applications. For external forces, the evaluation of the mesh dependence is required. It will be shown that the finer mesh results in

more displacements and bending moments in the pile. Besides, the evaluation of the *strength reduction factor R_{inter}* of the interface assigned around the volume pile is made in order to find the best approximation between the two PLAXIS pile models. For the cause of soil movements in embankment applications, the embedded pile is considered in an extension of the imaginary example of the construction of an embankment on soft soils by Brinkgreve (2007). The main point is to investigate the increase of bending moments in the pile and pile deformations due to lateral soil displacements. Even with the same profile of soil displacement distribution, the embedded pile is also influenced by pile properties (pile length, pile diameter). Besides, again a comparison with the volume pile is made to evaluate how good the embedded pile is able to resemble the volume pile in the situation of undergoing lateral soil movements in the same test conditions. It will be shown that the small difference of pile displacements and bending moments between the two pile models may be caused from the small difference in the generated meshes.

- In a PLAXIS model of a real case study, only cause of soil movements induced by the construction of an embankment on soft soil is considered. The influence of the fixity of the pile head connection on the distributions of bending moments in the pile is evaluated. Then the best model of this connection, in which the embedded pile gives distributions of bending moments along the pile comparable to the real pile, will be shown. A comparison between PLAXIS predictions and measurements is made by an investigation of bending moments at the end of each consolidation phase. This is aimed to evaluate the capability of the embedded pile in modelling the real pile undergoing lateral soil movements. Furthermore, in order to see whether the embedded pile is able to resemble the volume pile behavior, a comparison between the two pile models in the same test conditions is made. Note that the validation of the embedded pile is made based on the assumption that the clay layer is modelled with the SSC model. Therefore the evaluation of the SSC model is also required. The evaluation is made by comparing with measured data in terms of soil displacements at the end of each consolidation phase. It will be shown that although there is a deviation from measurements, the SSC model is able to resemble the real soil behavior. The SSC model is applied with a very low *modified creep index μ^**, it seems to yield very little in the short term. Therefore in order to consider the influence of creep in the longer term, a comparison with SS model is also discussed. The finding shows that there is no difference between the SS model and the SSC model during loading and consolidation phases, only a small difference during creep phases (due to a very low modified creep index μ^*).

From the research, the limitations and the possibilities of the laterally loaded embedded pile are clearly observed. Recommendation for further research in which the embedded pile model is improved in the situation of being subjected to lateral loading will be given.

TABLE OF CONTENTS

CHAPTER 1   INTRODUCTION

1.1   General introduction

Foundation piles are primarily meant to sustain vertical forces. However piles are also assigned to sustain lateral soil movements, for instance piles supporting bridge abutments adjacent to embankments and existing pile foundations close to deep excavations. In this type of working condition, the lateral soil movements actually lead to increase displacements and bending moments in piles which may result in failure of the structures. The following part shows some typical examples of piles undergoing lateral soil movements.

Piles undergoing soil movements induced by excavations and adjacent pile driving

Finno et al. (1991) reported a case of a 17.7 m excavation which was made through granular soils within the frame-work supported by groups of piles. The excavation was temporarily supported by a tie-back sheet pile wall. However, by the time the sheet pile wall was pulled out, the main column pile heads moved 6.4 cm towards the excavation.

A case of driving of adjacent piles giving effects on the existing piles was discussed by De Beer (1977). He represented that the bending moments of the existing piles were increased approximately 40kN.m.

Hagerty and Peck (1971) reported another case of significant pile head displacements caused by driving of adjacent piles. Some piles were already installed behind the bulkhead, afterwards other piles nearest to the bulkhead were driven first and subsequent driving was successively further from the bulkhead. An investigation was made to consider that the heads of the existing piles nearest to the bulkhead displaced laterally by approximately 58 cm.

Piles undergoing soil movements induced by embankments

Schmidt (1977) reported two cases of bored piles supporting bridge abutments. As a result of strong forces, the piles were displaced significantly from the adjacent embankments and failed.

Another case of pier piles adjacent to an embankment was presented by Hull and McDonald (1992). They concluded that the piles with free pile-heads were damaged due to unacceptable deflections.

Piles for slope stabilization

There are many examples of piles used to stabilize slopes. Fukuoka (1977) reported a case in which steel H-piles were used to support an unstable slope in Ushinotani. He showed that the piles failed due to the strong forces of the slopes. Another case of pile damage due to strong slope forces was also presented by Kalteziotis (1993). Furthermore, a report by Bea (1971) described a seafloor slide initiated a pile-supported platform to move some meters downward and the pile foundation was severely damaged. Similar cases were also reported by Sterling and Strohbeck (1973).

1.2 Problem definition

As previously mentioned, piles undergoing lateral soil movements have been identified by different causes. However, in this thesis only the cause of the embankment construction on soft soils is considered. Although the situations have been studied by different researchers, there is no clear guideline about which method may reflect the real behavior of the piles in the best way.

The main purpose of this thesis is to validate the PLAXIS embedded piles undergoing lateral soil movements induced by the adjacent construction of an embankment on soft soils by means of PLAXIS 3D. Within this research, the lateral pile displacements and the bending moments in the piles are investigated. It should be noted that the validations of the PLAXIS embedded piles will be made by comparisons with the PLAXIS volume piles as well as with measured data from real tests. Besides, this thesis also takes into account an evaluation of the Soft Soil Creep (SSC) which is applied for the soft soil in embankment applications.
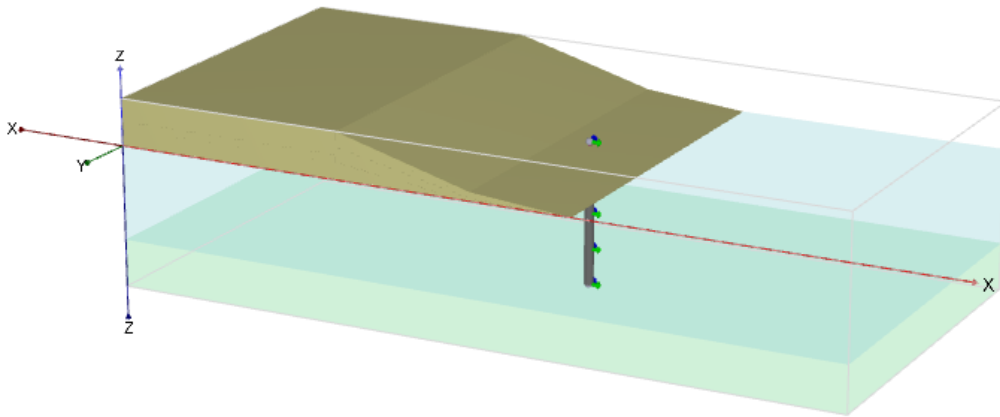
Figure 1.1 Imaginary example of the pile undergoing lateral soil movements
induced by an embankment in PLAXIS 3D

1.3 Limitations

The limitations of the embedded pile in the situation of undergoing lateral loads are considered as below:

- The first limitation regards the model geometry. It should be taken into account that the embedded pile is considered as a line element. Therefore, when either *a line load or a line prescribed displacement* is applied along the pile, the mesh generation cannot be finished with "overlapped" lines. In short, it's impossible to move the embedded pile laterally by applying another line element along the pile.

- The second limitation regards the pile-soil interaction model. By PLAXIS setting, a "slide" is used to model a relative pile-soil displacement in axial direction. However in horizontal directions, the "slide" is not considered. In the other words, the embedded pile doesn't take into account the pile-soil friction in the situation of being loaded laterally. (More details are elaborated in *part 2.3.1.3*).

1.4 Objectives

The objectives of this research include the following aspects:

- The main objective is validating the PLAXIS embedded piles undergoing lateral soil movements induced by the construction of an embankment on soft soils. The validation is made by comparisons with measurements from real tests as well as with the PLAXIS volume piles. In addition, an evaluation on how good the embedded pile is able to resemble the real pile behavior is discussed.

- The secondary objective is evaluating the SSC model which is applied for the soft soil in embankment applications by comparisons of soil displacements with the measured data. Besides, the influence of creep in the long term is also discussed.

1.5 Layout of report

Within the content of the research, the report is structured in the following main parts:

- Chapter 1 briefly describes the existing situations of laterally loaded piles, defines the present research, remarks the limitations of the PLAXIS embedded pile, determines the objectives of the research, and draws the outlines.

- Chapter 2 reviews the literature relating to the main research. This is aimed to provide the basic knowledge, which is required for the analysis of the research as well as for the interpretation of the results. With this purpose, three main points are described as follows:

    + The first one summarizes different research methods on situations of the piles loaded laterally by soil movements in order to provide an overview of the laterally loaded pile behavior. In addition, by these previous methods the helpful information will be selected to support the analysis of the present research;

    + The second one elaborates the background of the PLAXIS embedded pile to consider its benefits in comparison with the PLAXIS volume pile. It should be taken into account that although the PLAXIS embedded pile is a relatively new feature, it has been validated in the previous research. The validation will be summarized in order to recognize how good the embedded pile is able to resemble the real pile behavior;

    + The third one describes the theory of Soft soil behavior. Within this content, such aspects: the background of stress paths in subsoil under an embankment, the theory of undrained behavior and the theory behind the time-dependent soil model in PLAXIS, will be discussed.

    The chapter is ended with a brief conclusion.

- Chapter 3 simulates a simplified model in which a "short" embedded pile is moved laterally into soils. This chapter is mainly aimed to get insight in the behavior of the laterally loaded embedded pile by investigating the surrounding soil as well as the pile-soil interaction. In addition, the benefits in the embedded pile properties are also evaluated by a comparison with the volume pile in order to consider whether embedded pile is able to resemble the volume pile behavior.

- After the evaluation of the laterally loaded embedded pile in a simplified model, Chapter 4 continues to pay attention to validate the embedded pile in "advanced" models. In this part, the lateral loading is caused by both external forces and soil movements. Different from Chapter 3 which gives the validation of the embedded pile by an investigation of the surrounding soil, this chapter will validate the embedded pile by investigating lateral pile head displacements and bending moments in the pile. With this purpose, the outline of this chapter is drawn in two main parts:

    + The first one focuses on validating the embedded pile undergoing lateral loading caused by external forces. This validation is made by evaluating the influence of mesh dependence on deformations and bending moments in the pile as well as comparing with the volume pile in the same test conditions;

    + The second one validates the laterally loaded embedded pile caused by soil movements induced by the construction of an embankment on soft soil. The validation is made by comparing with the volume pile and evaluating the influence of the embedded pile properties.

    The chapter is closed with a conclusion.

- Chapter 5 is mainly aimed to validate the PLAXIS embedded pile undergoing later soil movements induced by the construction of an embankment on soft soils by comparing with measurements from a centrifuge test as well as comparing with the PLAXIS volume pile. The comparison is made in terms of predictions on bending moments in the pile. In addition, an evaluation of the SSC model applied for the soft soil layer is considered as the secondary purpose of this chapter. The evaluation is made by a comparison of soil displacements between the PLAXIS predictions and the measured data. The chapter is ended with conclusions on how good the PLAXIS embedded pile is able to resemble the real pile behavior and what the limitations of the comparisons are.

- Chapter 6 ends the research by drawing conclusions of main results. Furthermore, recommendations for the improved embedded pile models are considered.

CHAPTER 2   LITERATURE REVIEW

2.1   Introduction

The literature review, which has the function of "a bridge" connecting between the basic knowledge and the main goal of the research, is necessarily required. As already mentioned in the previous chapter, this project mainly concerns the validations of the PLAXIS embedded piles loaded by lateral soil movements induced by an embankment constructed on soft soils. Therefore this chapter is firstly aimed to review previous research on situations of the piles undergoing lateral soil movements in order to get insight the pile behavior as well as to extract the useful information for the analysis of the present research. Besides, the background of the PLAXIS embedded pile is desirably elaborated to consider its benefits of properties in comparison with the PLAXIS volume pile. The elaboration is made by providing the philosophy design of the embedded pile in PLAXIS 3D as well as discussing the previous validations to consider whether the embedded pile enables to resemble the real behavior. Furthermore it should be noted that an evaluation on the SSC model applied for the soft soil layer in embankment applications is considered as the secondary purpose of this thesis. Therefore the theories of Soft soil behavior, which consist of the background of stress paths in the sub-soil under the construction of an embankment, the theory of undrained behavior and the theory behind the time-dependent soil model in PLAXIS, are also discussed. As a result, the outline is divided into the following main parts:

- *Section 2.2* briefly reviews previous research on situations of the piles loaded laterally by soil movements under the construction of an embankment with different methods such as theoretical methods, experimental tests and site-investigation tests.
- *Section 2.3* elaborates the philosophy design of the PLAXIS embedded piles to consider its benefits of properties. In addition, the PLAXIS volume pile which will later be used to validate the PLAXIS embedded pile is described. Moreover, this section also considers the validation of the embedded pile by previous research in order to assess whether the PLAXIS embedded pile is able to resemble the real pile behavior.
- *Section 2.4* studies the theories of Soft soil behavior which consist of the background of stress paths in sub-soil under the construction of embankment, the theory of undrained behavior and the theory behind the time-dependent soil model in PLAXIS.
- *Section 2.5* gives a summary.

2.2   A summary of previous research on situations of the piles loaded by lateral soil movements

This section gives a review of considerably previous research on situations of the piles subjected to lateral soil movements with different methods: theoretical methods, laboratory tests and in situ tests in order to get insights the pile behaviors as well as to extract the useful information taken from these methods for the analysis of the present research. In addition, the overview of soil-displacement

distributions along the piles is summarized that is considered as the starting point for reasonable predictions of pile behavior by the theoretical methods. In brief, the outlines are made as below:

- *Section 2.2.1* introduces typical situations of laterally loaded piles by soil movements.
- *Section 2.2.2* reviews soil displacement distribution along the pile.
- *Section 2.2.3* summarizes the theoretical methods.
- *Section 2.2.4* summarizes the experimental tests.
- *Section 2.2.5* summarizes the in-situ tests.
- *Section 2.2.6* gives a conclusion.

2.2.1   Introduction of situation

Before going to the previous research, a general introduction of the typical situation of a pile undergoing lateral soil movements is shown by Chen (1994) (see Figure 2.1). In this situation, soil mass is divided into an unstable layer and a stable layer. The pile portion in the upper part is subjected to lateral soil movement and is referred as a "passive" portion, whereas the pile portion in the lower part is subjected to lateral loading transmitted from the upper pile portion and is referred as an "active" portion. It can be seen that the soil surrounding the pile at any depth is at equilibrium under the initial stress state before the soil starts moving. When the soil begins displacing, the stress in soil surrounding the pile will change from the initial state to a new equilibrium state.
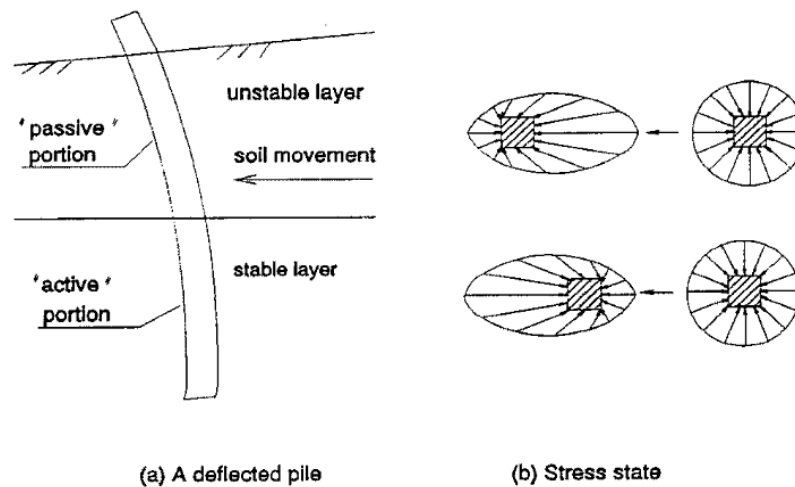
Figure 2.1 Pile loaded by lateral soil movement (Chen 1994)

2.2.2   Soil displacement distribution

Heyman and Boersma (1962) presented lateral soil displacement profiles along the pile caused by an adjacent embankment (Figure 2.2). The embankment was constructed sequentially to create a total height of 5m. The soil displacements were measured at the ends of each step.

De Beer (1972) showed another profile of soil displacements along the pile caused by an embankment. The soil displacements were measured by a flexible plastic pipe which was installed

vertically near the edge of the embankment. The measurement under an embankment load of 18T/m^2 is shown in Figure 2.3. Furthermore, Ingold (1977) described another profile of soil displacements as in Figure 2.4.

From the Figures below, it is worthy to note that the different soil displacement profiles depend much on the distance between the embankment and the pile as well as the stiffness of the soil layers.
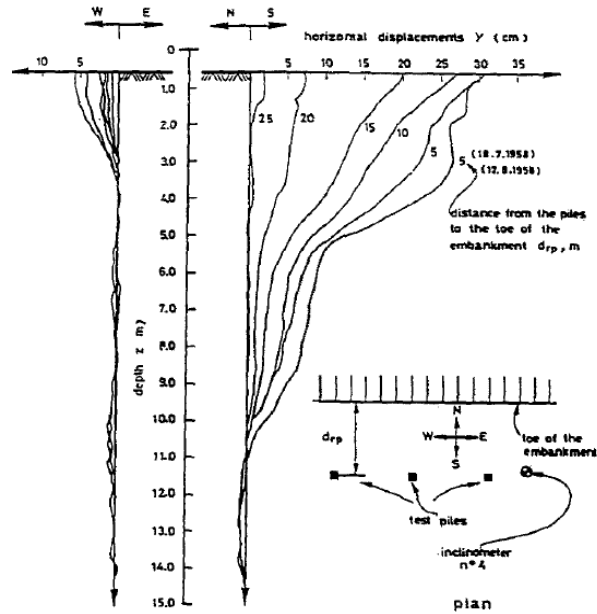
Figure 2.2 Distribution of lateral soil displacement (Heyman and Boersma 1962)
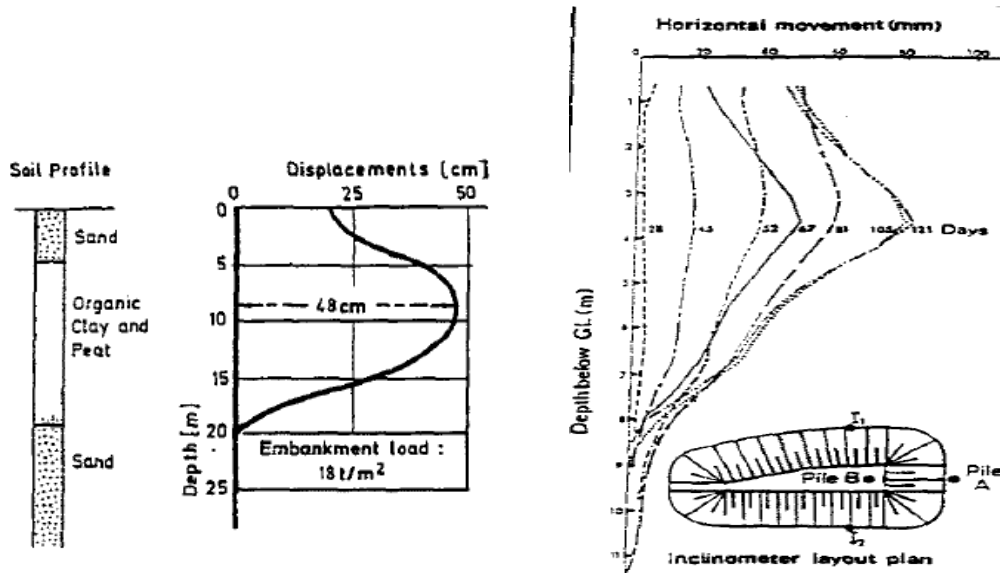
Figure 2.3 Lateral soil displacement profile (De Beer 1972)

Figure 2.4 Lateral soil displacement profile (Ingold 1977)

2.2.3   Theoretical methods

2.2.3.1 Pressure-based methods

De Beer and Wallays (1972) experienced a case of the pile loaded by lateral soil movements caused by an embankment as in Figure 2.5. They proposed a semi-empirical method to calculate the soil pressure acting on the pile. The clear limitation of the method is that it only predicts the maximum value of bending moments and is not allowed to estimate the distribution of bending moments along the pile shaft.

$$p = \frac{\epsilon - \phi/2}{\pi/2 - \phi/2} \gamma H$$
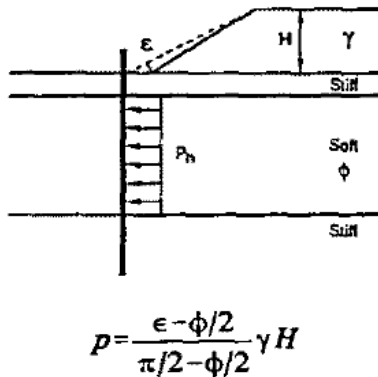
Figure 2.5 Method of De Beer and Wallays (1972)

Thereafter this method was continued to study by giving different assumptions regarding the prediction on distribution of lateral soil pressure along the pile. Tschebotarioff (1973) presented an empirical method which assumed the soil pressure distribution along the pile shaft was of triangular shape (Figure 2.6); the bending moment in the pile was then calculated based on this distribution.
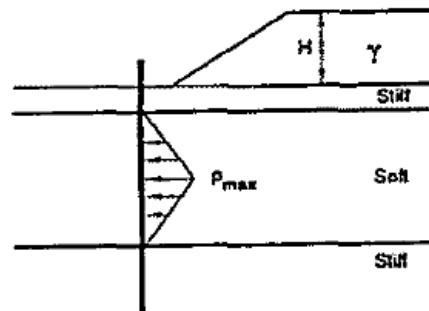
Figure 2.6 Method of Tschebotarioff (1973)

The triangular shape of soil pressure distribution was continued to research by Springman (1989). She used results of a centrifuge model test to propose a relatively simple design method which predicts the distribution of lateral soil pressure along the pile in shape of parabolic curve as in Figure 2.7. The method took the differential pile-soil movement into account and also accommodated for pile group analysis.
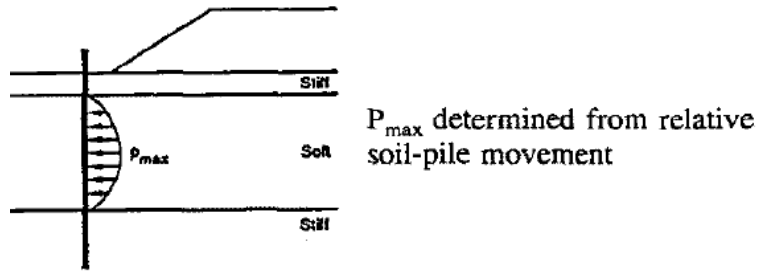
Figure 2.7 Method of Springman (1989)

Ito and Matsui (1975) used plasticity theory to propose a method to predict the soil pressure and bending moment in the pile. The authors noted that this method was only applied as the soil around the pile become plastic. According to Popescu (1991), this method was used in situations of designing the bored piles for slope stabilization in which the piles were treated as lateral loaded piles. Based on the evaluations of results, Popescu concluded that the conditions of the fixity at the pile head had a significant effect on the bending moments in the pile.

In 1990, Gabr and Borden used a force-equilibrium model to derive a theoretical solution for the lateral capacity of rigid piers embedded in non-cohesive soil under a slope. The lateral soil resistance was derived by considering the pier as a translating cylinder moving into the soil.

2.2.3.2 Displacement-based methods

In addition to the pressure-based methods, the displacement-based methods were also studied by considerable research. However, this part is not aimed to mention all aspects of the methods, only several main points made by Poulos (1973), Hull et al. (1991) and Byrne et al. (1984) are summarized:

Poulos (1973) mentioned a boundary element method to analyze a single pile subjected to lateral soil movements. The soil was assumed to be elastic; the parameters of Young's modulus and yield pressure were allowed to vary with depth. The method required an input of the magnitude of the free-field soil movement at each depth and the ultimate soil pressure acting on the pile in order to predict the behavior of the pile. Based on comparisons between the method predictions and the measured data, the author concluded that it was in quite agreement with the measurements. The method gives the interpretation for the continuous nature of soil, but a good prediction depends on the accurate magnitude of soil movement and ultimate soil pressure. This method is used for analyzing the single pile as well as the pile group.

Later, the method of Poulos was modified by Hull et al. (1991). He raised different failure modes which were identified for the pile-soil interaction when the pile was subjected to lateral soil movements. The modified method was considered to be good in practical applications. However this method still depends on an accurate input of both of the magnitude of soil movement and ultimate soil pressure.

Another method for estimating the behavior of the piles loaded by soil movements was proposed by Byrne et al. (1984). The method assumed that the soil was replaced by a system of non-linear springs. The method gives the predictions on the bending moments, shear forces and deformations of the piles based on the implementation of the iterative procedure to solve the differential equations,

2.2.4   Experimental tests

In addition to theoretical methods, the situation of the pile subjected to lateral soil displacements has been investigated with laboratory tests by different researchers. It should be noted that this thesis concentrates on validating the PLAXIS embedded piles by comparing with measurements from laboratory tests described in Chapter 5, thus the results of these previous tests become very helpful for the analysis of the present research.

A laboratory test of laterally loaded pile regarding the evaluation of the influence of pile stiffness was carried out by Fukuoka (1977). The model pile was installed in an iron box filled with soils. The pile was instrumented with strain gauges along the pile shaft to measure the deformations. The uniform distribution of soil movements was incrementally applied to the pile. The pile model is varied with different materials (steel pile, wooden pile) to investigate the influence of pile stiffness on its deformations. As a result of test, it could be concluded that the deformed shape of the pile depends much on the flexural rigidity of the pile.

Furthermore, variations of pile diameters were carried out by Matsui (1982) to investigate their influences. He conducted a series of experimental tests on the model piles loaded laterally by soil movements to predict lateral pressures acting on the piles. The model piles were inserted through clay layer and sand layer filled inside a steel box. The soils were moved towards the piles by the loading plates. Loads on the piles were recorded using the load cells. It was found that the increases of pile diameters result in increasing pressure acting on the piles.

Stewart (1992) utilized a geotechnical centrifuge to carry out a series of model tests on the pile adjacent to the construction of an embankment. The tests were conducted on both single piles and pile groups. The model piles were plane-strain gauged so that the bending moments induced in piles could be measured. The piles were installed through a soft clay layer and a dense sand layer. The construction of an embankment was carried out sequentially and the bending moments in the piles were measured at each stage of embankment construction. From the results, it could be considered that the maximum bending moments are found at the pile heads and the interface between the soft layer and the stiff layer. In comparison with the results from the field test, this method was generally in good agreement. The centrifuge tests give insight in the pile behavior and the results are considered to be of significant practical values.

2.2.5   In-situ tests

The in-site tests on the piles loaded laterally by soil movements have been considered as the best practical methods which reflect the real pile behaviors. Many instrumented field tests have been

reported by different researchers, for example, Heyman & Boersma (1962), Heyman (1965), Leussink & Wenz (1969), Nicu (1971). Most of them involved the piles supporting the bridge abutments where lateral soil movements were caused by the construction of embankment, while the others involved the piles for slope stabilization and the piles for retaining structures. However in term of this part, only two reports made by Esu & D'Elia (1974) and Ingold (1977) are mentioned in order to gain the overview of the pile behaviors.

Esu and D'Elia (1974) described a field test relating to a landslide. A reinforced concrete pile with dimensions of 30m in length and 0.79m in diameter was instrumented with pressure cells along the pile shaft and an inclinometer inside. It could be seen from the measurements that, the pile head deformed significantly and the pressures acting on the pile gradually increased.

Ingold (1977) presented a field test where the steel pile was installed approximately four months after the construction of embankment. The pile was located at the embankment toe and inserted through the soft clay layer & the stiff sand layer. The bending moments and the pile deflections were recorded by vibrating-wire strain-gauges and inclinometer respectively. In short, the measurements showed that the maximum bending moments acting on the pile could be generally found at the pile top, the middle of the soft layer and the interface between two different layers

2.2.6 Conclusion

The part gave an overview of the behavior of piles undergoing lateral soil movements by theoretical methods as well as measurements from laboratory tests and field tests. Some conclusions were drawn:

- In terms of theoretical methods, the pressure-based methods have the limitation of applicability because they only respond for some specific cases, and depend much more on the assumption of the distribution of soil pressures along the pile. Besides, the displacement-based methods can be used for any types of problem. However, the clear limitation of these theoretical methods is that the proper predictions compulsorily required the exact assumptions and inputs which are often uncertain.
- In terms of laboratory tests and in-situ tests, the real behavior of the piles could be obtained based on the measured data. However, there is no general guideline for practical uses because the piles behave differently from case to case.

2.3 Background of embedded pile and volume pile in PLAXIS 3D

The purpose of this part is to describe the background of the PLAXIS embedded pile in order to consider its benefits of properties (see *section 2.3.1*). Furthermore, the previous research on validation of the embedded piles by comparing with measurements will be discussed in *section 2.3.2*. In addition, the background of PLAXIS volume pile (*section 2.3.3*) is also necessarily shown because it will later be used to validate the embedded pile.

2.3.1   PLAXIS embedded pile

2.3.1.1 Philosophy design of PLAXIS embedded pile

The PLAXIS embedded pile is considered as a beam which can cross the soil volume elements at any arbitrary location and with any arbitrary orientation (Figure 2.8a). The pile is connected to the surrounding soils by means of special interfaces which are skin interfaces and foot interfaces. Although volume is not considered according to the philosophy design of the embedded pile, a particular elastic volume around the pile (*elastic zone*) whose dimension is equivalent to the pile diameter is assumed, in which the plastic behavior is neglected (Figure 2.8b). This makes the embedded pile almost behave like a volume pile. However, the installation effects of the pile are not taken into account and pile-soil interaction is modeled at the centre rather than at the circumference. Therefore the embedded pile model may be applied effectively in modeling the piles in which installation process results in low disturbance, such as in case of bored piles and actually not in case of driven piles or soil-displacement piles.
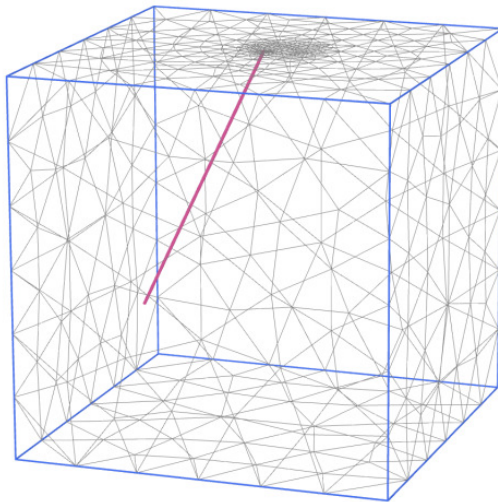
Figure 2.8a Embedded pile   *Figure 2.8b Elastic region*
with arbitrary direction   *around embedded pile*
Figure 2.8 Schematization of single embedded pile (PLAXIS 3D)

In comparison with the volume pile which is created by volume elements, the embedded pile has its benefits. Firstly, when creating the embedded pile no corresponding geometry points are created, thus contrary to the volume pile, the embedded pile doesn't give influence on the mesh as generated from the geometry model. Therefore mesh refinement is lower and time for numerical calculations is reduced. Furthermore because of being considered as a beam structure, the embedded pile can directly give the results of Force in PLAXIS 3D Output which can't be obtained from the volume pile model which is assigned with Soil material. In general, the embedded pile composing of line elements is considered as a simplified model of the volume pile. For more understanding of the PLAXIS embedded pile, the following aspects: *pile-soil interaction*, *influence of coefficient R_{inter}* and *required material parameters*, are discussed:

2.3.1.2 Pile-soil interaction

After the mesh is generated, new nodes on the pile are created. Thus, the special interfaces modelling the pile-soil interaction are made by a connection between the new pile nodes and the existing soil nodes. An elasto-plastic model is used to describe the behavior of the interfaces. The interaction may involve a skin resistance (in unit of force per length) and a tip resistance (in unit of force) whose sum is considered as the bearing capacity of the embedded pile. For both the skin resistance and the tip resistance, a failure criteria is applied to distinguish between the interface elastic behavior and the interface plastic behavior.

The skin resistance of the interface is represented the in constitutive equation

$$t^{skin} = K^{skin}.\Delta u_{rel} \tag{2.1}$$

Where t^{skin} is the force at the integration points; K^{skin} is the material stiffness matrix of the interface; $\Delta u_{rel} = u^p - u^s$ is the relative displacement vector between the soil and the pile. Furthermore, the above equation can be represented in the 3D local coordinate system (n, s, t) as in Eq. (2.2)

$$\begin{bmatrix} t_n \\ t_s \\ t_t \end{bmatrix} = \begin{bmatrix} K_n & 0 & 0 \\ 0 & K_s & 0 \\ 0 & 0 & K_t \end{bmatrix} \begin{bmatrix} u_n^p & - & u_n^s \\ u_s^p & - & u_s^s \\ u_t^p & - & u_t^s \end{bmatrix} \tag{2.2}$$

Where,

t_n	Shear stress in axial direction
t_s and t_t	Normal stress in horizontal directions (remain elastic)
K_n	Elastic shear stiffness
K_s and K_t	Elastic normal stiffness in horizontal directions
u^p	Displacement of the pile
u^s	Displacement of the soil
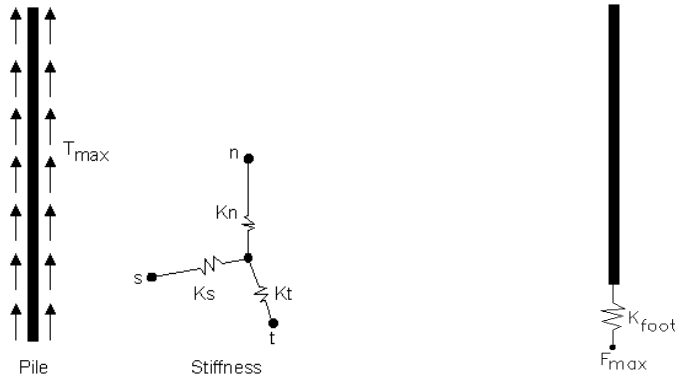
Figure 2.9a Shear resistance T_{max} along the pile   Figure 2.9b Maximum force at the pile tip

Figure 2.9 Shear resistance and tip resistance

Figure 2.9a gives a visualization of constitutive Eq. (2.2). It should be considered that *the skin resistance T_{max}* is defined as the capacity of the interface to sustain the *shear force t_n* along the pile (in axial direction of the pile). For elastic behavior of the shaft, the *shear force t_n* at the particular point has to be smaller than local skin resistance at that point T_{max} $(/t_n/ <T_{max})$. Therefore, the plastic behavior occurs if $|t_n| \geq T_{max}$.

In addition to the skin resistance, the tip resistance is governed by a non-linear spring at the pile tip (Figure 2.9b). The tip resistance presents the capacity against the maximum force acting at the interaction between the pile tip and the soil. It can be formulated in the equation below

$$0 \leq F_{tip} = K_{tip}.(u_{tip}^p - u_{tip}^s) \leq F_{max} \tag{2.3}$$

Where F_{tip} is the force at the pile tip; K_{tip} represents the material stiffness matrix of the spring element at the pile tip; $(u_{tip}^p - u_{tip}^s)$ is the relative displacement vector between the soil and the pile at the foot. It can be seen that the force at the pile tip F_{tip} is zero in case of pulling out (tension behavior). The failure occurs when the force at the pile tip F_{tip} is equal to the maximum resistance at the pile tip in case of compression.

2.3.1.3 The influence of coefficient R_{inter} on the behavior of the pile-soil interaction
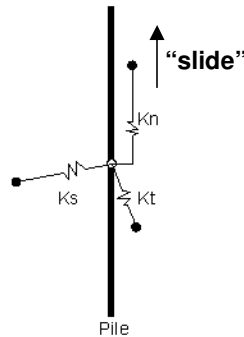
Figure 2.10 Node model for the pile-soil interaction

It should be taken into account that the skin resistance is the shear resistance of the interface in the axial direction of the pile, which is determined based on a "slide" between the pile node and the soil node. In PLAXIS, the skin resistance can be described by means of *linear, multi-linear or layer-dependent* traction models. Within the third option, the skin resistance directly relates to the strength of the surrounding soil by the *interface strength reduction factor R_{inter}*, which is set up in the material data set of the soil. Therefore, it's clearly recognized that R_{inter} can be used to control the "slide" between the pile and the soil in the axial direction of the pile. In the other words, the value of R_{inter} gives an influence on the relative displacement between the pile and the soil when the pile is subjected to the axial loading (in n-direction) (see Figure 2.10).

However this thesis examines the embedded pile which is subjected to lateral loading. Therefore it is questionable whether R_{inter} can be also used to control the pile-soil friction in case of being subjected to lateral loading. The question may be answered based on the node model at the interface (see

Figure 2.10). By PLAXIS setting, the "slide" is used to model the pile-soil interaction in axial direction (n-direction). However in horizontal directions (t-direction & s-direction), the normal stresses totally remain elasticity that result in no relative displacement between the pile and the soil in these directions. Consequently, R_{inter} doesn't give any influence on the displacements in terms of laterally loaded pile.

2.3.1.4 Parameters of the embedded pile

In PLAXIS 3D, the embedded pile is defined in separate material data sets: the parameters for the beam and the parameters for the pile-soil interaction. It should be taken into account that the bearing capacity of a pile is considered to be an input parameter rather than the result of Finite Element calculation. Therefore to make the behavior between the embedded pile and the real pile comparable, the input data should be based on a pile load test.

Because of being considered as a beam, the pile is set up in linear elastic properties of a beam element which is presented in parameters of *the Young modulus E and the unit weight γ* of pile material. Subsequently, geometric properties of the pile are defined in terms of both *predefined shapes* (*Massive circular pile, Massive tube, Massive square pile*) and *real pile diameter* which determines the *elastic zone* around the pile. Alternatively, a "*user defined*" type may be used to define the pile shape by means of *pile's cross section, A and Moments of inertia, I_2, I_3*. On the other hand, the properties of the pile-soil interaction are defined by *skin resistance and base resistance*, which were already elaborated in the previous part. Table 2.1 below shows an example of the required material set of the PLAXIS embedded pile.

Table 2.1 Example of required parameters of the embedded pile

Parameters	Name	Value	Unit
Predefined pile type	Massive circular pile	-	-
Diameter	Diameter	1.5	m
Young's modulus	E'	3.10^7	kN/m^2
Unit weight	γ	6	kN/m^3
Skin resistance	Type	Linear	-
Maximum traction allowed at the pile top	$T_{top,max}$	200	kN/m
Maximum traction allowed at the pile bottom	$T_{bot,max}$	500	kN/m
Base resistance	F_{max}	10000	kN

2.3.2 Validation of the embedded piles by previous research

Although the embedded pile is a relatively new feature in PLAXIS 3D, it has been validated in the previous research to see how good the embedded pile is able to resemble the real pile. Therefore, this part is aimed to summarize the validation of the embedded piles in terms of compression loading, tension loading and lateral loading by comparing with measurements. It should be taken into account

that the validation made by Kelesoglu (2009) on the embedded pile undergoing lateral soil movements induced by the construction of an embankment on soft soils described in the last sub-part is very helpful for the interpretation of the results in case studies later.

2.3.3.1 Validation of the embedded pile in case of being subjected to compression loading

The real case of the Alzey Bridge pile load test (El-Mossallamy et al. 1999) was modelled by means of PLAXIS using the embedded pile. The real test can be summarized as follows. At the construction site, load cells were set up at the pile base to directly measure the base load. In addition, skin friction was obtained by subtracting the base load from the total load. Soil structure is totally described as over-consolidated clay. The model of the pile load test in PLAXIS can be visualized in Figure 2.11.
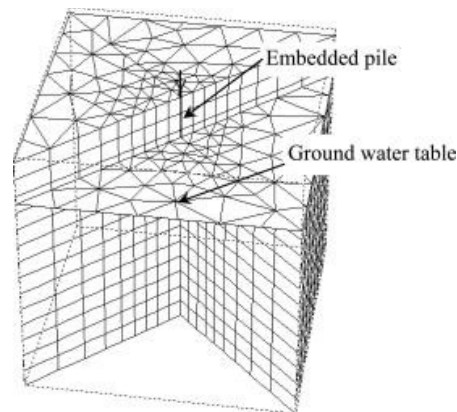
Figure 2.11 Model of Alzey Bridge pile load test in PLAXIS 3D Foundation (Engin et al. 2007)

Figure 2.12 shows the results of a comparison between the measurement and the PLAXIS model. It can be seen that although the embedded pile seems to overestimate the base resistance, it predicts similar results of the pile capacity. Therefore, a conclusion could be made is that the embedded pile is able to resemble the real pile behavior.
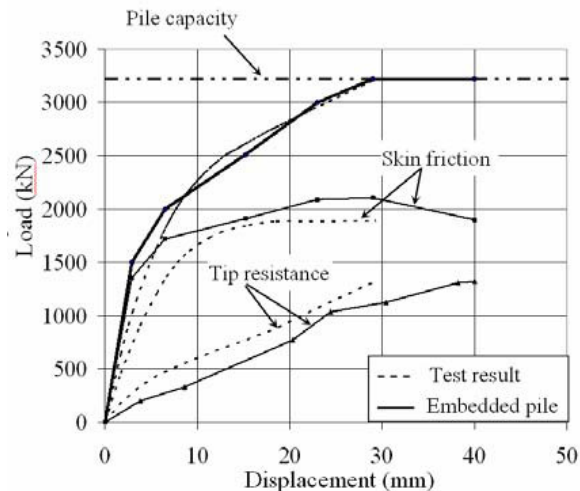
Figure 2.12 Load-displacement behavior (Engin et al. 2007)

Another pile load test carried out in Amsterdam was also modelled by PLAXIS 3D Foundation using the embedded pile. In this case, the validation of the embedded piles was made by comparisons not only with measurements, but also with the volume piles. The geometries of the PLAXIS models are described as in Figure 2.13. The pile is inserted through five different layers. The mesh could be considered to be medium to fine. In addition, it should be noted that in order to make a good comparison between the embedded pile model and the volume pile model, their generated meshes need to be similar.
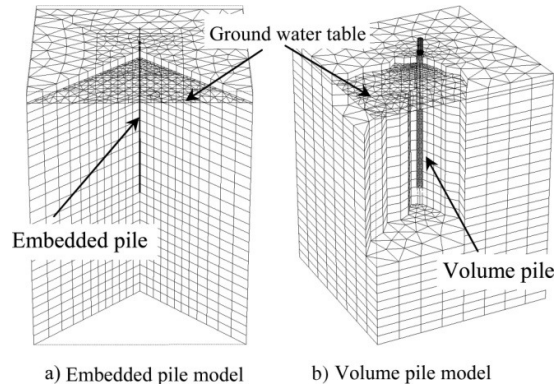
Figure 2.13 Model of Amsterdam pile load test in Plaxis 3D Foundation

Figure 2.15 shows a comparison between the PLAXIS predictions and the measurements. It can be considered that the embedded pile is able to catch the real behavior in terms of investing the load-displacement behavior (Figure 2.14a). Besides, it can be seen that the volume pile gives an overestimation of pile capacity, and behaves stiffer than the embedded pile. However, the result of axial load distribution along the depth (Figure 2.14b) shows that a good agreement of the embedded pile in comparison with the real test pile can be achieved.

a. Load-displacement behavior   b. Distribution of axial load with depth
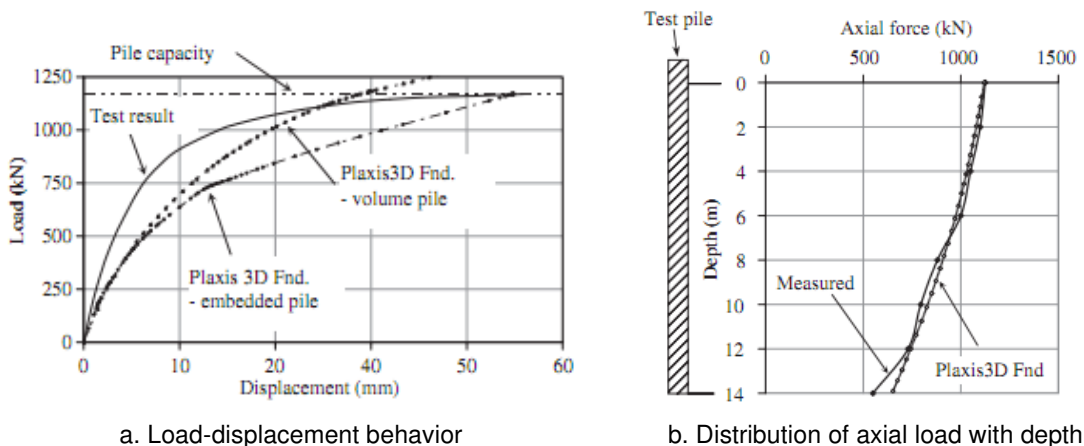
Figure 2.14 Comparison between the embedded pile model and the real test pile

(Engin et al. 2007)

2.3.3.2 Validation of the embedded pile in case of being subjected to tension loading

The real tension tests on the bored piles in cemented desert sands at two sites (South Surra test site and Umr Gudayr test site) were modelled in PLAXIS 3D using the embedded piles (Engin et al. 2007). The details of geometry and soil parameters were given in Ismael et al. (1994). The field tests investigated load transfer of the bored piles which were installed at different sites. Two bored piles were tested in axial tension to failure.

The load-displacement behavior of the PLAXIS embedded piles and the real test piles at South Surra site is shown in Figure 2.15. It can be seen that in both cases of the "short" pile and the "long" pile, the embedded pile is in very good agreement with the real pile behavior.
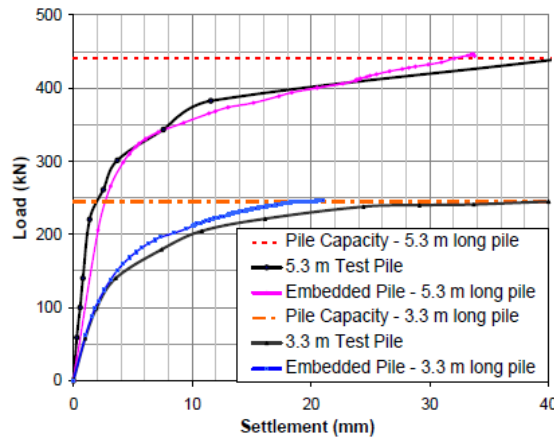
Figure 2.15 Load-displacement behavior in case of the South Surra test site (Engin et al. 2007)

Figure 2.16 represents the comparison between the PLAXIS embedded pile and the Umr Gudayr test pile in terms of load/unload-displacement behavior. It can be seen that in the part of unloading, the embedded pile does not reflect the real behavior because loading is in elastic part in the FE model. However, in general the embedded pile is able to resemble the real behavior.
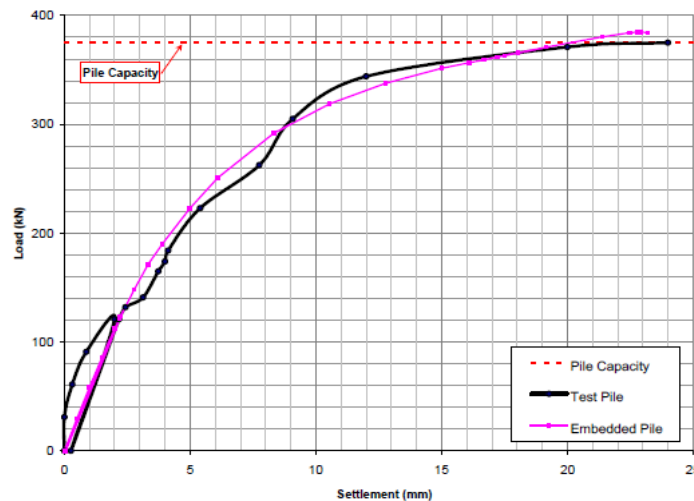
Figure 2.16 Load-displacement behavior in case of the Umr Gudayr test site (Engin et al. 2007)

2.3.3.3 Validation of the embedded pile in case of being subjected to lateral loading caused by soil movements

A case study of the single pile located at the embankment's toe was modeled in PLAXIS 3D Foundation v2.1 by Kelesoglu (2009) in order to validate the embedded pile by comparing with the measured data. The model geometry is shown in Figure 2.17 and Figure 2.18.
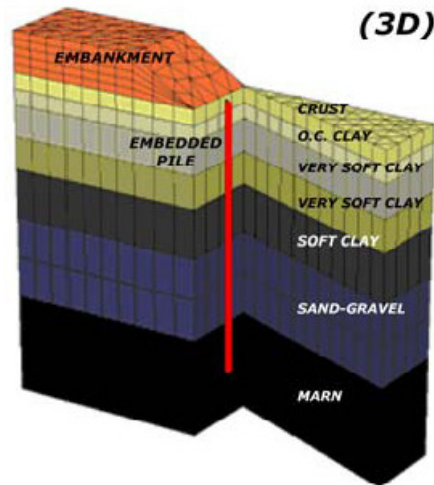
Figure 2.17 Model in PLAXIS 3D Foundation v2.1 *(Kelesoglu 2009)*
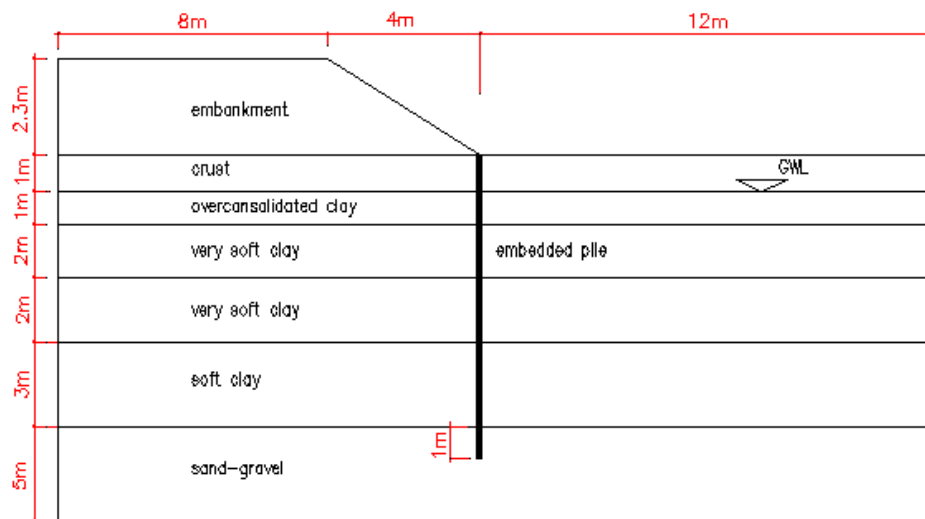
Figure 2.18 Dimensions of the model

In PLAXIS, the pile was modelled using the embedded pile and the soft soil layers of the Cubzac-les-Ponts test site were modelled using the Soft Soil Creep (SSC) model. Creep parameters of these layers were defined with the equation proposed by Mesri and Choi (1985) as $C_\alpha/C_C \cong 0.05$. The stiff layers were modelled with the Hardening Soil (HS) model to consider the soil nonlinearity and hardening. The properties of the stiff soil, the embankment and the pile are summarized in Table 2.2. In addition, the parameters of the soft soil layers are also shown in Table 2.3 that were obtained as a result of an extensive research provided in Magnan et al. (1983) and Wood (1990).

Table 2.2 Parameters of piles and soils (Kelesoglu 2009)

Soil Type	Model	Depth [m]	E_i [MPa]	E_{50} [MPa]	ϕ [°]
Embankment	MC	-2.3–0.0	15.0		30.0
Sand-Gravel	HS	9.0–14.0	50.0	27.5	30.0
Marn	HS	14.0–20.0	100.0	87.5	35.0
Pile Model	**d** [m]	**L** [m]	E_P [GPa]	A_P [m²]	I_P [m⁴]
Beam	1.0	17.0	28.0	0.78	0.049

E_i and E_{50} : initial and half-ultimate stress modulus of the soil,
$E_i = (2.E_{50}) / (2-R_f) \rightarrow R_f=0.90$ (Brinkgreve et al. 2006),
d: pile diameter, L: pile length, E_P: young's mod. of pile,
A_P: cross-sect. area of pile, I_P: moment of inertia of pile sect.

Table 2.3 Material parameters of the soft soil

(Magnan et al. 1983 & Wood 1990)

Material	Depth	ϕ	σ'_{vc}	γ	κ	λ	e_{CS}	M	G	k_X	k_Y
Crust	0.0 – 1.0	32.0	80.0	17.0	0.017	0.12	1.0	1.29	930	4.6×10^{-9}	9.0×10^{-9}
Over cons.cl.	1.0 – 2.0	29.0	68.0	16.0	0.022	0.53	2.6	1.16	1670	1.4×10^{-9}	1.2×10^{-9}
Very soft cl.	2.0 – 4.0	26.0	36.0	14.0	0.085	0.75	3.2	1.03	400	2.6×10^{-9}	7.0×10^{-10}
Very soft cl.	4.0 – 6.0	26.0	42.0	15.0	0.048	0.53	2.25	1.03	670	1.5×10^{-9}	1.0×10^{-9}
Soft cl.	6.0 – 9.0	26.0	58.0	15.2	0.043	0.52	2.3	1.03	1050	1.5×10^{-9}	1.0×10^{-9}

ϕ : friction angle [°], σ'_{vc} : precons. press. [kN/m²], γ : unit weight [kN/m³], κ : swelling index, λ : comp. index, e_{cs} : crit. void ratio, M : slope of the crit. state line, G : shear mod. [kN/m²], k_X, k_Y : coef. of vertical and horizontal perm.[m/s]

The test results are displayed as the graphs of "bending moment-depth" and "lateral pile head displacement-time". Two reference times selected for the investigation are at 15 days and 817 days. Figure 2.19 indicates that the embedded pile predicts larger values of bending moments than the real pile in the early phases and it tends to better approach to the real one towards the later phases. Figure 2.20 shows the comparison between the PLAXIS 3D model and the real test in terms of horizontal displacements at the pile top as a function of time. It can be seen that the good approximation between the embedded pile and the real pile is revealed at the later phases. In general, it can be concluded that the embedded pile shows a good performance in terms of being subjected to lateral soil movements induced by the construction of an embankment on soft soils.

15 days   817 days
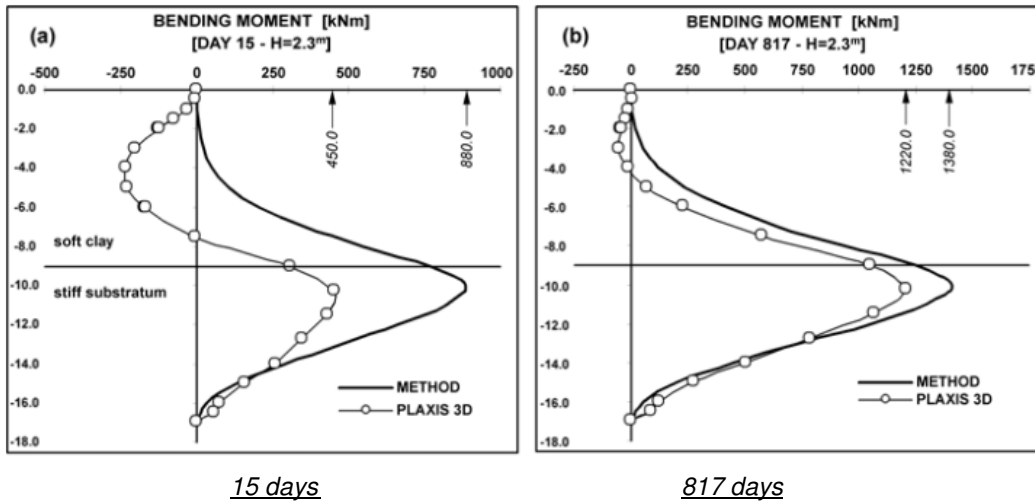
Figure 2.19 Bending moment-depth

(Kelesoglu & Cinicioglu, 2009)
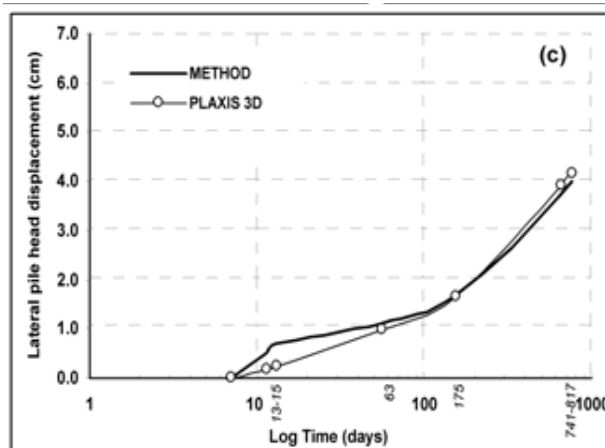
Figure 2.20 Lateral pile head displacement – time

(Kelesoglu & Cinicioglu, 2009)

2.3.2   PLAXIS volume pile

In this research, the PLAXIS volume pile will later be used to validate the PLAXIS embedded pile by comparisons between them. Thus before reaching this purpose, the background of the PLAXIS volume pile needs to be discussed. The volume pile consists of volume elements in which the interaction with surrounding soil is modelled by means of interface elements. In PLAXIS 3D, the volume pile may be created by two options. The first one relates to the use of "*Insert Solid*" function which allows to set up *the shape and the location of volume element* (see Figure 2.21). The second one relates to use the "*command box*" in which the volume pile is defined by the length, the radius and the numbers of segments of the pile shaft.
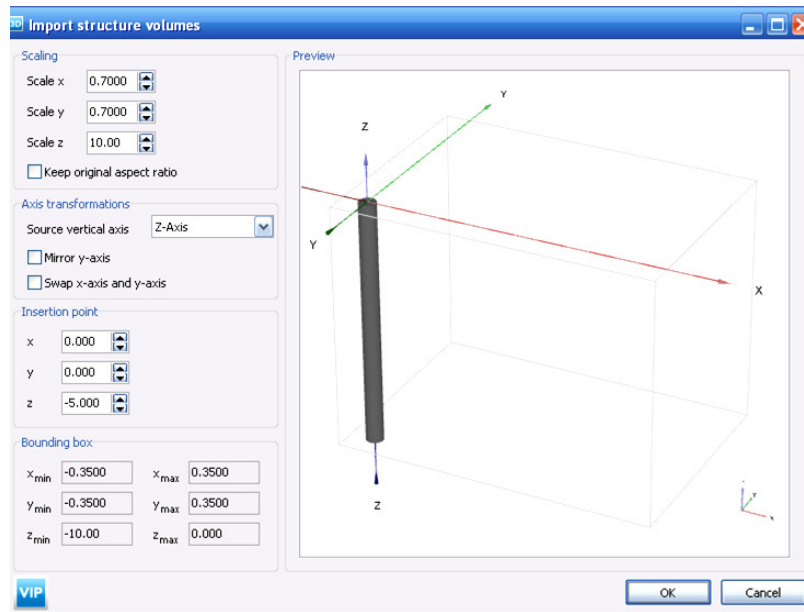
Figure 2.21 Shape and location of volume structure in Plaxis 3D

The properties of the volume pile are assigned with a material data set for soil but with concrete properties. For example, in order to assign the volume pile which has properties of the *unit weight* $\gamma = 25(kN/m^3)$ *and the Young's modulus E=3.10^7(kN/m^2)*, *"soil and interface"* material type and *"linear elastic"* material model are set up. The other material parameters are shown in Table 2.4. Due to being volume element with soil material, the volume pile can't give results of Force like the embedded pile. Therefore in order to investigate the results of Force, a beam element is inserted at the axial axis of the volume pile. This beam is set up with the same properties as the volume pile except for the E modulus which is 10^6 times lower than E modulus of the volume pile material. With the set of material properties, the deformations of the beam will be as similar as that of the volume pile. However, to obtain the actual result of the bending moment in the pile, the bending moment value of the beam in PLAXIS output has to be multiplied by the factor "10^6". The details of the volume pile will be elaborated in *section 4.2.3.1*.

Table 2.4 Material data set of the PLAXIS volume pile

Parameter	Name	Value	Unit
Material model	-	Linear elastic	-
Drainage type	-	Non-porous	-
Unit weight	γ	25	kN/m^3
Young's modulus	E	3.10^7	kN/m^2

2.4 Theory of soft soil behavior

In addition to the basic background of the PLAXIS piles, the basic theories of soft soils as well as knowledge from the former studies on this type of soil are also presented here. In order to make an overview of relevant parts relating to soft soil behavior, it's supposed to imagine a situation as in Figure 2.22.
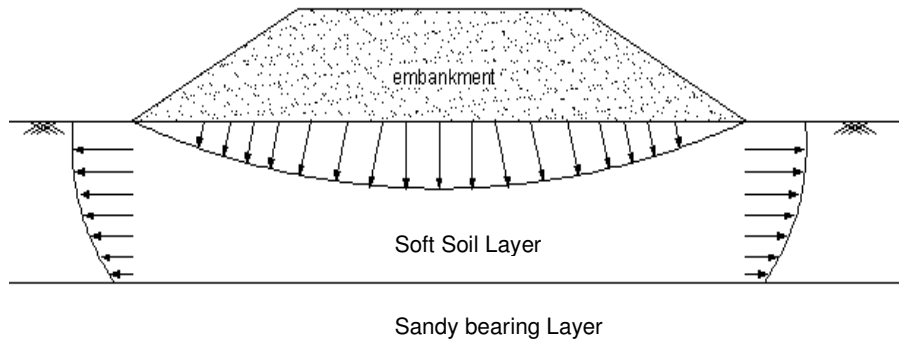
Figure 2.22 Imaginary example of an embankment on soft soil

It can be seen that when the soft soil is subjected to an external load of the embankment, the stress in the sub-soil is developed. Thus, an analysis of the stress path given in *sub-section 2.4.1* is aimed to make a good understanding of the state of stability and failure of soils. Besides, a sufficient knowledge of the stress paths is a basic factor to select the proper model for numerical analysis. Furthermore, saturated soft soil under embankment loading in the short term is likely to behave in an undrained manner in which the change of excess pore pressure is taken into account. Therefore in order to obtain the main factors of this state of soil, the next *sub-section 2.4.2* gives general description of undrained behavior which will be later used for the simulation of embankment applications. It should be considered that the dissipation of excess pore pressure in the soft soil with time due to embankment loading results in consolidation deformation, after which an additional deformation occurs with time (creep). Creep deformation is considered as a gradual rearrangement of soil skeleton. Both deformations are time-dependent that will be elaborated in the last *sub-section 2.4.3*. Moreover, in order to get insight in how the time-dependent soil model, which will later be used to model soft soils, works in PLAXIS, the theory of Soft Soil Creep (SSC) model is shortly discussed.

2.4.1 Analysis of stress path in soil

A stress path shows the stress development of a small volume in the subsoil. A difference could be between total stress (stress in soil skeleton and pore pressure) and effective stress (only stress in soil skeleton). In terms of this research, the stress path is used to assess the stress development within the subsoil under the loading caused by an embankment constructed on soft soil.

Under embankment loading, the normal stress and the deviatoric stress develop with time. However, it should be taken into account that the lateral effective stress, vertical effective stress and shear

stress are different depending on the stress points in the subsoil (Zdravkovic et al. 2002). The different stress conditions can be shown in Figure 2.23.
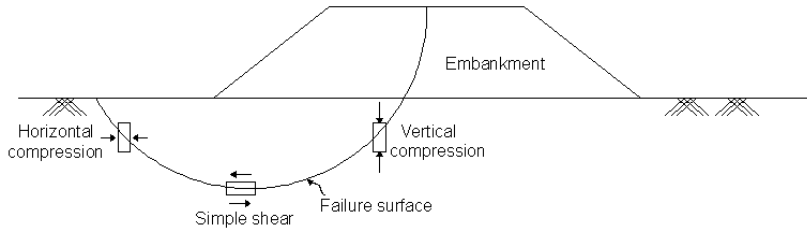
Figure 2.23 Stress conditions under an embankment (Zdravkovic' et al., 2002)

It can be seen that the vertical compression in the subsoil gets the maximum value at the centre of embankment ($\Delta\sigma_v > \Delta\sigma_h$). In the direction towards the embankment toe, the shear stress increases and reaches the highest value under the embankment toe ($\Delta\sigma_v = \Delta\sigma_h$). When moving away from the embankment toe, the stress condition changes from shear stress into horizontal stress ($\Delta\sigma_v < \Delta\sigma_h$).

For stress description, the following parts are structured from "general" stress description in coordinate systems (*sub-part 2.4.1.1*) to "particular" stress description in the subsoil under an embankment (*sub-part 2.4.1.2*).

2.4.1.1 Global stress description

Stresses in soil mass are caused from self weight and external force. Stress states can be expressed in different coordinate systems such as the Cartesian system (x, y, z) and the Cylindrical coordinate system (r, θ, z). In this research, the Cartesian system (x, y, z) with Stress tensor (Formula 2.4) is selected to describe Stress states

$$\sigma = \begin{bmatrix} \sigma_{xx} & \sigma_{xy} & \sigma_{xz} \\ \sigma_{yx} & \sigma_{yy} & \sigma_{yz} \\ \sigma_{zx} & \sigma_{zy} & \sigma_{zz} \end{bmatrix} \qquad (2.4)$$

The stress tensor can be presented in principal stresses σ_1, σ_2, σ_3 when the system of axis is such that shear stress components are zero (formula 2.5)

$$\sigma = \begin{bmatrix} \sigma_1 & 0 & 0 \\ 0 & \sigma_2 & 0 \\ 0 & 0 & \sigma_3 \end{bmatrix} \qquad (2.5)$$

In reality, the soil body is composed of discrete particles in which the properties between neighboring crystals widely vary. However for the engineering purpose, it is convenient to describe the soil on

macroscopic level (Valliappan 1981). According to Terzaghi (1943), the description of difference between total stress and pore water pressure for saturated soil is shown in the matrix form

$$\begin{bmatrix} \sigma'_{xx} & \sigma_{xy} & \sigma_{xz} \\ \sigma_{yx} & \sigma'_{yy} & \sigma_{yz} \\ \sigma_{zx} & \sigma_{zy} & \sigma'_{zz} \end{bmatrix} = \begin{bmatrix} \sigma_{xx} & \sigma_{xy} & \sigma_{xz} \\ \sigma_{yx} & \sigma_{yy} & \sigma_{yz} \\ \sigma_{zx} & \sigma_{zy} & \sigma_{zz} \end{bmatrix} - \begin{bmatrix} u & 0 & 0 \\ 0 & u & 0 \\ 0 & 0 & u \end{bmatrix} \qquad (2.6)$$

Where σ are total stress components; σ' are effective stress components and u is pore water pressure components. From the formula above, it can be recognized that pore water pressure can't sustain shear. Consequently, the soil particles have to resist all shear forces. In addition, Skempton (1984) experienced that the behavior of soil in nearly all circumstances is controlled by the effective stresses.

2.4.1.2 Stress path in soft soils under an embankment

After passing the "general" stress descriptions, this part forwards to analyze the stress path in the "particular" case of an embankment constructed on soft soils. According to Ladd et al. (1994), the estimation of soil displacements depends much on the correct incorporation of stress path. Therefore, a proper determination of total stress path (TSP) and effective stress path (ESP) is highly required to accurately predict the strain before and after yielding. Leroueil et al. (1990) showed a scheme to visualize the development of TSP and ESP in slightly over-consolidated soft soil under the embankment (Figure 2.24). However, it should be taken into account that the interaction between the undrained deformation and deformation due to consolidation is very complicated in reality. Therefore for the convenience of analysis the assumption is made that each type of deformation occurs separately (Matsuo and Kawamura, 1977)
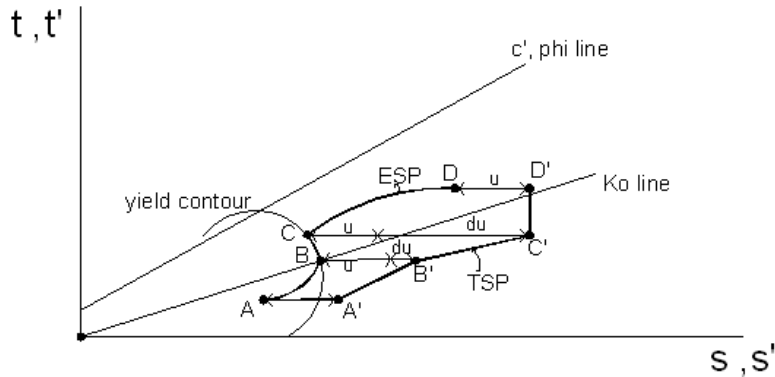
Figure 2.24 Schematic overview of TSP and ESP under an embankment (Leroueil et al., 1990)

The first phase of effective stress path (from A to B) is initial quasi-elastic response, which relates to the over-consolidated state of soil. In this phase, the consolidation process happens quickly and only a very small amount of excess pore pressure can develop (small du). Conventionally, this phase is assumed fully drained behavior (Tavenas and Leroueil, 1980). After passing the pre-consolidation

stress point B, the path follows an undrained state of plastic shearing, in which the stress path follows the yield contour and the excess pore pressure develops strongly. In this phase the mean effective stress stays equal that means soil mass is volume preserving, which is typical for undrained behavior. After the undrained response, the consolidation process (from C to D) takes place, which leads to the increase of vertical effective stress with time due to the dissipation of excess pore pressure. Point D shows the end of consolidation process where excess pore pressures have fully dissipated.

Furthermore, according to Leroueil (1990) the development of the effective stress path in soft soil can be also considered in the relationship between lateral displacement of embankment toe and vertical displacement under the centre of embankment. This is shown in Figure 2.25.
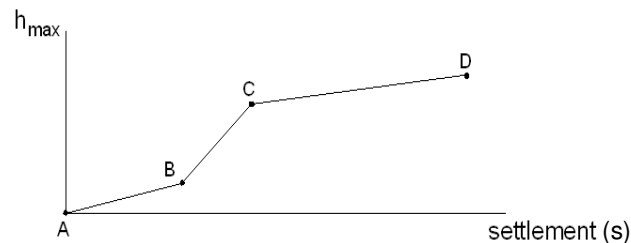
Figure 2.25 Relation between horizontal deformation at toe and settlement under centre embankment

It can be seen that a very small lateral displacement can take place at the embankment toe during the reconsolidation phase (A to B). In this phase the effective stress path stays close to the K_0-line (see Figure 2.24) (generally K_0 stress condition relates to zero lateral strain, which is similar to oedometer test condition in which the sample is confined in lateral directions (Peters and Steenbrink 2008)). When the soil behaves consolidated again (from B to C), the horizontal displacement develops almost at the same level as the vertical displacement. Afterwards, this development of the horizontal displacement becomes lower during the consolidation phase (from C to D). Moreover, according to Marche and Chapuis (1974), the relationship between settlements s, and lateral displacements h_{max} in the consolidation phase, was estimated based on a function ξ (where $h_{max}=\xi.s$). ξ depends on embankment width, embankment slope, thickness of soft soil deposit and safety factor of embankment. In most cases, this value was assumed to be approximately 0.16 (Matsuo and Kawamura 1977).

2.4.2 Undrained behavior of soft soil

Undrained behavior of soft soil is studied by two main sub-parts. The first one gives a general description of undrained state in soils as well as factors for determining undrained condition of soil. The second one focuses on undrained shear strength which is considered the maximum soil resistance in undrained analysis.

Undrained behavior of soft soil may be understood as the situation of soils under external loading in which water can't drain out of soil in the short term (Whitlow 1983), because the rate of loading is much quicker than the rate at which pore water is able to dissipate. As a result, most of external loading is transferred into pore water, leading to an increase of excess pore pressure. The existence

of drained or undrained state depends on some main factors such as types of soil (fine-grained soil or coarse-grained soil), rate of loading. Normally, undrained state is experienced with fine-grained soil (clay, peat,…). However, if the rate of loading is fast enough, the coarse-grained soil also experiences undrained behavior.

According to Whitman (1979), undrained shear strength of soil s_u is defined as strength of fine-grained soil which describes the capacity to sustain shear stress under undrained condition. In aspect of soil properties, the undrained shear strength only depends on the initial void ratio or the initial water content. Furthermore unlike the critical state of friction angle, the undrained shear strength is not a fundamental soil parameter. Its value s_u depends on the value of effective confining stress (Figure 2.26). It can be considered that an increase of effective confining stress results in an increase of undrained shear strength.
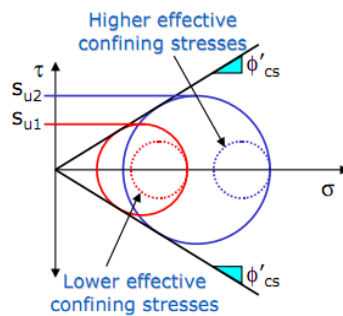
Figure 2.26 Relationship between effective confining stress and undrained shear strength
(Whitman 1979)

It should be considered that the behavior of saturated soft soils subjected to embankment loading in the short term is considered in undrained state. The failure surface is formulated, along which soil grains slide over each other (Figure 2.27). The undrained shear strength of soil in this situation is defined as the maximum shear stress at which the soil starts failing.
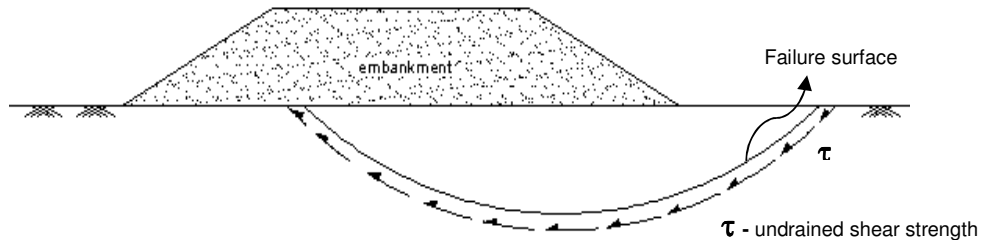
Figure 2.27 undrained shear strength in embankment application

According to Silva (2009), the undrained shear strength parameters could be estimated by laboratory tests as well as in-situ tests. Such an example of the range of undrained shear strengths for a fine-grained plastic soil is defined by Atterberg Limits (see Figure 2.28). It may be interpreted from this example that at its Liquid Limit ($I_L=1$) and Plastic Limit ($I_L=0$), the undrained shear strength s_u is

approximately equal to 1.5kPa and 150kPa respectively. Therefore, it can be considered that s_u can be predicted by knowing the water content of the soil.
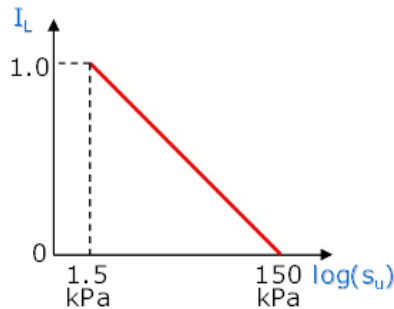
Figure 2.28 Diagram of Atterberg Limits

2.4.3 Theories of consolidation and creep behavior

As mentioned above, under external loading in undrained state of soil, excess pore water pressure develops. Thereafter, water gradually drains out of soil with time that leads to consolidation phase, after which additional deformation occurs with time (creep). Creep is reasonably understood as the gradual rearrangement of soil grains in more stable configuration (Leroueil et al., 1985 and Floquet, 2006). Besides, another understanding is that creep is caused by a very slow drainage of water from micro-pores to macro network (Berry and Poskitt, 1972). It can be said that the mechanism which causes creep deformation is still not fully understood due to different opinions of previous research.

Before going further to different theories of consolidation, some important aspects should be learned to get more understanding about the definitions and the factors relating to the later soil deformation. For example, the definition of *continuity equation* is firstly mentioned. According to Gibson (1967), this is the starting point of all consolidation theories. The continuity equation is differential equation which describes the transport of a conserved quantity. The equation form can be given in the Formula below

$$\frac{\partial \rho}{\partial t} + \nabla(\rho.u) = 0 \qquad (2.7)$$

The application of this equation to saturated soil can be described in Figure 2.29. This shows a typical flow regime under an embankment during consolidation phase. The embankment load produces excess pore pressure, which flows with time to drainage boundaries. It should be considered that in outer parts of the embankment, the horizontal water flow gives a certain influence on the rate of deformation. Therefore, the deformation in these parts becomes larger and the rate of deformation is quicker than this calculated by Terzaghi theory of one-dimensional consolidation (Larsson 1997). Due to this reason, to determine horizontal deformation at the embankment toe, at least two-dimension method needs to be used for the analysis.
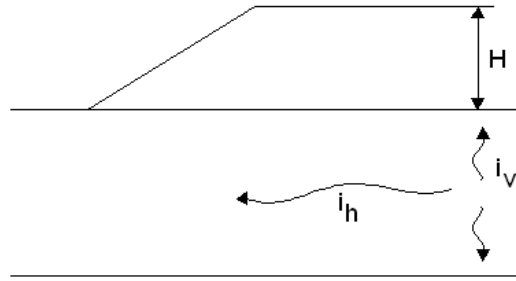
Figure 2.29 Typical flow's scheme during consolidation under embankment (Leroueil et al., 1990)

In addition, the concept of *isotropy* and *anisotropy* should be mentioned. In most of theories and models, *isotropy* is described during consolidation because axisymmetric condition is assumed. However, *anisotropy* is conferred to soil structure in reality because soil is almost subjected to plane-strain loading or three-dimensional loading and soil properties in all directions are not the same.

Furthermore, the magnitude of *shear strains* at the embankment toe is another important aspect for the development of lateral deformations with time. It should be considered that there is a distinction between a slow embankment construction and a fast embankment construction in response of *shear strains*. Tavenas et al. (1979) showed that for *a slow embankment construction*, the deformations mainly result from volumetric strains. In addition, other factors which reduce the relative importance of shear strains are the slope of embankment, the width of embankment and the safety factor of embankment. Furthermore, shear strains could be ignored if the safety factor of embankment is higher than 1.3 (Leroueil et al. 1990). However, it should be taken into account that, for *a fast embankment construction*, the *shear strains* can't be disregarded. In fact, accumulated from such an example of a fast embankment construction reported by Landva and Rochelle (1982), 30% of the total strains are the result of shear strains (see Figure 2.30).
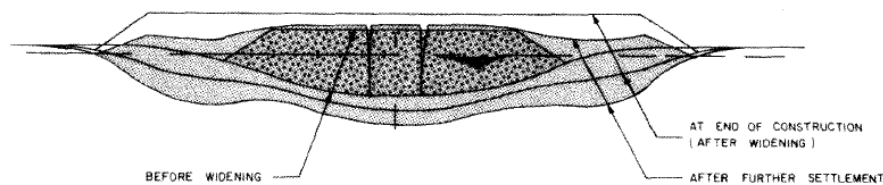
Figure 2.30 Embankment suffered excessive shear deformations (Landva and Rochelle 1982)

2.4.3.1 Development of time-dependent theories

As already mentioned, consolidation deformations and creep deformations, which are time-dependent behavior, have been studied in different theories. These theories are summarized in this part. However, it should be noted that this part does not intend to mention all aspects, only some important points regarding the developments from 1D consolidation to 3D consolidation are briefly discussed:

One-dimensional consolidation

In 1923, Terzaghi proposed a theory for one-dimensional consolidation. So far this theory has still played an important role in basic formation for several soil models. However, the validation of this theory was not in good agreement with experimental results. It was shown that the theory gives a good estimation only in the initial phase of consolidation, but during the secondary phase the experiment gives more rate of consolidation than estimated theoretically (Leonards and Girault 1961). According to Leroueil and Tavenas (1980), the limitations of Terzaghi's theory are that it uses a lot of assumptions which are not in full agreement with the real soil behavior. Firstly, the theory is only applicable for relatively small strains, while in reality strains could be in the order of 50% for peaty soil deposits as shown by Landva and La Rochelle (1982). Secondly, Terzaghi assumes one-dimensional flow during consolidation, while at least two-dimensional flow occurs in realistic situations that lead to more rapid rate of consolidation than estimated theoretically. Thirdly, this theory assumes that permeability is constant that can't be agreed in reality (Berry and Poskitt 1972). Afterwards, these limitations of Terzaghi's theory have been improved by other researchers. For example, the limitation of small strains was removed and the allowable changes in soil compressibility and permeability were considered by Gibson et al. (1967).

The secondary phase of consolidation was continued to be researched by others. Buisman (1940) found that the deformation pattern of soft soils in a consolidation test did not approach a constant final value and continued in very long time. On a logarithmic scale the secular deformations can be represented by an inclined straight line as shown in Figure 2.31. However, it can be seen that his theory is only valid for common time spans in civil engineering.
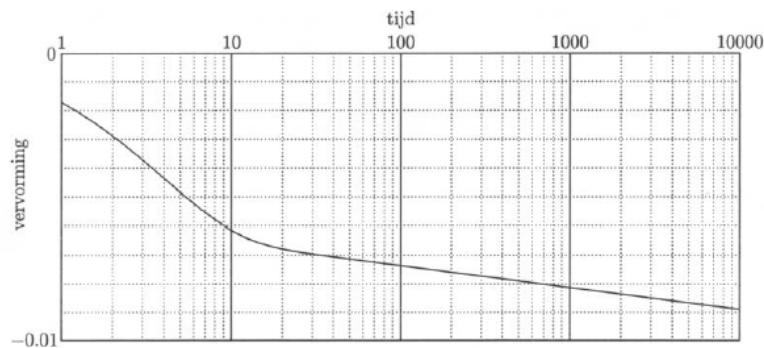
Figure 2.31 Simulation of secondary deformation in consolidation test (Buisman 1940)

Furthermore, modifications of Terzaghi's theory for secondary consolidation were developed in formulations by Taylor and Merchant (1940). The formulations gave a reasonable description of the phenomenon of secondary consolidation, which at least provided a partial interpretation of the discrepancies between full-scale measurements and estimations based on Terzaghi's theory. In addition, the formulations also described creep deformations (Christie 1964).

Three-dimensional consolidation

As mentioned above, the theory of Terzaghi (1923) has been the basis for the consolidation, but it is restricted to one-dimensional consolidation. Afterwards, more mathematical works on the one-dimensional theory have been continued and extended to theory of three-dimensional consolidation. It should be kept in mind that the 3D consolidation problems at first were coped with by making simplifications and deriving an approximately 1D problems which could be solved using Terzaghi's one-dimensional theory (Cryer 1962). Subsequently, several theories of 3D consolidation have been proposed. However this part doesn't pay attention to cover all aspects of theories, just some main points which display the development of the theories are discussed as below:

Terzaghi's 3D theory and Biot's 3D theory can be considered as typical theories of 3D consolidation which are based on Terzaghi's equations and Biot's equations (the details of these theories are shown in Terzaghi (1943) and Biot (1941) respectively). It can be summarized that the solution of Terzaghi's equations is often used in experiments, whereas the solution of Biot's equations has recently been paid good attention. However, neither Terzaghi's theory nor Biot's theory can show a complete picture of consolidation. An example of comparing between Terzaghi's theory and Biot's theory on the case of a sphere of soil loaded hydrostatically reported by Cryer (1962) presented that, the two theories give good estimations in volume changes, but predictions for the water pressure at the centre of the sphere differ significantly. The Terzaghi's theory predicts that the water pressure could steadily decrease, while the Biot's theory predicts that the water pressure could increase initially. Another example of comparing between these theories on predicting the settlements around the pumping well was represented by Debbarh (1988). He concluded that Biot's theory accurately predict subsidence phenomena as opposed to Terzaghi's theory especially in the close surrounding of the well. However, the Terzaghi's theory might be used effectively in estimations of the soil settlements far away from the pumping.

From the discussion above, it can be considered that each theory has its owned applications and both of them are in incomplete state of consolidation. Therefore, it can be recommended that more laboratory tests and in-situ tests may be required for validating these theories.

2.4.3.2 Soft Soil Creep (SSC) in PLAXIS

Theories of consolidation and creep have been studied by considerable research. However, it is remarked that there is still a disagreement about which theory is valid. Buisman (1936) might be the first one who proposed a creep law in clay after considering that soft soil settlements could not be fully explained by classical consolidation theory. He found that the deformation pattern of soft soils in a consolidation test did not approach a constant final value, and the deformation continued in very long time that means the tail of deformation curve is not horizontal. His invention proved that there was an existence of a secondary consolidation. Thereafter, this law of 1D-secondary compression was continued to research by others such as Bjerrum (1967), Adachi & Oka (1982), Borja & Kavaznjian (1985) and then was extended to 3D creep law.

The part is aimed to give a summary of SSC model which is implemented in PLAXIS Finite Element code. The SSC model is an extension of Modified Cam Clay model. However, the main differences between them are that SSC model uses criteria of MC failure with *strength parameters c' & φ'* and takes into account secondary compression. Furthermore, the SSC model is defined as an elastic viscoplastic model, formulated as a relationship between stress rates and (total) strain rates (Vermeer & Neher 1999).

SSC model for isotropic stresses

The total volumetric strain in SSC model is defined in Eq. (2.8) where ε_v is total volumetric strain due to an increase in effective mean stress from p'_o to p' in a time period of t_c to t'. The total volumetric strain is divided into an elastic part (ε^e) and a visco-plastic creep part (ε^{cr}). In addition, the visco-plastic part can be also decomposed into two parts which are one part during primary consolidation (ε_c^{cr}) and the other after primary consolidation (ε_{ac}^{cr}). Furthermore, the relationship between the volumetric strain and the mean effective stress was clarified by Janbu (1969) as in Figure 2.32.

$$\varepsilon_v = \varepsilon^e + \varepsilon^{cr} = \varepsilon^e + \varepsilon_c^{cr} + \varepsilon_{ac}^{cr} \qquad (2.8)$$

$$\varepsilon_v = k^*.\ln\left(\frac{p'}{p'_0}\right) + (\lambda^* - k^*).\ln\left(\frac{p'_{pc}}{p'_{po}}\right) + \mu^*.\ln\left(\frac{\tau_c + t'}{\tau_c}\right) \qquad (2.9)$$

In Eq. (2.9), the parameters k*, λ* and μ* is modified swelling index, modified compression index and modified creep index. It can be recognized that the first two parts relate to Modified Cam Clay model and the third one is new. The first part relates to unloading/reloading behavior of soil which is assumed to be elastic and follows the Hooke's law. The second part only acts if isotropic compression situations occur. The third part implies for secondary compression (Vermeer & Neher 1999).
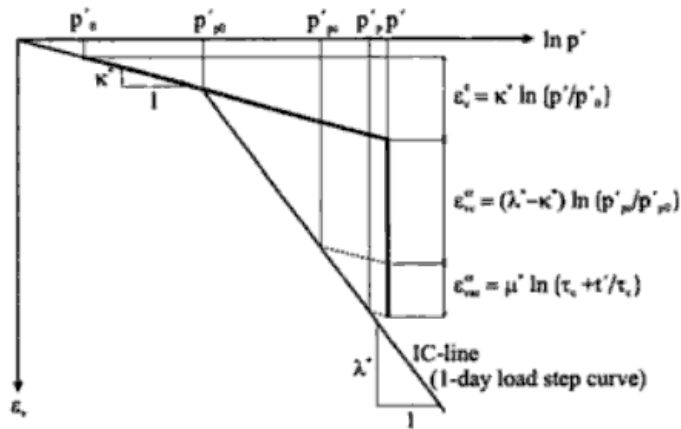
Figure 2.32 Logarithmic relationship between volumetric strain and mean stress including creep

The Eq. (2.9) is only valid for the constant mean effective stress. Therefore, for continuous loading problems, this equation needs to be formulated in differential form as in Eq. (2.10). The more details of formulation are described in Vermeer & Neher (1999). Thus, here only shows the final form of creep strain part as:

$$\varepsilon^{cr} = \int d\varepsilon^{cr}.dt \text{ and } \varepsilon^{cr} = \frac{\mu^*}{\tau}\left(\frac{p'}{p'_p}\right)^{\frac{\lambda^*-K^*}{\mu^*}}$$ (2.10)

Where τ is intrinsic time parameter (1 day) and $(p'/p'_p) = OCR^{-1}$ is inverse of over-consolidation ratio.

It can be seen that the creep strain rate, ε^{cr} depends on the inverse of the over-consolidation ratio. If the stress state remains unchanged, the creep process continues and the pre-consolidation stress keeps on increasing, but at a decreasing rate (more details are shown in Vermeer & Neher (1999)).

SSC model for arbitrary stress

The above part describes the SSC model in the situation of isotropic stress. To extend the model for the situation of arbitrary stress, the concepts of equivalent stress p^{eq} and equivalent pre-consolidation pressure p_p^{eq} are introduced (the formulations of the parameters are shown in Vermeer & Neher (1999)).

$$p^{eq} = \frac{q^2}{M^{*2}.(p'+c'.\cos\varphi')} + (p'+c'.\cos\varphi')$$ (2.11)

$$p_p^{eq} = p_{po}^{eq}.\exp\left(\frac{\Delta\varepsilon^{cr}}{\lambda^* - k^*}\right)$$ (2.12)
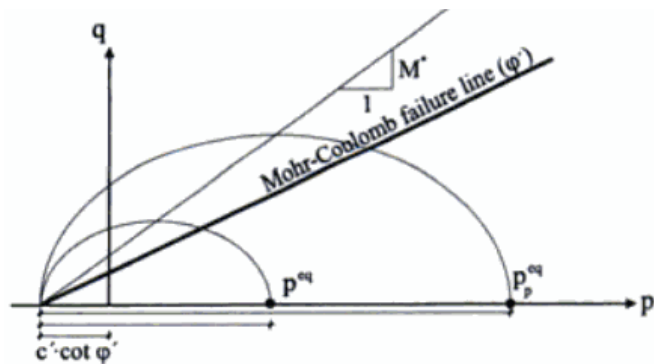
Figure 2.33 Yield surface of SSC-model in p'-q plane

From Figure 2.33, it can be understood that any stress state is described by a point lying on the surface homologous to the yield surface of the Modified Cam Clay (MCC) model represented in p'-q plane. The top of the surface is located on the M*-line (in MCC model, M*-line is Critical State Line). It should be kept in mind that SSC model uses MC failure criteria with the strength parameters c' and φ'.

Both MC line and M*-line are moved from the origin of the coordinate system by an offset which is equivalent to the amount of $c'.cos\varphi'$. Furthermore, it can be seen in the Figure that MC line is fixed, but the cap with p_p^{eq} may move due to volumetric strain.

2.4.3.3 Parameters of Soft Soil Creep model in Plaxis

After summarizing the main points of SSC model as above, the last part briefly presents the required parameters of SSC model which will later be used for assigning material properties of the soft soils in embankment applications (Table 2.5). In addition, Figure 2.34 shows the determination of consolidation parameters and creep parameters from isotropic compression test.

Table 2.5 Required parameters of the SSC model

Required parameter	Name
λ^*	Modified compression index
k^*	Modified swelling index
μ^*	Modified creep index
ν_{ur}	Poisson's ratio for unloading/reloading
c'	Cohesion
φ'	Friction angle
ψ	Dilatancy angle
K_{nc}^0	Horizontal/vertical stress ratio in normally consolidated 1D compression
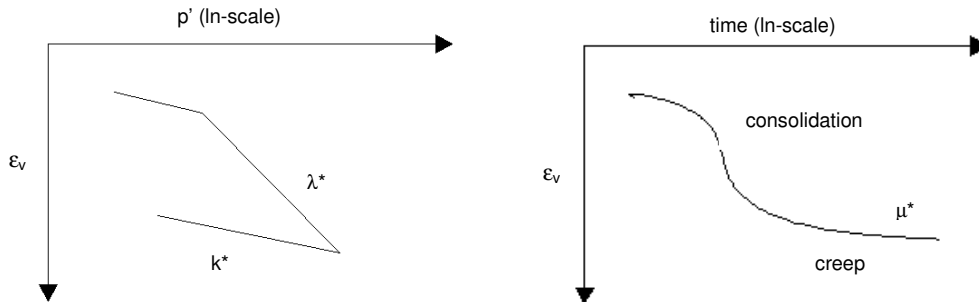
Figure 2.34 Determination of λ^*, k^*, μ^* from isotropic compression test

2.5   Summary of the literature review

This chapter not only reviewed the previous research on the piles undergoing lateral soil movements, but also provided the basic background of the PLAXIS embedded pile and the theories of soft soil behavior. Some conclusions were drawn:

+ There are many theoretical methods as well as practical methods for solving the situation of laterally loaded piles caused by soil movements. However, many uncertainties still remain in terms of theoretical methods and the proper predictions vary from case to case in terms of practical methods.

+ The background of the PLAXIS embedded pile is elaborated in order to consider its benefits of properties in terms of simulating the pile in PLAXIS 3D. On the other hand, the previous validation of the embedded pile concludes that the embedded pile is in quite good agreement with the real behavior.

+ The theory of soft soil is mentioned regarding the problem of an embankment constructed on soft soil. Many theories have been studied by different researchers. However, this part only mentions some main points which show the overview of soft soil behavior and the developments from one-dimensional consolidation to three-dimensional consolidation. Furthermore, the SSC model is paid more attention for further usage in embankment applications.

CHAPTER 3   EVALUATION OF THE EMBEDDED PILE UNDERGOING LATERAL LOADING IN A PLAXIS SIMPLIFIED MODEL

3.1   Introduction

Before considering the embedded pile behavior in 'advanced' models shown in the next chapters, it's firstly desirable to study the embedded pile behavior in a 'simplified' model. This 'simplified' model is considered, where only a 1m cross-section of the 'advanced' model is simulated. The cross-section is taken at a certain distance below the ground surface. This is shown in Figure 3.1. More details of the 'simplified' model will be described in *part 3.2.1*.
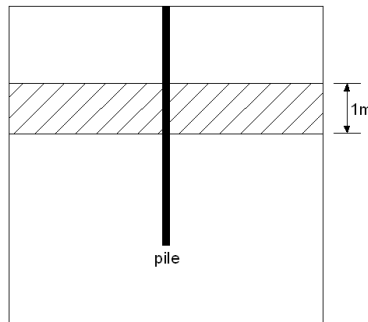
Figure 3.1 Model of 1m cross-section

In this model, the embedded pile is moved laterally into soils, and then the embedded pile itself will be studied by investigating the behavior of surrounding soils as well as the behavior of pile-soil interaction. In addition, it should be reminded that the embedded pile model is considered as the 'simplified' volume pile model, thus the evaluation of the embedded pile is also made by a comparison with the volume pile. It's expected to get insight in the behavior of the embedded pile in case of being subjected to lateral loading as well as to consider how good the embedded pile is able to resemble the volume pile.

3.2   Description of the simplified model

3.2.1   Geometry

3.2.1.1   Embedded pile model

The PLAXIS model is created with dimensions of 8m in both X direction and Y direction, 1m in Z direction. The soil is assumed with total 1m thick layer. The 'short' embedded pile with length of 1m is inserted at the origin of the coordinate system. The overview of the model in half way is shown in Figure 3.2.
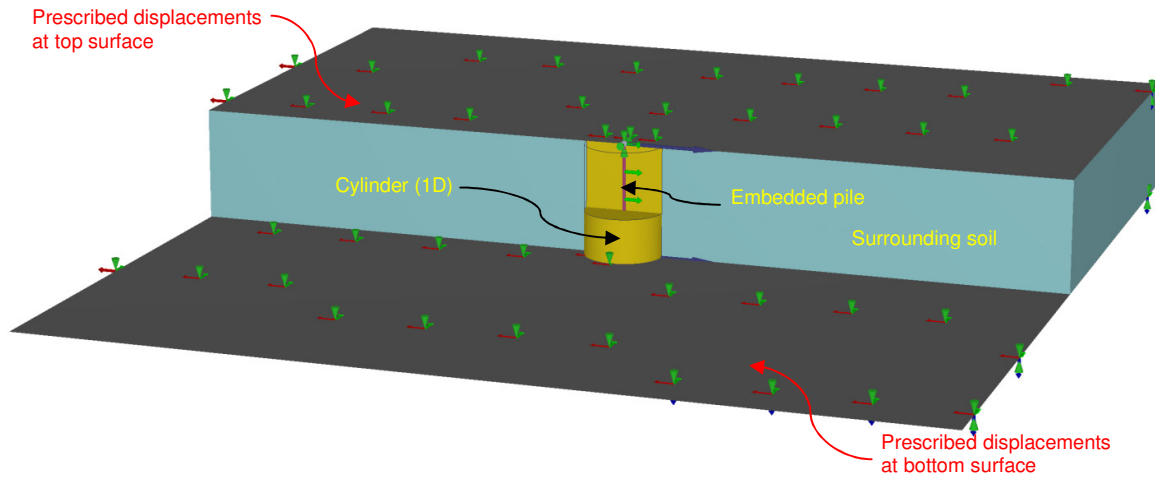
Figure 3.2 Sketch of the model with embedded pile in PLAXIS 3D

It can be seen that the pile foot is connected to the model bottom boundary. By PLAXIS default, this boundary is totally fixed in all directions that make the pile foot impossible to move. Therefore, a *surface* is added at the model bottom boundary in which the displacements in X and Y direction are allowed and the displacement in Z direction is fixed. With this assignment, the constraint of movements in X direction and Y direction at the pile foot is completely released. Furthermore, another *surface* with the same prescribed displacements is also made at the model top to prevent the movements of the soil and the pile in Z direction.

Although the embedded pile is composed of line elements, *a particular elastic region* around the pile whose dimension is equivalent to pile diameter is assumed according to the embedded pile concept. In addition, to make a good comparison between the embedded pile model and the volume pile model as shown later, the geometries of the two pile models have to be similar. Therefore, a cylinder which has a diameter of 1D (m) is inserted around the embedded pile. The cylinder is set up with the same properties as the surrounding soil. Moreover, the mesh around the embedded pile should be fine enough to make good contacts between the pile and the soil, thus the local mesh in the cylinder is refined with the *fineness factor of 0.1*.

In order to move the embedded pile laterally in the surrounding soil, *point prescribed displacements* are applied at the pile top and the pile foot. The point displacements are prescribed with 0.2m in X-direction and fixed in Y direction & Z direction that only allow the pile to displace with the maximum value of 0.2m in X-direction (see Figure 3.3).
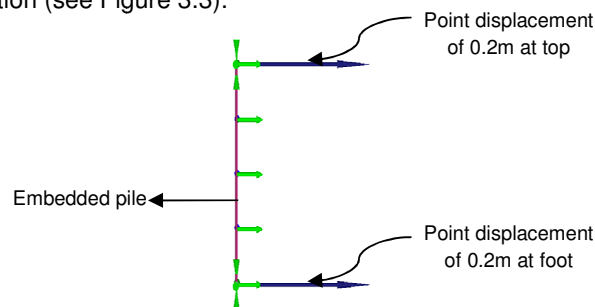
Figure 3.3 Visualization of the point prescribed displacements at the pile top and pile foot

3.2.1.2 Volume pile model

In addition to studying the embedded pile itself, the chapter is also aimed to consider how good the embedded pile is able to resemble the volume pile. Therefore, in order to make a good comparison between them, the volume pile model has to be created with the same conditions as the embedded pile model. The volume pile model in half way is sketched as in Figure 3.4. However, it should be taken into account that the volume pile is assigned with *a material data set for soil* but with *concrete properties* instead of *a material data set for structures* like the embedded pile.
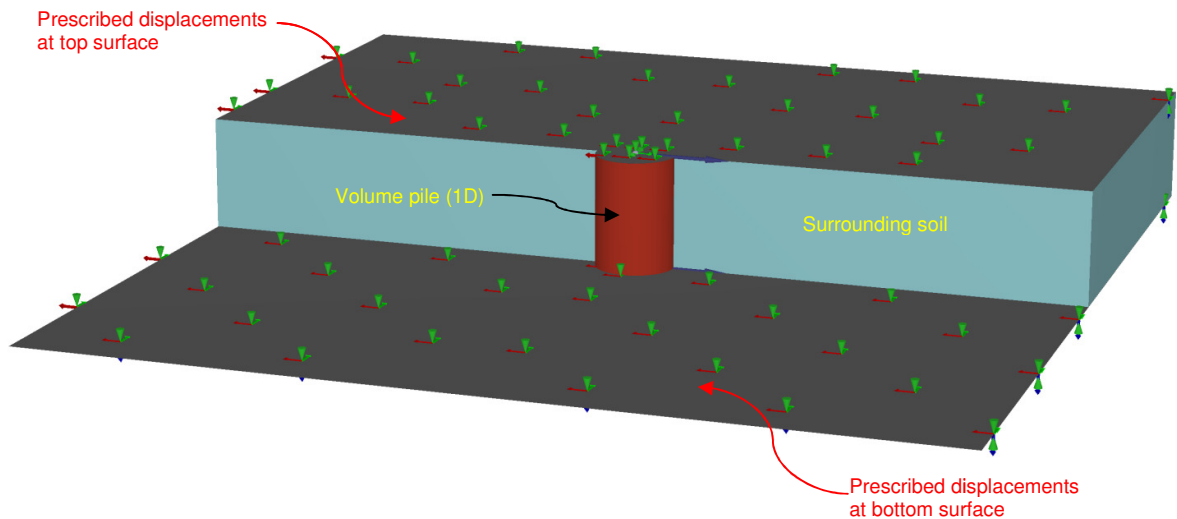
Figure 3.4 Sketch of the volume pile model in PLAXIS 3D

Furthermore, to make the same conditions of *prescribed displacements* as the embedded pile, the *surface prescribed displacements* of 0.2m in X-direction are applied at the pile top surface and the pile bottom surface. In addition, these displacements are fixed in other directions to ensure that the volume pile is only allowed to move in X-direction (see Figure 3.5).
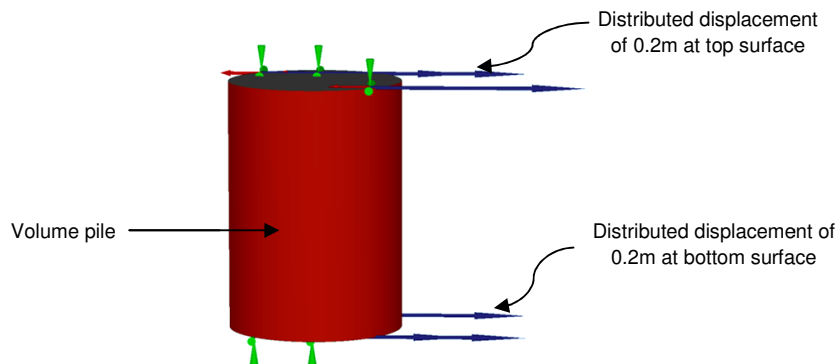
Figure 3.5 Visualization of the distributed displacements at pile top surface and pile bottom surface.

3.2.2 Property

The properties of the volume pile and the embedded pile as well as the properties of the surrounding soil are shown in the Tables below

Table 3.1 Properties of the volume pile in PLAXIS 3D

Parameter	Name	Value	Unit
Material model	-	Linear elastic	-
Drainage type	-	Non-porous	-
Unit weight	γ	0	kN/m^3
Young modulus	E	3.10^7	kN/m^2

Table 3.2 Properties of the embedded pile in PLAXIS 3D

Parameter	Name	Value	Unit
Predefined pile type	-	Massive circular pile	-
Young's modulus	E	3.10^7	kN/m^2
Unit weight	γ	0	kN/m^3
Pile diameter	d	0.7	m
Pile area	A	0.3848	m^2
Inertia moment	I	0.01179	m^4
Skin resistance type	Type	Linear	-
Maximum traction allowed at the pile top	$T_{top,max}$	500	kN/m
Maximum traction allowed at the pile bottom	$T_{bot,max}$	500	kN/m
Base resistance	F_{max}	10000	kN

Table 3.3 Properties of the surrounding soil in PLAXIS 3D

Parameter	Name	Value	Unit
Material type	Type	MC	-
Drainage type	Type	Drained	-
Unit weight	γ_{unsat}	0	kN/m^3
	γ_{sat}	0	kN/m^3
Effective Young's modulus	E'	10^4	kN/m^2
Effective Poisson's ratio	ν'	0.3	-
Effective cohesion	c'	10	kN/m^2
Effective friction angle	φ'	0	^{0}
Tension cut-off	Type	Deselected	-
Strength reduction factor of the interface	R_{inter}	0.5	-

In Table 3.3 showing the material data set of the surrounding soil, some main points should be taken into account as follows. Firstly, the "*Drained*" type is considered, which enables to simulate the drained behavior using an effective stress analysis. In addition, the *effective friction angle φ'* is assumed to be equal to zero, thus the drained shear strength of the soil is fully modelled using the *effective cohesion* c' (see Figure 3.6). Furthermore, in order to neglect the *initial stress* in the soil as

well as the increase of the *drained shear strength* with depth due to the soil weight, the *unit weight* of the soil γ has to be equal to zero. By this set of material data, the maximum shear stress resistance of the soil is fully controlled with the value of 10kN/m^2. Moreover, the option of "*tension cut-off*" is deselected, which means that the soil is assigned with a very large tensile strength in order to avoid the failure due to tensile stresses. On the other hand, the property of the interface around the volume pile is related to the property of the surrounding soil by the *strength reduction factor R_{inter}* (for the comparison between the embedded pile and the volume pile 'with' interface which will be shown later, R_{inter} is assumed to be equal to 0.5).
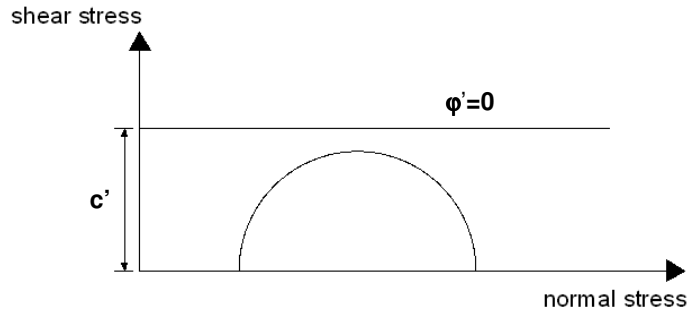
Figure 3.6 Drained shear strength c'

3.2.3 Test phase conditions

For both the volume pile model and the embedded pile model, the test is conducted with two calculation phases. After the *Initial phase* with K_0 analysis, the *First phase* is implemented by activating the *prescribed displacements* at the pile top and the pile foot to move the pile into the soil. The PLAXIS calculation phases may be summarized as in Table below. The results will be discussed in the next part.

Table 3.4 Calculation phases

Phase	Analysis type	Elements	Activated	Value
Initial	K_0	(1) Surrounding soil	✓	-
		(2) Top/bottom boundary surface	x	-
		(3) Top/bottom prescribed displacements	x	-
		(4) Embedded pile/Volume pile	x	-
1	Plastic drained	(1) Surrounding soil	✓	-
		(2) Top/bottom boundary surface	✓	-
		(3) Top/bottom prescribed displacements	✓	u_x=0.2 (m)
		(4) Embedded pile/Volume pile	✓	-

3.3 Discussion

The discussion analyzes the behavior of the laterally loaded embedded pile by an investigation of the surrounding soil as well as a comparison with the volume pile in terms of soil displacements and stress distributions in the soil. It's expected that the embedded pile is not only able to show efficient features in case of being loaded laterally, but also to resemble the volume pile behavior.

3.3.1 Analysis on the embedded pile by an investigation of the surrounding soil

It should be reminded that the embedded pile is assumed with the *elastic region* whose diameter is equivalent to the pile diameter. Therefore, when the pile displaces into the soil, it's expected that the soil in the *elastic region* will move with the same displacements as the embedded pile. This expectation is clearly seen in Figure 3.7, which shows the PLAXIS output shadings of total soil displacements around the pile.
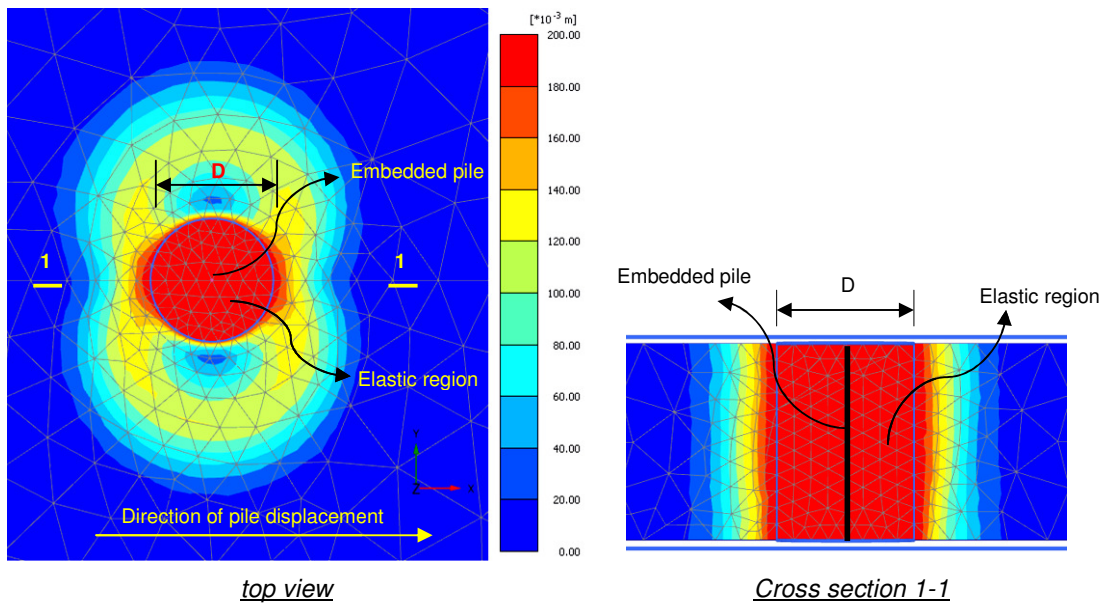
Figure 3.7 Shadings of total displacements around the pile in PLAXIS 3D output

Furthermore, Figure 3.8 shows the vector plot of soil displacements around the embedded pile. It can be seen that when the pile displaces forward, the soil surrounding immediately moves from the front towards the back that creates the flow of soil around the pile. The soil displacements decrease with increasing distance away from the pile. On the other hand, when the pile is pushed further into the soil, the stress becomes compressed at the front of the pile and tensile at the back of the pile. In this test, the *tension cut-off* is switched off that enables the soil to sustain tensile stresses. Therefore, the "gap" at the back between the surface of "imaginary" pile (the shaft surface of elastic region) and the soil is not allowed to open. Consequently at the back of the pile, the pile-soil contact is restored.
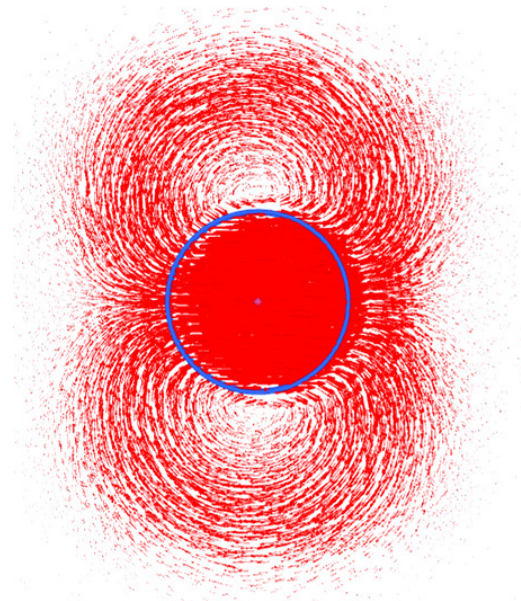
Figure 3.8 Vector plot of soil displacements around the PLAXIS embedded pile

In addition to the investigation of soil displacements, stress distribution in the surrounding soil is also considered. When the pile moves into the soil, it's expected to consider the compressive stresses at the front of the pile and the tensile stresses at the back of the pile. This expectation can be clearly seen in Figure 3.9 which shows direction plots of *major compressive stress and minor tensile stress σ_1* & *minor compressive stress and major tensile stress σ_3* around the shaft surface of the *elastic region* after loading.

Direction of the pile movement   Direction of the pile movement
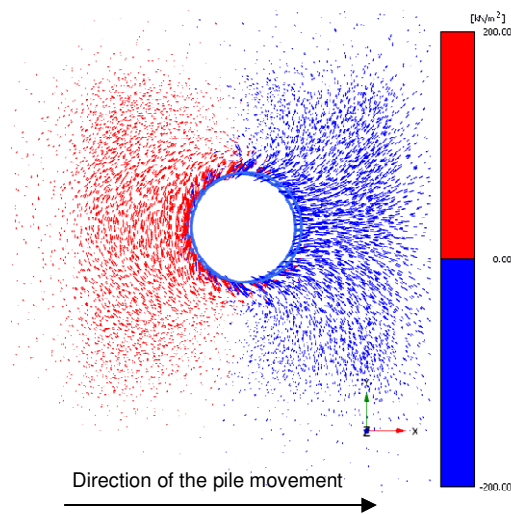
Figure 3.9a Major compressive stress   *Figure 3.9b Minor compressive stress*
and minor tensile stress σ_1   *and major tensile stress σ_3*
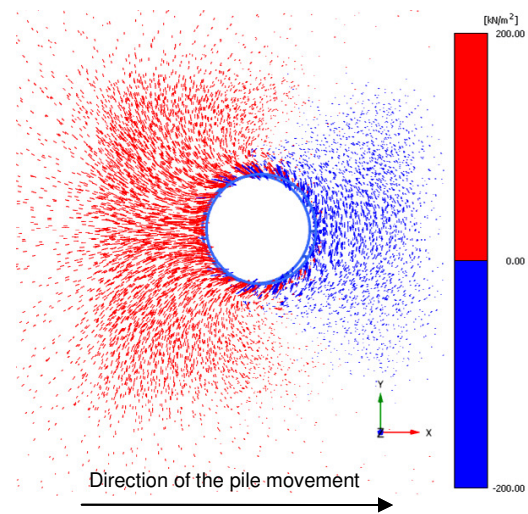
Figure 3.9 Direction plots of principal stresses around the surface shaft of elastic region

These results above may be interpreted based on a simplified model of stress points at the front of the pile and the back of the pile shown in Figure 3.10. It can be seen that each stress point of the soil

element in the horizontal plane composes of the principal stress components σ_1 and σ_3. Furthermore in this situation, the stress point at the front is in compression and the stress point at the back is in tension. Therefore if either *major compressive stress (minor tensile stress)* σ_1 or *major tensile stress (minor compressive stress)* σ_3 is plotted, Figure 3.10 will be changed into Figure 3.11a (complying with the trend as seen in Figure 3.9a) or into Figure 3.11b (complying with the trend as seen in Figure 3.9b)
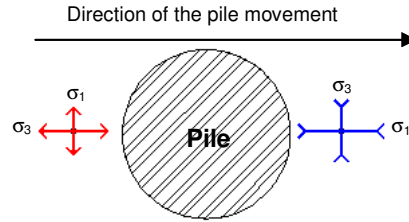
Figure 3.10 Simplified model of stress points at the front and the back.
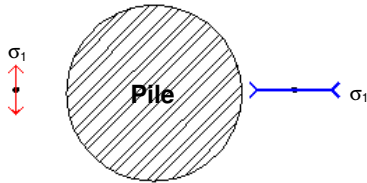
Figure 3.11a Major compressive stress and minor tensile stress $\boldsymbol{\sigma_1}$
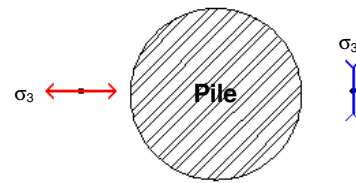
Figure 3.11b Minor compressive stress and major tensile stress $\boldsymbol{\sigma_3}$

Figure 3.11 Directions of Principal stress components.

In addition to the evaluation of stress distribution in the surrounding soil, the strain distribution is also considered. Figure 3.12 shows direction plots of *major compressive strain (minor tensile strain),* ε_1, and *major tensile strain (minor compressive strain),* ε_3, around the shaft surface of the elastic region after loading. It can be seen that the ε_1 is found at the front of the pile and ε_3 is found at the back of the pile, which is consistent with the trend as seen for the principal stresses displayed in Figure 3.9.
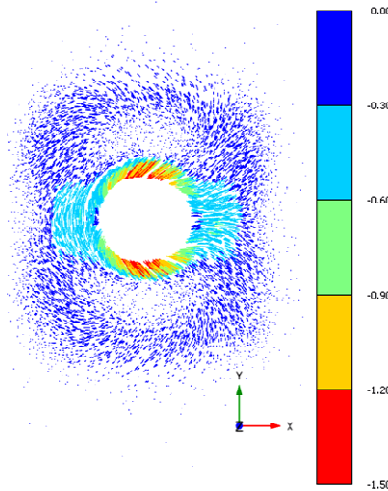
Figure 3.12a Direction of principal strain ε_1 Figure 3.12b Direction of principal strain ε_3
Figure 3.12 Directions of Principal strain components.
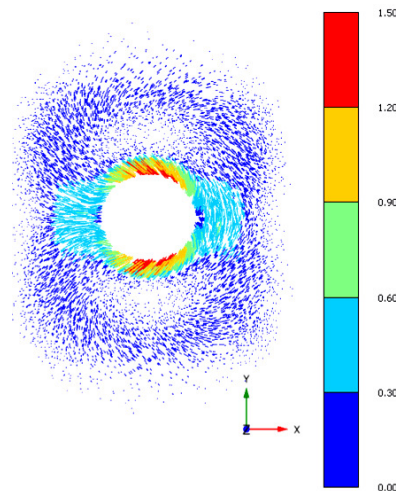
When the embedded pile is laterally pushed further, the soil remains elastic inside *the diameter region* and becomes plastic outside that region to create a *plastic zone* as displayed in Figure 3.13. It can be seen that the *plastic zone* expands more in the direction of the pile movement. In addition, Figure 3.14 shows the total strain of a particular point in the plastic zone. A clear indication is that over 90% of the total strain of this soil element is the result of the plastic strain.
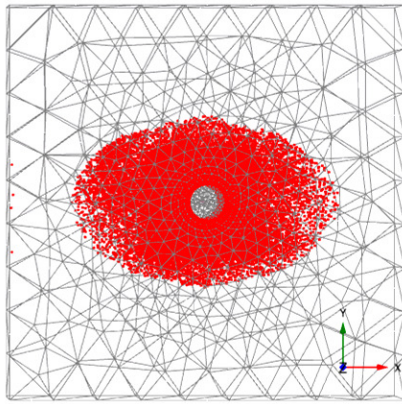
Figure 3.13 Plastic zone
Figure 3.14 Stress-strain relationship
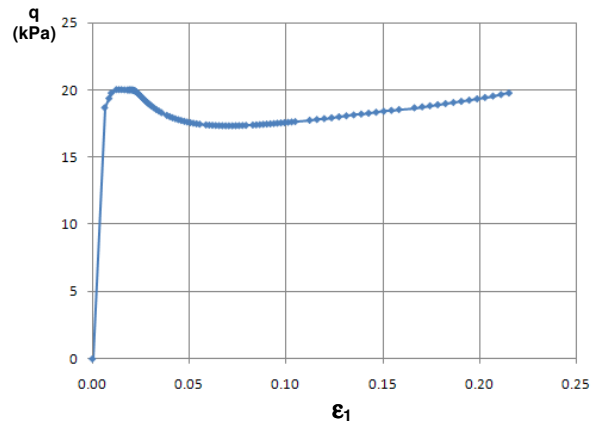
3.3.2   Validation of the PLAXIS embedded pile 'with' a cylinder around by a comparison with the PLAXIS volume pile

In order to make a good comparison between the embedded pile model and the volume pile model, the geometries of the two models have to be similar. Therefore, a *cylinder (1D)* in which the local mesh is refined with the fineness factor of 0.1, is added around the embedded pile (more details were elaborated in *part 3.2.1.1*). The comparison between the embedded pile and the volume pile is made by investigating the load-displacement behavior as well as the stress distribution in the surrounding soil. Besides, the volume pile model takes into account the roughness of pile-soil contacts which corresponds to the values of R_{inter} ($R_{inter}=1$ implies the "rough" pile-soil contacts and $R_{inter}<1$ implies the "smoother" pile-soil contacts), whereas it's not considered in the embedded pile model in the situation of undergoing lateral loading (more details were shown in *part 2.3.1.3*). Therefore, this comparison is also aimed to see the difference between the embedded pile model and the pile with "smoother" shaft surface (which corresponds to $R_{inter}<1$). In short, the validation of the embedded pile is made by comparisons with the volume pile in both cases *'without'* the interface and *'with'* the interface having $R_{inter} = 0.5$.

For the purpose of plotting the load-displacement curves, *point A* lying on the top surface of 1D-cylinder is selected (Figure 3.15).
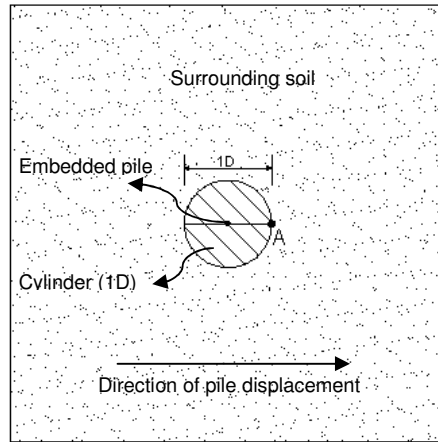
Figure 3.15 Selected point for load-displacement curves

The load-displacement behavior of the soil at point A is presented in Figure 3.16. It can be seen that the embedded pile and the volume pile 'without' interface completely match although a very slightly smaller displacement is revealed in the embedded pile model. However, in comparison with the volume pile 'with' interface having R_{inter}=0.5, the embedded pile overestimates the lateral load by approximately 15%. Therefore it can be concluded that in the situation of being subjected to lateral loading, the embedded pile shows a very good performance in modelling the pile with the "rough" shaft surface and has a trend of overestimation in modelling the pile with the "smoother" shaft surface.
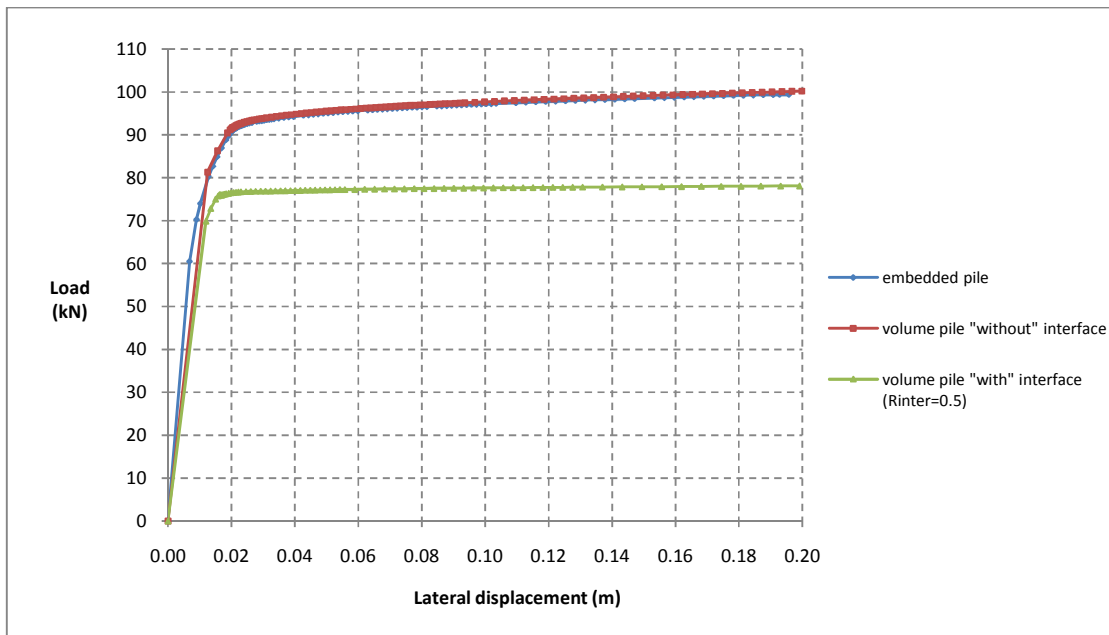
Figure 3.16 Load-displacement curves

In addition to the load-displacement behavior, distributions of the principal stresses around the pile are also investigated as seen in Figure 3.17. As expected, the compressive stresses and the tensile stresses are found at the front and the back of the volume pile respectively, complying with the trend

as seen for the embedded pile. In general, it can be concluded that the embedded pile is in good agreement with the volume pile in the same conditions of geometry.

Embedded pile   Volume pile without interface   Volume pile with interface
                                                                        (Rinter=0.5)
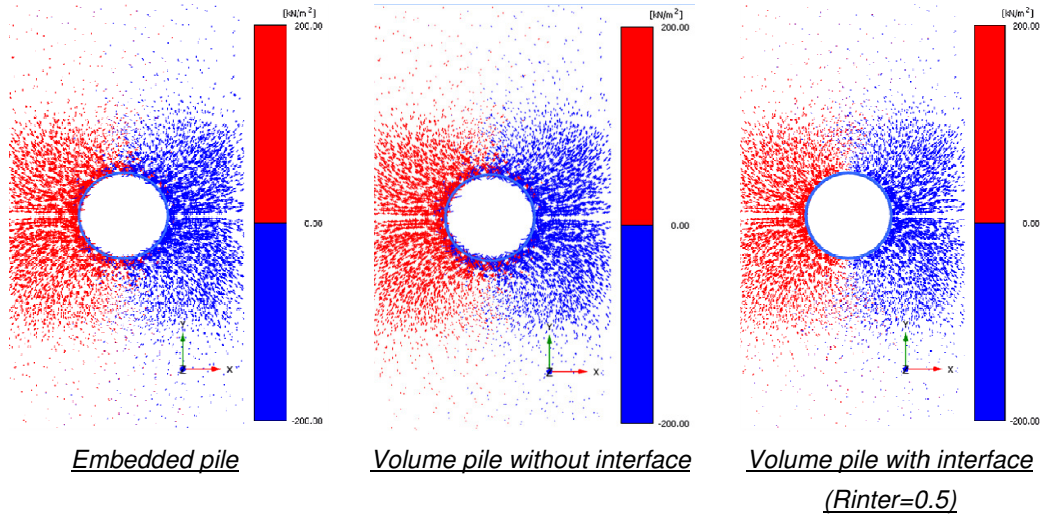
Figure 3.17 Distribution of total principal stress.

3.3.3 Validation of the PLAXIS embedded pile 'without' a cylinder around by a comparison with the PLAXIS volume pile

The above part shows that to make a good comparison with the volume pile, the cylinder (1D) in which the local mesh is refined, needs to be created around the embedded pile. However in practical applications, the embedded pile is usually modelled without any local mesh refinement. Therefore, it is questionable whether the embedded pile 'without' a cylinder around is also able to show a good performance in comparison with the volume pile. This question will be discussed by a comparison between the embedded pile 'without' a cylinder around and the volume pile as below.

Figure 3.18 shows the top view of the two models after the meshes are generated. It should be noted that the local mesh refinement which is seen in the embedded pile model (Figure 3.17b) only occurs at the pile top and no refinement is revealed in the deeper part. The results of surrounding displacements are shown in Figure 3.19 below.
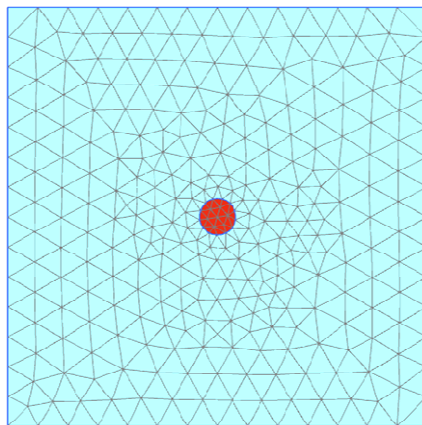
Figure 3.18a Volume pile model   Figure 3.18b Embedded pile model
Figure 3.18 Generated mesh in embedded pile model and volume pile model.
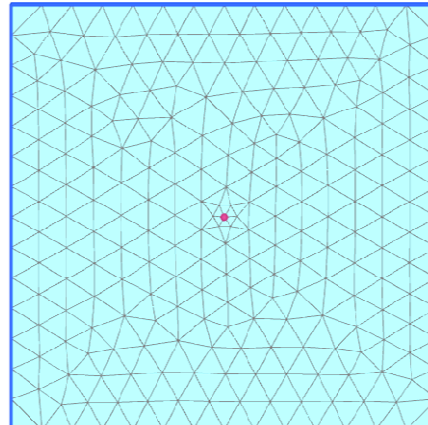
Remark: In Figure 3.19 which shows the distribution of total soil displacements, *a 'white circle' with diameter 1D* doesn't really exist in the embedded pile model (Figure 3.19b). This circle is only made to determine the boundary of *the elastic region* that makes it convenient to compare with the volume pile model.

It can be seen that the embedded pile predicts slightly smaller soil displacements in the elastic region than the volume pile. However the embedded pile gives the larger "*radius*" of an area in which the soil is displaced due to the pile displacement.

In addition to the investigation of the distribution of total soil displacements, lateral loads induced in both models are also considered. Figure 3.20 shows load-displacement behavior at a particular point in *the 'elastic region'*. It can be seen that the embedded pile, in spite of predicting slightly smaller soil displacement than the volume pile, overestimates the lateral load by approximately 25%.
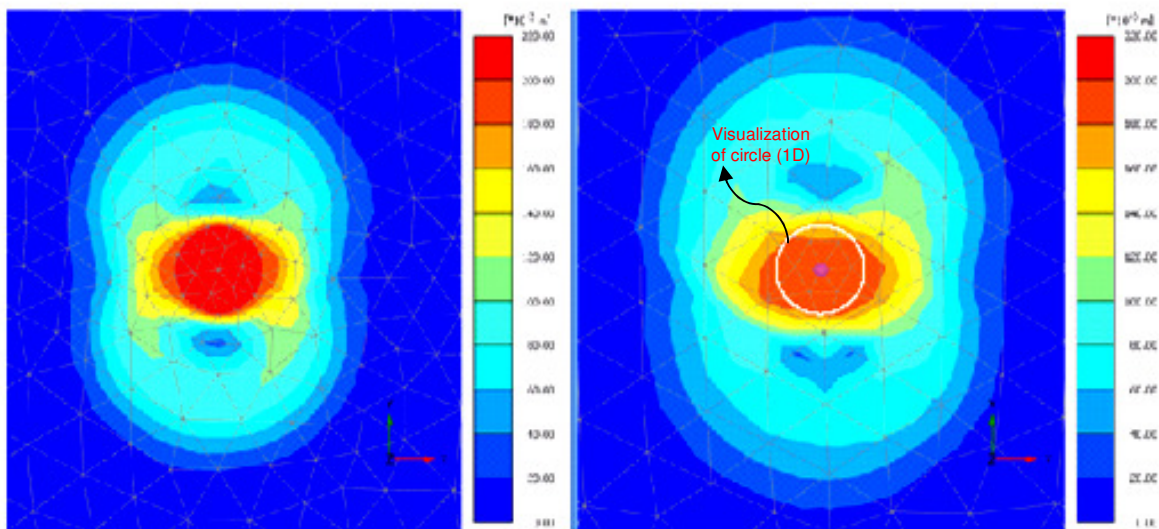
Figure 3.19a Volume pile model   *Figure 3.19b Embedded pile model*

Figure 3.19 Total soil displacements (m)
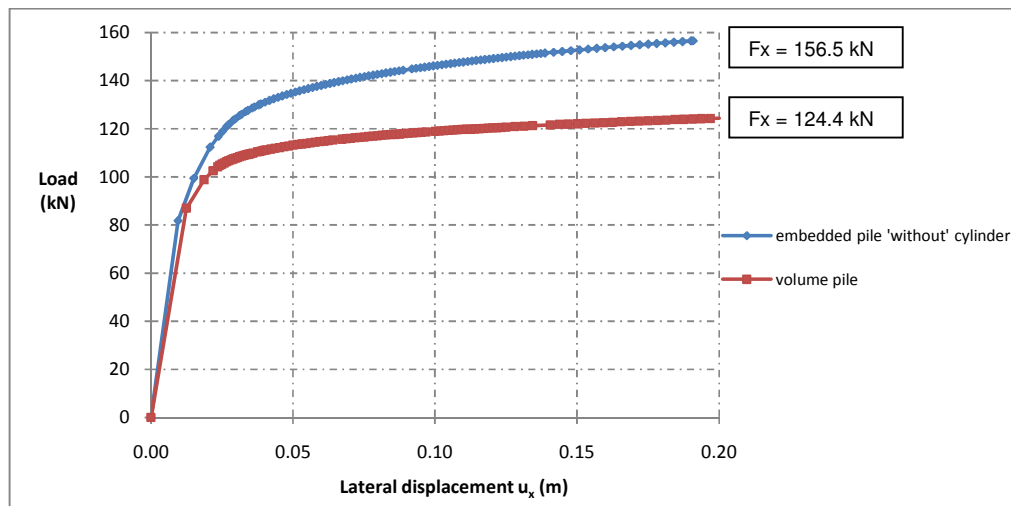
Figure 3.20 Load-displacement curves

3.4   Conclusion

The embedded pile undergoing lateral loading was evaluated by investigating the surrounding soil and comparing with the volume pile. Some conclusions were drawn:

➢ In the part of investigating the surrounding soil (based on the assumption that a 'cylinder' with local mesh refinement is added around the embedded pile), soil displacements as well as stress-strain distributions were considered. It can be recognized that the soil is fully elastic inside *the 'diameter' region* and becomes plastic outside this region. In addition, a clear indication is that total strains of soil elements in the plastic zone mostly result from plastic strains. Moreover, compressive stresses and tensile stresses are found at the front and the back of the pile shaft, complying with the trend as seen for strain distributions. Therefore it can be concluded that the embedded pile shows a good performance in modelling the laterally loaded pile.

➢ In the part of comparing with the volume pile (based on the assumption that the embedded pile model with a 'cylinder' around to have the same geometry with the volume pile model), the pile-soil interaction was considered. It can be recognized that the embedded pile is perfect in modelling the pile having "rough" surface and has a trend to overestimate the displacement-load behavior in modelling the pile having "smoother" surface. This is because the embedded pile doesn't take into account a 'slide', which is used to model the pile-soil interaction, in the horizontal directions. Besides for a more realistic application (based on the assumption that the embedded pile 'without' any local mesh refinement around), the embedded pile overestimates the load-displacement behavior by approximately 25%.

In addition to this 'simplified' model, the embedded pile will be worked out more in "advanced" models in next chapter.

CHAPTER 4   VALIDATION OF THE EMBEDDED PILES FOR LATERAL LOADING IN PLAXIS 3D

4.1   Introduction and objectives

In the previous chapter the laterally loaded embedded pile is only validated by investigating the behavior of the surrounding soil in a 'simplified' model. Therefore this chapter continues to validate the embedded pile in "advanced" models, in which pile displacements and bending moments in the pile are examined. Furthermore in terms of this chapter, the lateral loading acting on the pile is classified into two causes of external forces and soil movements. For external forces (_section 4.2_), the embedded pile is validated by evaluating mesh dependence and comparing with the volume pile in the same test conditions. For soil movements (_section 4.3_), the validation of the embedded pile is made based on an extension of the example of the embankment constructed on soft soils by Brinkgreve (2007). The validation in this case requires the following aspects: evaluating the influences of pile locations, pile lengths, pile diameters and comparing with the volume pile. In brief, this chapter is structures as below:

+ _Section 4.2_ validates the embedded pile undergoing lateral loading caused by external forces;

+ _Section 4.3_ validates the embedded pile undergoing lateral loading caused by soil movements;

+ _Section 4.4_ draws the conclusions.

4.2   Validation of the PLAXIS embedded pile undergoing lateral loading caused by external forces

This section is structured with the following subsections:

• _Subsection 4.2.1_ introduces the PLAXIS model in which geometries, properties of the soil, properties of the pile and external forces are described;

• _Subsection 4.2.2_ validates the embedded pile by evaluating the influence of mesh coarseness;

• _Subsection 4.2.3_ validates the embedded pile by comparing with the volume pile in the same test conditions;

• _Subsection 4.2.4_ gives a short conclusion.

4.2.1   Introduction and Description

An imaginary example is simulated in PLAXIS 3D. The model geometry is created with dimensions of 20m in both X direction, Y direction and Z direction. The soil is assumed to have one layer in which the water level is at 1m below the ground surface. Because this test isn't aimed to pay attention on time-dependent behavior, the soil is modelled with MC model which has the material properties set up as in Table 4.1. The embedded pile is located at the origin of the coordinate system with the pile head at the ground surface. In addition, the pile has the dimensions of 0.7m in diameter & 10m in length and is assigned with the material properties as in Table 4.2. At the pile head, a point load of 1000 kN is applied in X direction. The overview of the model is shown in Figure 4.1.
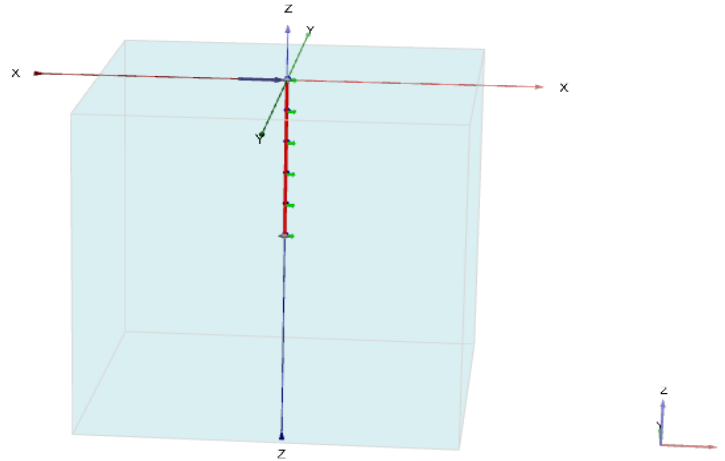
Figure 4.1 Model of the embedded pile subjected to the external force

Table 4.1 Mohr-Coulomb model property in PLAXIS 3D

Parameter	Name	Value	Unit
Material type	Type	MC	-
Drainage type	Type	Drained	-
Unit weight	γ_{unsat}	17	kN/m^3
	γ_{sat}	18	kN/m^3
Young's modulus	E'	10^4	kN/m^2
Poisson's ratio	ν'	0.3	-
Cohesion	c'	10	kN/m^2
Friction angle	φ'	30	^{0}
Dilatancy angle	ψ	0	^{0}
Tension cut-off	Selected	0	kN/m^2

Table 4.2 Properties of the Embedded pile in PLAXIS 3D

Parameter	Name	Value	Unit
Predefined pile type	-	Massive circular pile	-
Young's modulus	E	3.10^7	kN/m^2
Unit weight	γ	25	kN/m^3
Pile diameter	d	0.7	m
Pile area	A	0.3848	m^2
Inertia moment	I	0.01179	m^4
Maximum traction allowed at the pile top	$T_{top,max}$	200	kN/m
Maximum traction allowed at the pile bottom	$T_{bot,max}$	500	kN/m
Base resistance	F_{max}	10000	kN

4.2.2   Evaluation of mesh dependence

To perform Finite Element calculation, the model geometry has to be divided into elements. A composition of Finite Elements is called Finite Element mesh. In PLAXIS, the mesh coarseness is considered to have a significant influence on the calculation results. Furthermore, the mesh should be fine enough to get the accurate numerical analysis. In order to evaluate the mesh dependence, the model is implemented with five types of mesh coarseness ("Very Coarse" mesh, "Coarse" mesh, "Medium" mesh, "Fine" mesh and "Very Fine" mesh) which indeed result in different numbers of the generated mesh elements (see Table 4.3).

Table 4.3 Mesh generation

Type of mesh	Number of elements generated	Number of nodes generated
"Very Coarse"	10,342	16,237
"Coarse"	12,442	17,659
"Medium"	28,738	40,729
"Fine"	33,877	48,625
"Very fine"	88,906	125,760

In PLAXIS 3D, the test is implemented in two *calculation phases*. After the *Initial Phase* with K_0 procedure, the *First phase* is activated with the point load of 1000kN in X-direction at the pile head. The Figures and the Table below show the results on the lateral deformations at the pile head and the bending moments acting in the pile with different meshes. It can be seen that the model using the finer mesh gives more displacements and more bending moments, which is consistent with the mesh dependence. The difference in deformations at the pile head is about 20% when the mesh changes from *"very coarse"* into *"very fine"*, whereas the difference in bending moments is about 6%.

Table 4.4 Maximum pile head displacements and maximum bending moments in the pile

Types of mesh generation	Lateral displacement at the pile top U_x (m)	Maximum bending moment of the pile (kN.m)
"Very coarse"	0.172	1,884
"Coarse"	0.177	1,903
"Medium"	0.190	1,957
"Fine"	0.198	1.972
"Very fine"	0.208	1,999
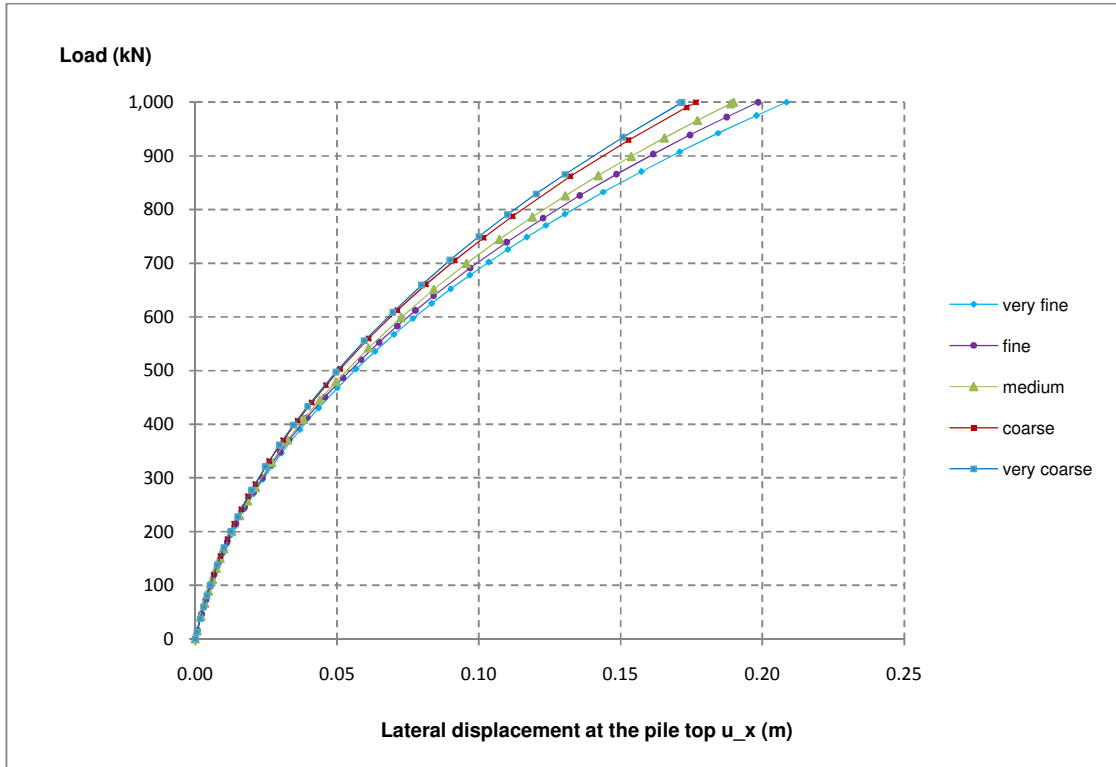
Figure 4.2 Load-displacement curves
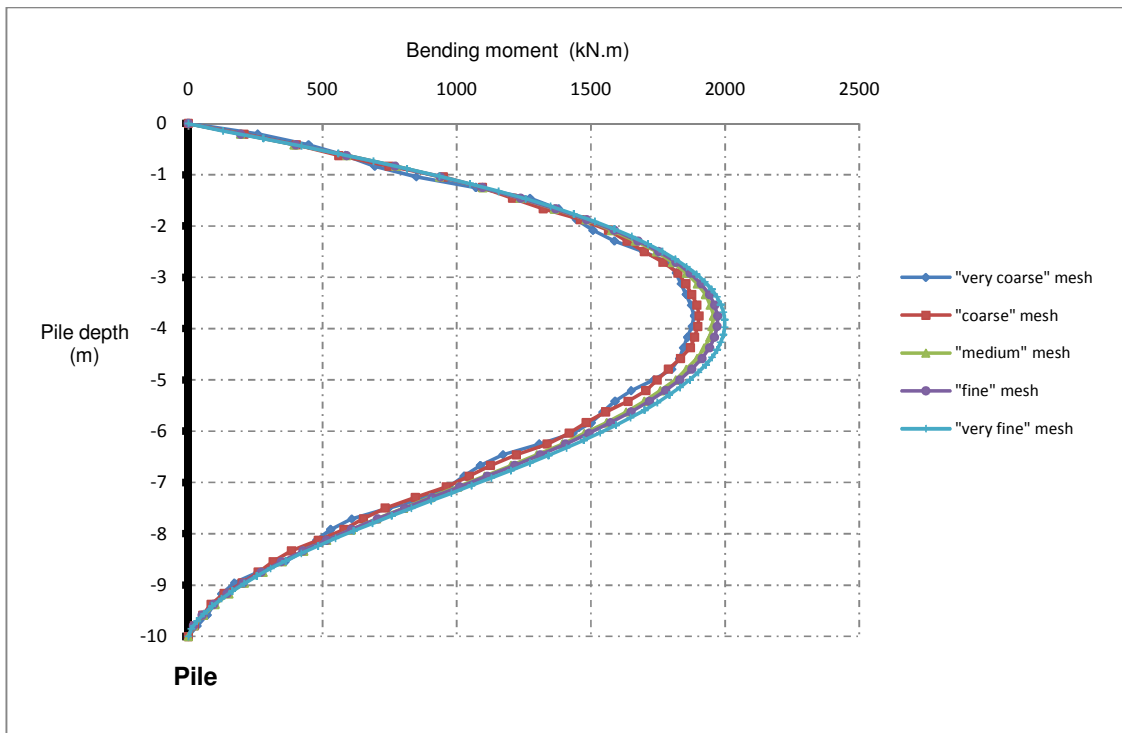
Figure 4.3 Distribution of bending moments along the embedded pile

4.2.3   Validation of the PLAXIS embedded pile by a comparison with the PLAXIS volume pile

In addition to the validation made by an investigation of mesh dependence, the embedded pile is also validated by a comparison with the volume pile. It should be noted that PLAXIS 3D allows to assign the interface around the volume pile shaft to model the pile-soil interaction and the strength of the interface is related to the strength of the surrounding soil by the *strength reduction factor R_{inter}*. Therefore in order to compare with the embedded pile, the volume pile is considered in both cases *"with"* interface around and *"without"* interface around. In addition to this main purpose, the part is secondarily aimed to consider the possibility of loss of contact between the volume pile and the surrounding soil near the ground surface. This may be interpreted that the surrounding soil close to the pile undergoing lateral loading is highly constrained at the front of the pile and stretched at the back of the pile where it has a tendency to break away from the pile.

This part is structured with following parts:

- Description of the model with the volume pile;
- Properties of the interface;
- Results of the comparison between the volume pile and the embedded pile.

4.2.3.1 Description of the model with the PLAXIS volume pile

In PLAXIS 3D, the volume pile may be created by two options. The first one relates to the use of "*Insert Solid*" function which allows to set up the shape and the location of volume structure. The second one relates to use the "*command box*" in which the volume pile is defined by *the length, the radius and the numbers of segments of the pile shaft*. Furthermore, in order to make a good comparison with the embedded pile model, the volume pile model needs to be created with the same test conditions of geometries and soil properties as the embedded pile model. In this case, the volume pile is set up with the dimensions of 0.7m in diameter, 10m in length (Figure 4.4) and the material properties as in Table 4.5.
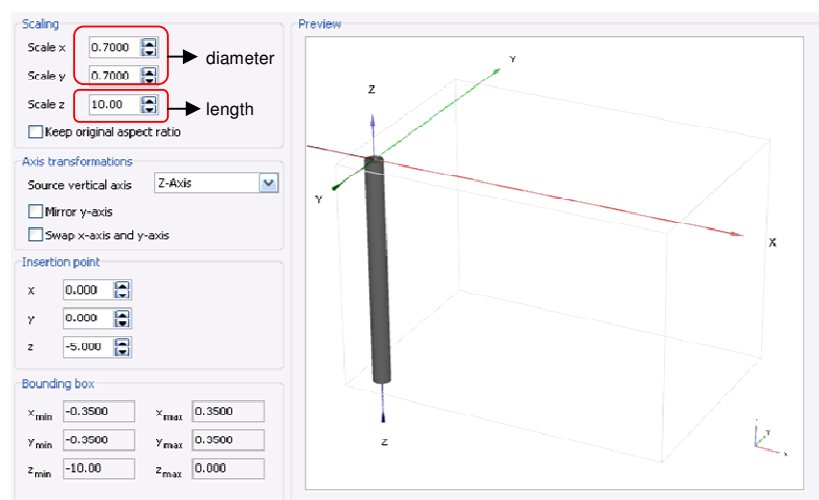
Figure 4.4 Dimension of Volume pile

Table 4.5 Input parameters of the PLAXIS volume pile

Parameter	Name	Value	Unit
Material model	-	Linear elastic	-
Drainage type	-	Non-porous	-
Unit weight	γ	25	kN/m^3
Young modulus	E	3.10^7	kN/m^2

It should be taken into account that Volume pile is created by volume elements with soil material, so it can't give results of force like the embedded pile. Therefore in order to investigate the results of force, a beam element is inserted at the axial axis of the volume pile. This beam is set up with the same material properties as the volume pile except for the E modulus which is 10^6 times lower than E modulus of the volume pile material (see Table 4.6). With this material set, the deformations of the beam will be as same as that of the volume pile. However, to obtain the actual bending moment in the volume pile, the bending moment of the beam in PLAXIS output has to be multiplied by a factor "10^6".

Table 4.6 Material properties of beam inside volume pile

Parameter	Name	Value	Unit
Cross-section area	A	0.3848	m^2
Unit weight	γ	25	kN/m^3
Young's modulus	E	30	kN/m^2
Inertia moment	I	0.01179	M^4

Moreover, to make the same condition of the lateral load at the pile head as the embedded pile, the volume pile is assumed to be subjected to a distributed load of 2598 KN/m^2 in X-direction at the pile top surface (see Figure 4.5 & Figure 4.6) which is equivalent to a point load of 1000kN at the top of the embedded pile.
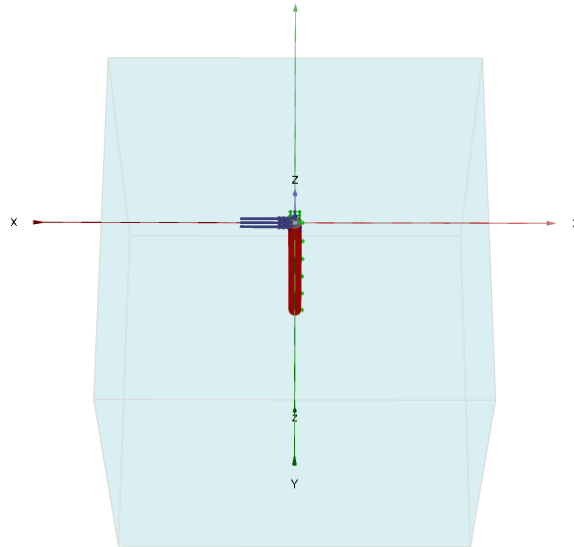
Figure 4.5 3_D view of the test of Volume pile in PLAXIS 3D

Volume pile in X-Y plane   Top surface of pile (X-Z plane)
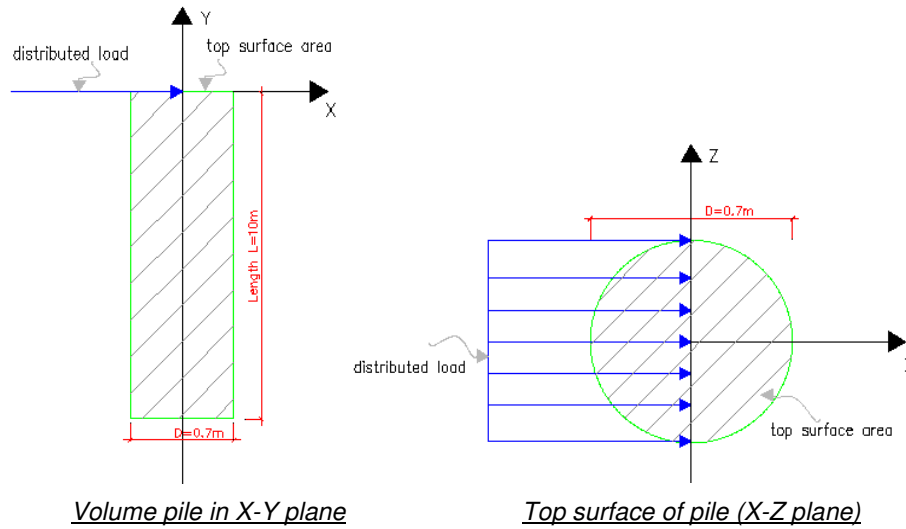
Figure 4.6 2D view of the volume pile model

Furthermore, similar condition of generated mesh between the two pile models has to be ensured for a good comparison between them. Therefore a *cylinder* which has the same dimension as the volume pile is created around the embedded pile. This cylinder is set up with the same material properties as the surrounding soil. In this test, at the default without mesh refinement, the embedded pile model with a cylinder around generates more mesh elements than the volume pile model with a beam inside. Therefore, the local mesh of the volume pile needs to be refined with *the fineness factor of 0.3*. As a result of mesh refinement, similar numbers of elements are obtained in both two models after the 'coarse' meshes are generated (13362 elements in the volume pile model and 13370 elements in the embedded pile model respectively) (see Figure 4.7).

Volume pile with the surface load   Embedded pile with the point load
(13362 mesh elements generated)   (13370 mesh elements generated)
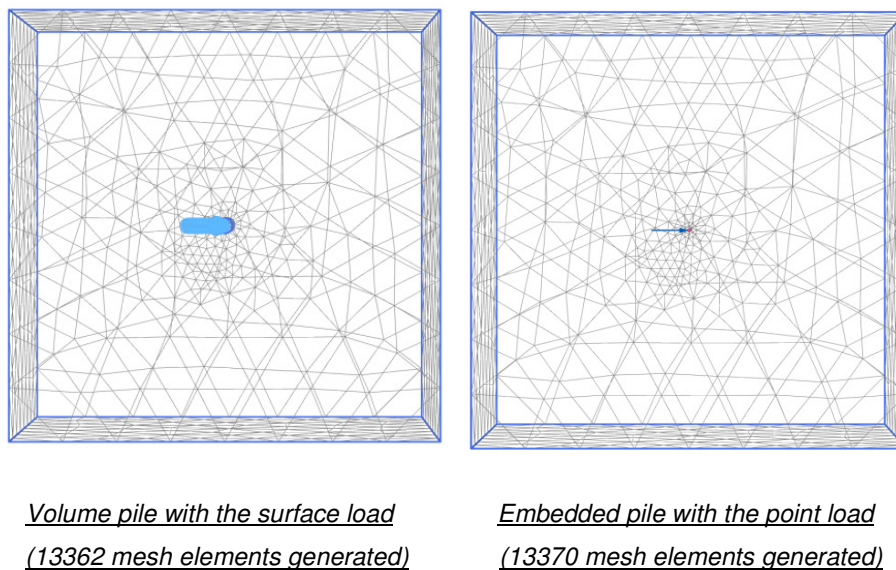
Figure 4.7 Top view of connectivity plot

4.2.3.2 Properties of interface

The property of the interface around the volume pile is related to the property of the surrounding soil by the *strength reduction factor R_{inter}*. Referenced from the *PLAXIS 3D Manual*, for real soil-structure interaction in general the interface is more flexible and weaker than surrounding soil which means R_{inter} should be less than 1.0. In this test, R_{inter} is assumed to be of the order of 2/3 (R_{inter}=2/3=0.67). By this value of R_{inter}, it is expected that the deformation of the volume pile 'with' the interface is larger than that 'without' interface.

In summary, the validation of the embedded pile is made by comparisons with the volume pile in both cases *'without'* the interface and *'with'* the interface whose strength is assumed regarding R_{inter} = 0.67.
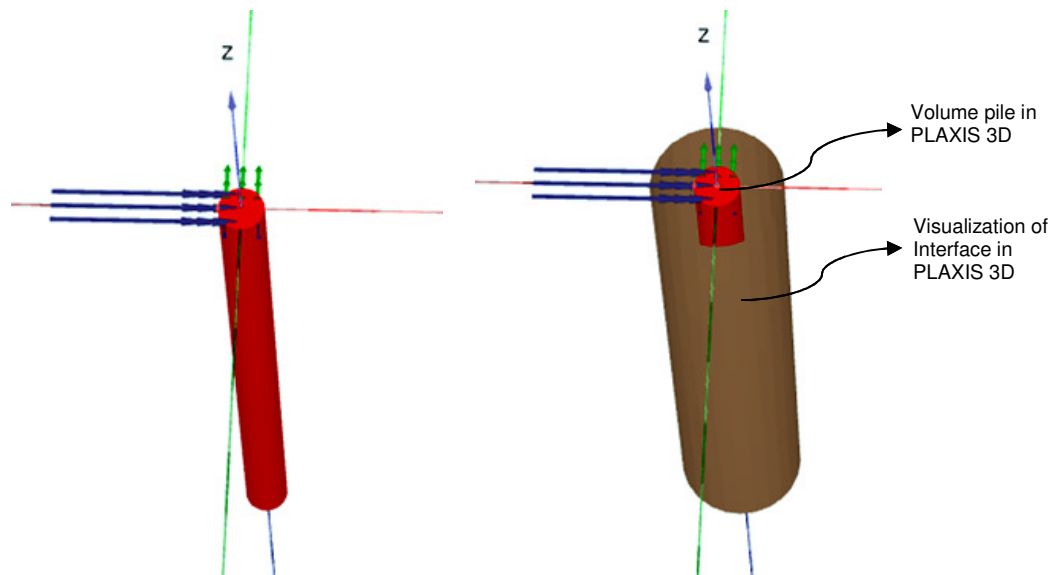
Without interface around volume pile shaft   *Interface around volume pile shaft*

Figure 4.8 Visualization of Volume pile 'with' and 'without' Interface around in Plaxis 3D

4.2.3.3 Results

Figure 4.9 shows the load-displacement behavior at the pile head. It can be seen that the behavior of the embedded pile looks more flexible than the behavior of the volume pile *'without'* interface and stiffer than the volume pile *'with'* interface having R_{inter}=0.67 (also see Table 4.7). From this identity, it may be predicted that the *strength reduction factor* can be used to control the better approximation between the embedded pile and the volume pile in terms of load-displacement behavior. Furthermore in Figure 4.10 which shows the distribution of bending moments along the pile, the behavior of the embedded pile and the volume pile *'without'* interface completely match. In short, the embedded pile is able to resemble the volume pile in the same test conditions.
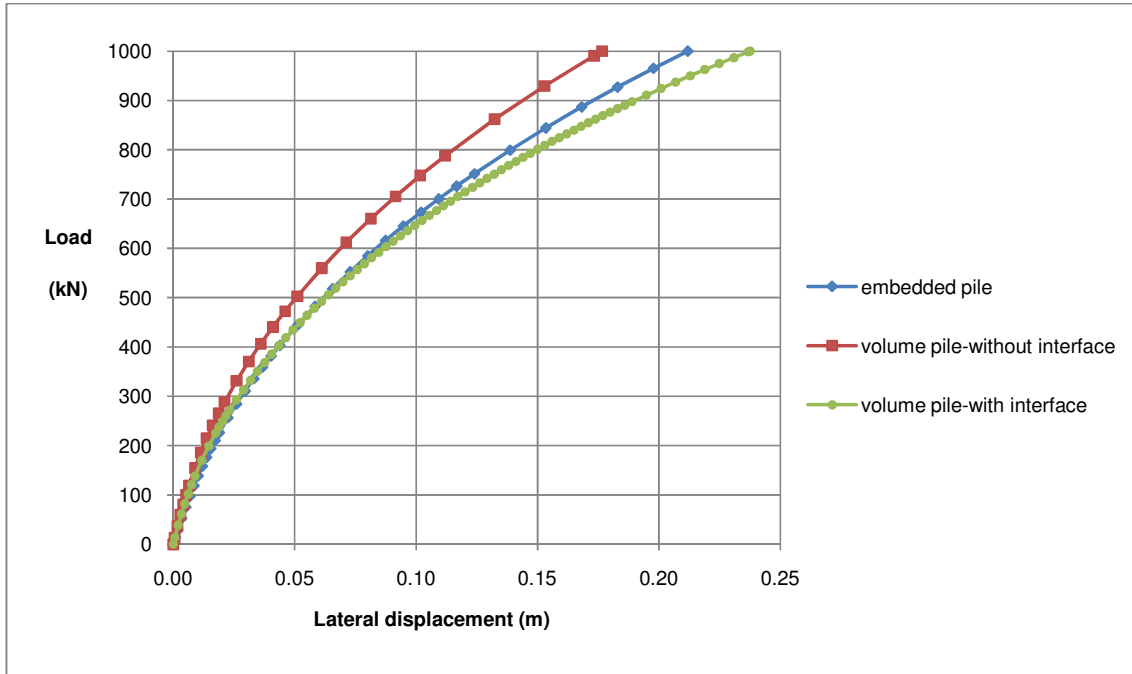
Figure 4.9 Load-displacement curves
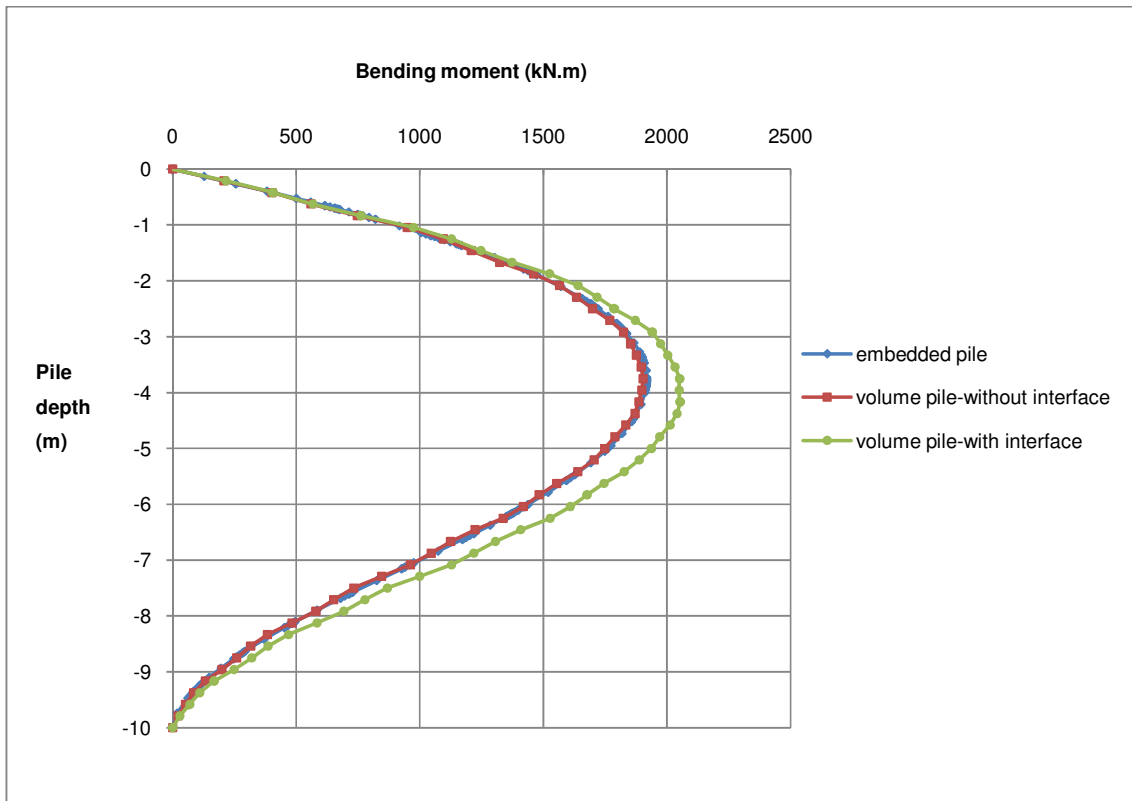
Figure 4.10 Distribution of bending moments along the pile

Table 4.7 Results of lateral displacements and bending moments of the piles

Pile type	Condition	Lateral pile head displacement (m)	Maximum bending moment (kN.m)
Embedded pile	-	0.212	1917
Volume pile	without interface	0.175	1913
	with interface R_{inter}=0.67	0.238	2054
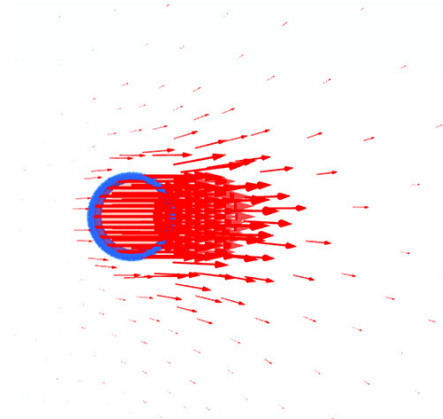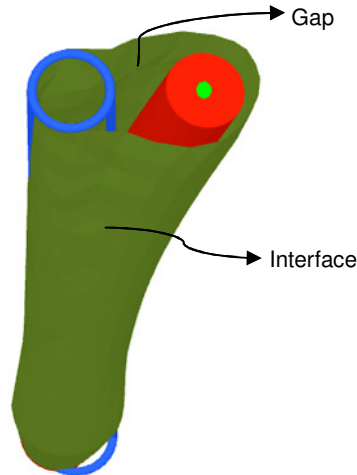
Figure 4.11a Gap at the back side   *Figure 4.11b Vector plot of total soil displacements*

Figure 4.11 Visualization of the gap at the back-side of the volume pile

Moreover, the volume pile model with the interface around may be used to simulate a 'gap' at the back of the pile (see Figure 4.11). It can be interpreted that when the lateral load applied to the pile increases, the soil at the front of the pile is in compression and the soil at the back of the pile is in tension. In this test, the surrounding soil is modelled with MC model in which, by default, the *tension cut-off* is applied with the tensile strength equal to zero. Therefore, the tensile strength of the soil at the back is unable to take any further tension that leads to open up a 'gap' at the back of the pile.

4.2.4   Summary

The validation on the embedded pile undergoing lateral loading caused by external forces was described above. A clear indication is that the finer mesh results in the more displacements and bending moments. Therefore, it can be concluded that the embedded pile is in good agreement regarding mesh dependence. Besides, when comparing with the volume pile in the same test conditions, the results show that the embedded pile is able to resemble the volume pile. In addition the value of *the strength reduction factor* (R_{inter}) of the interface has a significant influence of bending moments and displacements in the volume pile model.

4.3 Validation of the PLAXIS embedded pile undergoing lateral loading caused by soil movements

After validating the embedded piles undergoing lateral loading caused by external forces, the validation is extended to the cause of soil movement in an embankment application. In this part, the example of the construction of an embankment on soft soil by Brinkgreve (2007) is considered to be simulated in PLAXIS 3D. The part is structured as below:

- *Subsection 4.3.1* gives a summary of the example by Brinkgreve (2007) in which the results of a numerical study on the construction of an embankment on soft soil is simulated in PLAXIS 2D. Then an extension of the example simulated by means of PLAXIS 3D is described;
- *Subsection 4.3.2* validates the embedded pile by evaluating the influences of pile locations, pile lengths and pile diameters;
- *Subsection 4.3.3* validates the embedded pile by comparing with the volume pile in the same test situations;
- *Subsection 4.3.4* gives a brief summary.

4.3.1 Introduction and Description

The example by Brinkgreve (2007) gives an imaginary situation of an embankment constructed on 10m thick soft soil layer which has a phreatic level 1m below ground surface (see Figure 4.12).
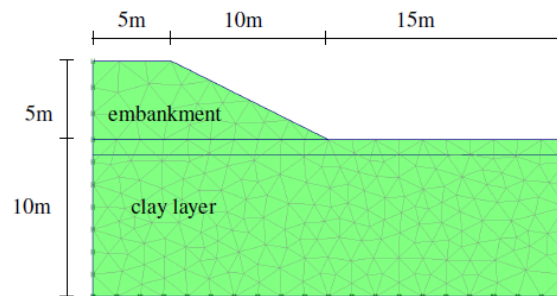
Figure 4.12 Embankment on soft soil (Brinkgreve 2007)

The clay layer is modelled with the SSC model and the embankment is modelled with the MC model as in Table 4.8 & Table 4.9. The test is implemented in two *calculation phases* which are defined as consolidation analysis. The *first phase* involves the staged construction of the full embankment in 100 days. The *second phase* involves 900 days of creep behavior. The purpose of this test is to take into account the settlement of the ground surface and the horizontal displacement of the embankment toe as a function of time. In addition, from the example Brinkgreve gave a conclusion about the influence of two parameters, which are K_0^{nc} determined by the M-parameter and OCR, on the ground surface settlement under the embankment and the lateral displacement of the embankment toe. The variations of the parameters are considered in Table 4.10.

Table 4.8 Soil properties of soft clay

Parameters	Name	Value	Unit
Material type	Type	SSC	-
Drainage type	Type	Undrained	-
Unsaturated unit weight	γ_{un}	15	kN/m^3
Saturated unit weight	γ	18	kN/m^3
Permeability	k	0.01	m/day
Cohesion	c	1	kN/m^2
Friction angle	φ	25	^{0}
Dilatancy angle	ψ	0	^{0}

Table 4.9 Properties of embankment

Parameter	Name	Value	Unit
Material type	Type	MC	-
Drainage type	Type	Drained	-
Unit weight	γ	20	kN/m^3
Permeability	k	1	m/day
Young's module	E	5000	kN/m^2
Poisson ratio	ν	0.3	-
Friction angle	φ	30	^{0}
Cohesion	c	1	kN/m^2

Table 4.10 Variation of M and OCR in SSC model
(Brinkgreve 2007)

Model 3	Model 5	Model 6	Model 7
SSC	SSC	SSC	SSC
$\lambda^*=0.1$	$\lambda^*=0.1$	$\lambda^*=0.1$	$\lambda^*=0.1$
$k^*=0.02$	$k^*=0.02$	$k^*=0.02$	$k^*=0.02$
$\mu^*=0.004$	$\mu^*=0.004$	$\mu^*=0.004$	$\mu^*=0.004$
$\nu_{ur}=0.15$	$\nu_{ur}=0.15$	$\nu_{ur}=0.15$	$\nu_{ur}=0.15$
M=0.99	M=1.36	M=0.99	M=1.36
OCR$_0$=1.0	OCR$_0$=1.0	OCR$_0$=1.3	OCR$_0$=1.3
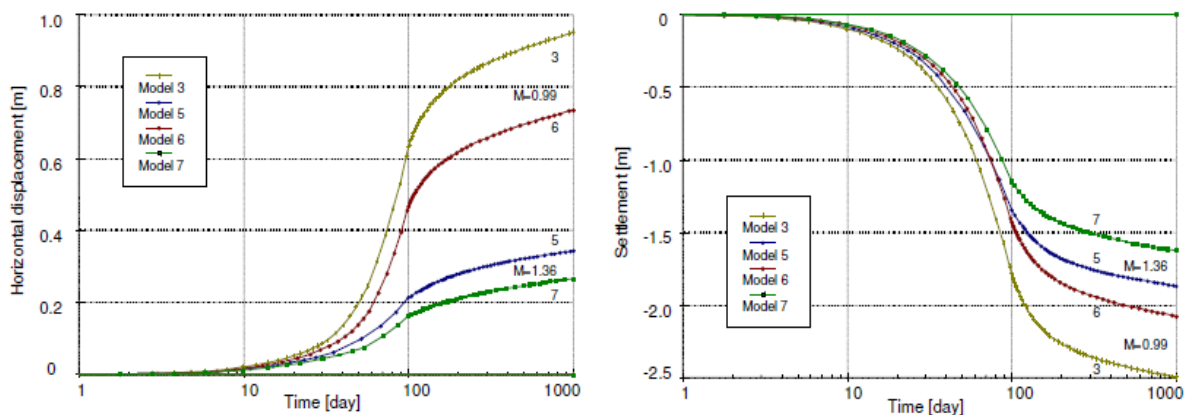
Figure 4.13 Horizontal Displacement of embankment toe and Surface settlement under embankment
(Brinkgreve 2007)

Table 4.10 presents different values of M-parameter and OCR-parameter which are applied in the SSC models namely model 3, 5, 6 & 7 in order to evaluate their influences on the soil displacements. From the calculation results shown in Figure 4.13, it can be seen that the higher value of the M-parameter (which means the lower value of the K_0^{nc}-parameter) results in less surface settlements and less lateral displacements at the embankment toe.

It can be recognized that the example by Brinkgreve (2007) is a good reference for the research of the pile undergoing lateral soil movements induced by the construction of embankment on soft soil. Therefore a new model is implemented in PLAXIS 3D by using the same test conditions of soil properties, calculation phases taken from the example. In addition, for the purpose of validating the embedded piles, the new model is added with two embedded piles which are located at 1m and 6m away from the embankment toe. The material properties of the embedded piles are set up with *the stiffness E=30.10^6 kN/m^2 and the unit weight γ=25 kN/m^3*. The model geometry is shown in Figure 4.14 & Figure 4.15.
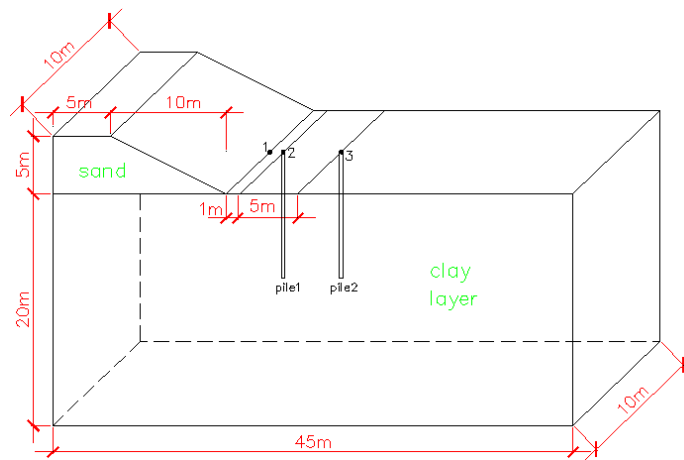
Figure 4.14 Geometry of the model
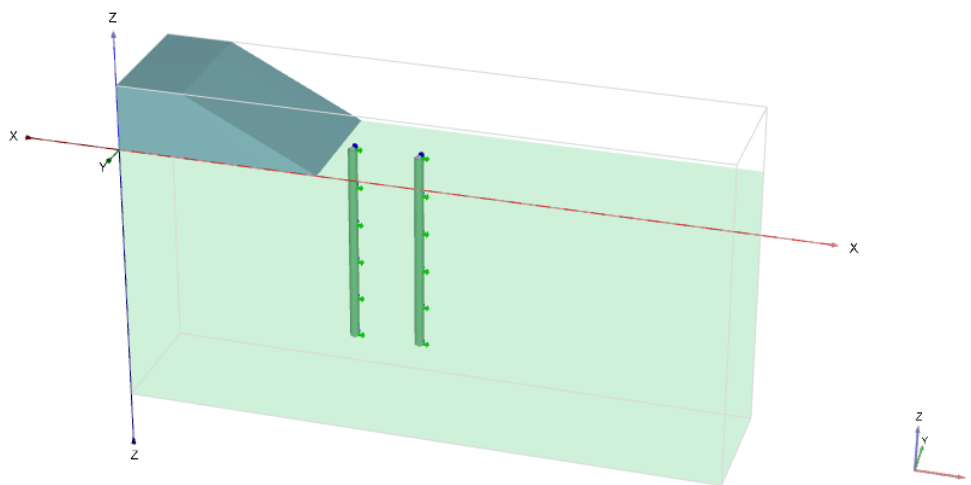
Figure 4.15 Visualization of the PLAXIS model of the embankment construction.

Table 4.11 and 4.12 show the input properties of the sand embankment and the soft clay layer. It should be taken into account that in terms of this analysis, the SSC model applied for clay layer is set up with the certain conditions of $K_0^{nc} = 0.72$ (M=0.9885) and OCR = 1.3. Furthermore, to neglect the mesh dependence, all tests will be implemented in the same *'medium'* mesh generation.

Table 4.11 Properties of the soft clay layer

Parameter	Name	Value	Unit
Material model	Model	SSC	-
Drainage type	Type	Undrained	
Modified compression index (lamda*)	λ^*	0.1	-
Modified swelling index (kappa*)	k^*	0.02	-
Modified creep index	μ^*	0.0004	-
Poisson ratio for unloading/reloading	ν_{ur}	0.15	-
Cohesion	c'	1	kN/m^2
Friction angle	φ'	25	^{0}
Dilatancy angle	ψ	0	^{0}
Horizontal/Vertical stress ratio in normally consolidated 1D compression	K^0_{nc}	0.72	-
Horizontal permeability	k_h	0.01	m/day
Vertical permeability	k_v	0.01	m/day
Over-consolidation ratio	OCR	1.3	-
Pre-overburden pressure	POP	0	-
Unit weight	γ_{unsat}	15	kN/m^3
	γ_{sat}	18	kN/m^3

Table 4.12 Properties of the embankment sand

Parameter	Name	Value	Unit
Material model	Model	MC	-
Drainage type	Type	Drained	-
Unit weight	γ_{unsat}	20	kN/m^3
	γ_{sat}	20	kN/m^3
Young's modulus	E'	5000	kN/m^2
Poisson's ratio	ν'	0.3	-
Cohesion	c'	1	kN/m^2
Friction angle	φ'	30	^{0}
Dilatancy angle	ψ	0	^{0}
Horizontal permeability	k_h	1	m/day
Vertical permeability	k_v	1	m/day

4.3.2   Validation of the PLAXIS embedded pile by evaluating the influence of pile location, pile length and pile diameter

4.3.2.1 Evaluation of the influence of pile location

In order to evaluate the influence of pile locations, two piles are installed at the locations of 1m and 6m away from the embankment toe (Figure 4.16). Both of them are set up with the same diameter of 0.3m and length of 15m.
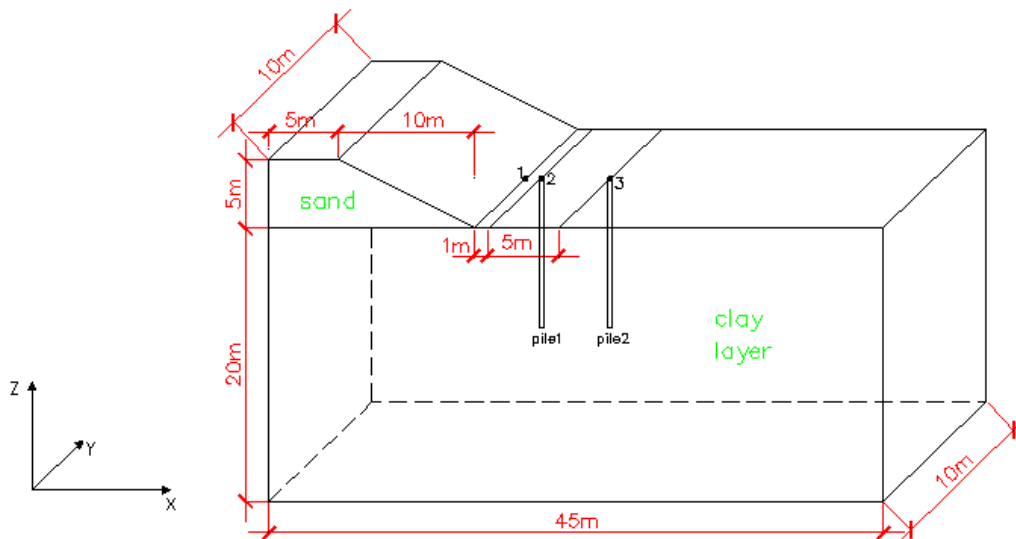
Figure 4.16 Locations of the embedded piles in the model

In this test, three points (1, 2 and 3) are considered as reference points for the investigation of the lateral displacements; point 1 (x=15m, y=5m, z=0m) is located at the embankment toe; point 2 (x=16m, y=5m, z=0m) and point 3 (x=21m, y=5m, z=0m) is at the top of the 'near' pile and the 'far' pile respectively.

Figure 4.17 shows a comparison of lateral displacements as a function of time. The similarity in shapes of three curves is meant that the lateral displacements of the pile tops almost follow the lateral soil surface displacements at the embankment toe. It may be concluded that the embedded pile shows a good performance in evaluating the influence of pile locations which is *"the closer pile is, the more lateral pile displacement"*. Furthermore, it's interesting to consider from Figure 4.18 that, in addition to the lateral displacement, pile 1 is also bended under lateral soil movements.
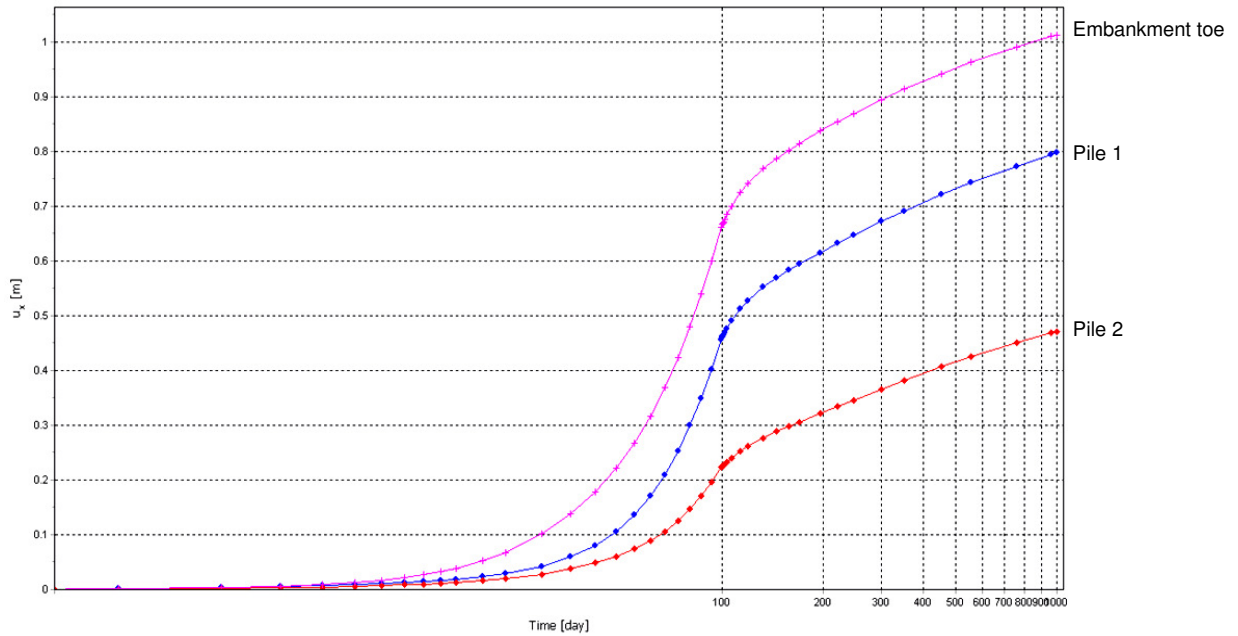
Figure 4.17 Lateral displacement u_x (m) at the embankment toe and the embedded pile tops
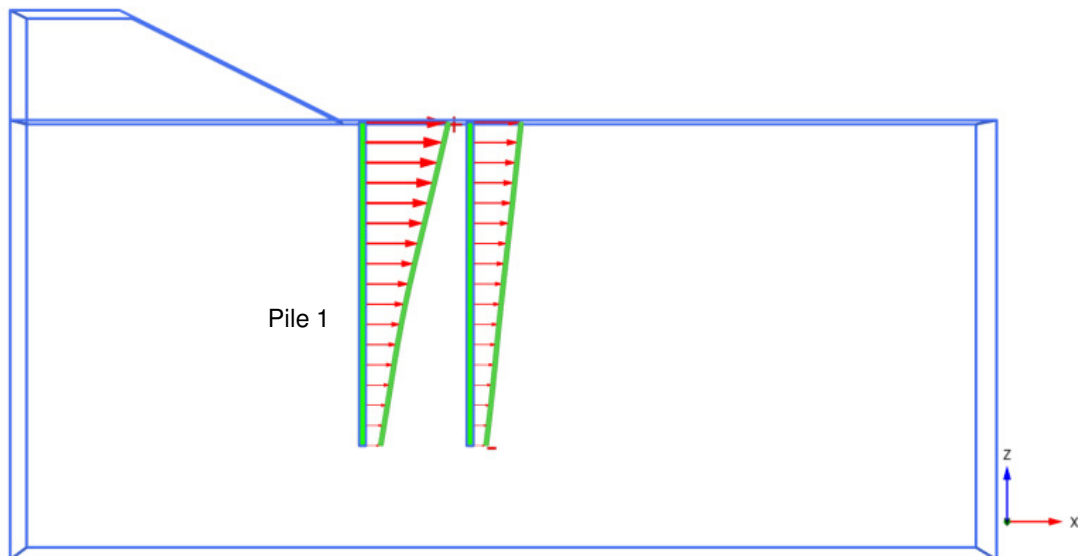
Figure 4.18 Visualization of the bending of Pile 1

4.3.2.2 Evaluation of the influence of pile length

To validate the embedded pile by evaluating the influence of the pile length embedded in the subsoil, only *pile 1* is selected for examining the results of the lateral pile top displacements and the bending moments in the pile. The pile whose length varies from 10m to 15m (L=10m, 11m, 12m, 13m, 14m, 15m) is tested under the same conditions. The reference time is at the end of the first phase of 100 days in consolidation analysis.

Figure 4.19 shows a comparison of the distribution of bending moments along the pile at the end of the first phase. It can be seen that the maximum bending moments in the pile increase with increasing

pile depth. However, it looks like that the increases of maximum bending moments are not linear with the increases of the pile depth (Figure 4.20) and the maximum bending moments increase very slightly when the pile depth is larger than 13m. The interpretation for these results may be made based on the distribution of soil displacements along the pile (Figure 4.21). It can be considered that there is less lateral soil movement subjecting to the deeper part of the pile. In addition, the range of the pile depth from L=13m to L=15m is in the same range of lateral soil displacements that leads to the similar bending moments in the piles. In brief, by the consistency of bending moments in the pile found in this case, it can be said that the embedded pile is good in agreement with the evaluation of the influence of pile length.
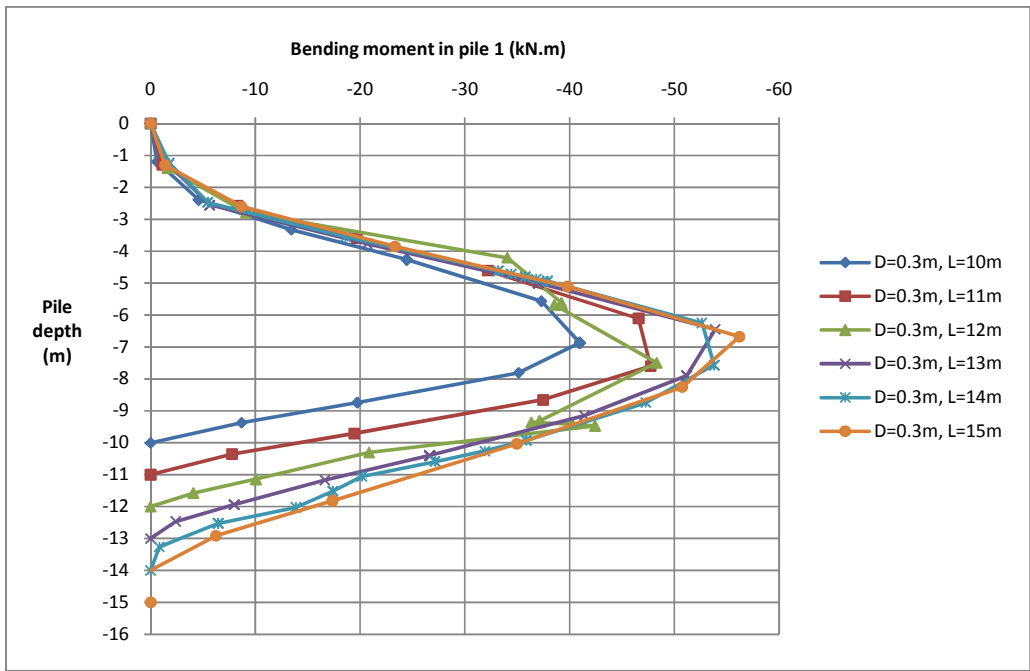
Figure 4.19 Distribution of bending moments along the pile (influence of pile depth)
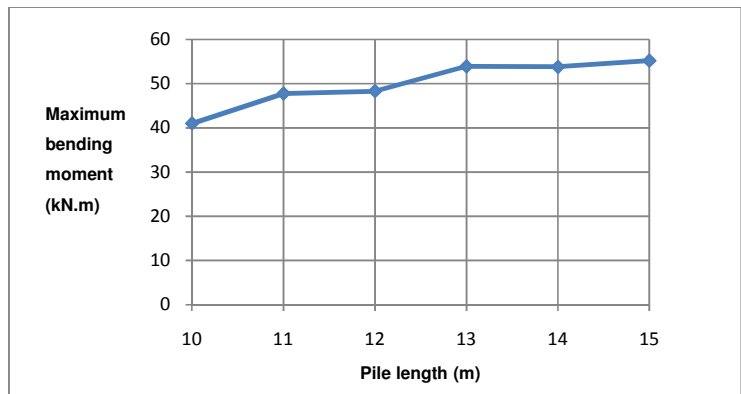
Figure 4.20 Maximum bending moment vs Pile length
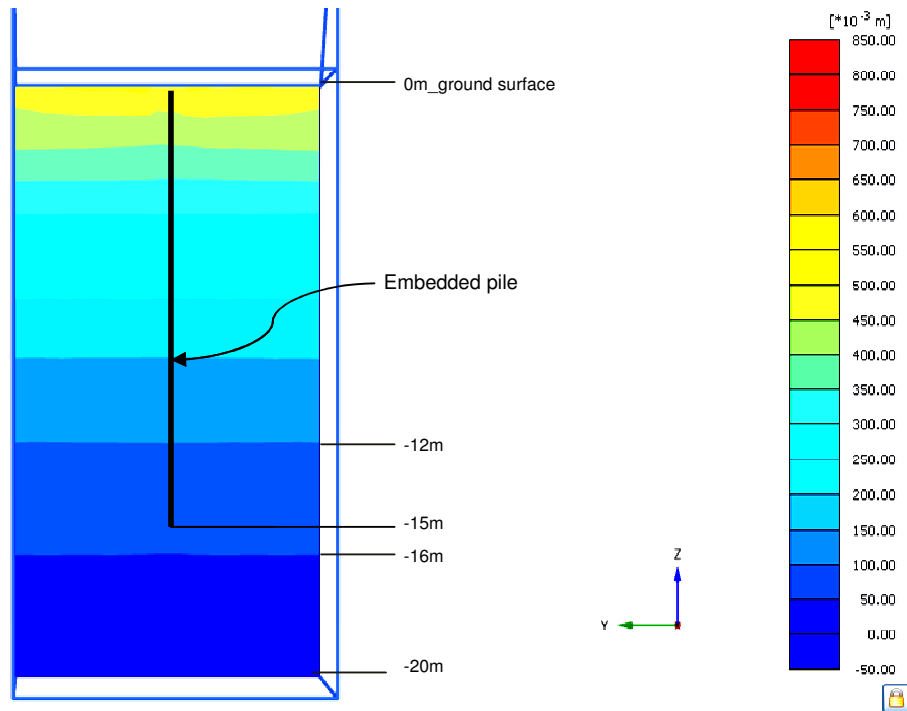
Figure 4.21 Distribution of lateral soil displacements with depth (PLAXIS 3D Output)

4.3.2.3 Evaluation of the influence of pile diameter

In order to validate the embedded pile by evaluating the influence of pile diameter, again *pile 1* is selected for examining the results of the lateral pile top displacements and the bending moments in the pile. The pile whose diameter varies from 0.2m to 0.5m (D=0.2m, 0.3m, 0.4m, 0.5m) is tested under the same conditions. The reference time is at the end of the first phase of 100 days in consolidation analysis.

Figure 4.22 shows the distribution of bending moments along the pile. It can be seen that the shapes of profiles are similar with the variations of pile diameter, but magnitude increases with increasing pile diameter. In addition, Figure 4.23 displays the pile head deflections with different diameters. It is clearly seen that with the same lateral soil movements, the pile head deflection decreases with increasing diameter.
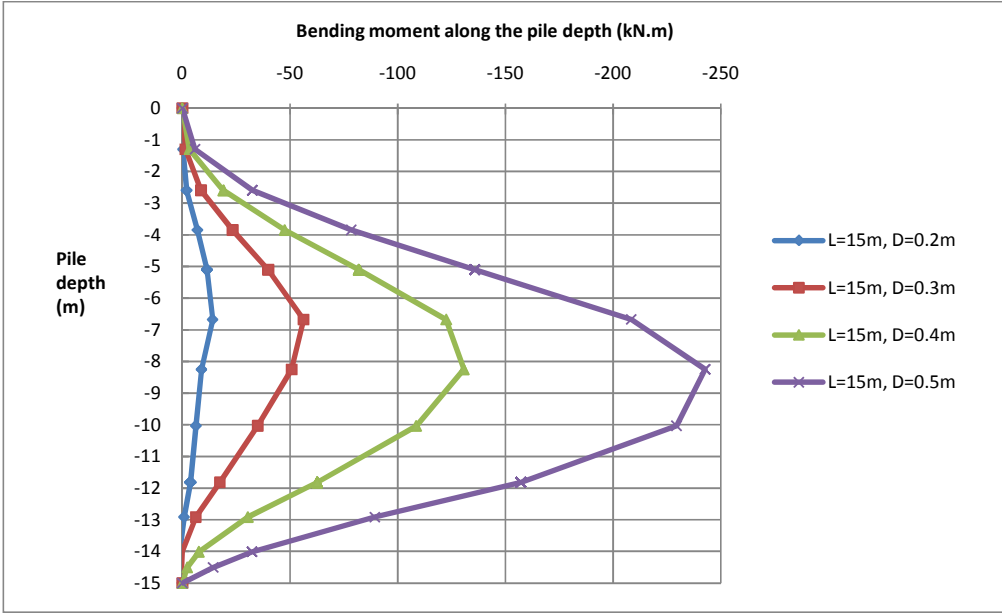
Figure 4.22 Distribution of bending moments along the pile (influence of pile diameter)
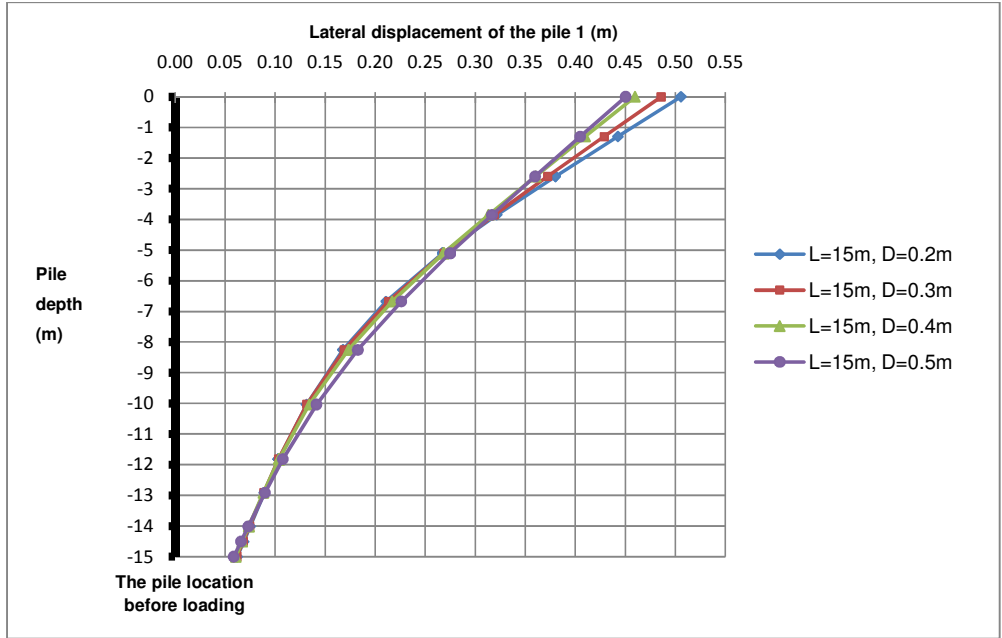
Figure 4.23 Lateral displacement u_x of the pile vs the pile depth

The interpretation for the results displayed in the Figures above may be made based on the Formula (4.1) and (4.2). It is clearly seen that the bending moment M is directly proportional with the pile diameter D and the lateral displacement is inversely proportional with D^3. In short, the consistency of distributions of bending moments and lateral pile head displacements in terms of varying the pile diameter can be found in the embedded pile model.

$$M = \frac{1}{\beta}.f.D.\sigma_{xx}.L^2_{pile} \tag{4.1}$$

$$u = \frac{\alpha.f.D.q.L^4_{pile}}{384.EI} = \frac{\alpha.f.D.q.L^4_{pile}}{384.E\frac{\pi.D^4}{64}} = \frac{\alpha.f.D.q.L^4_{pile}}{384.E\frac{\pi.D^4}{64}} = \frac{\alpha.f.q.L^4_{pile}}{6.E.\pi.D^3} \tag{4.2}$$

Where, D = pile diameter

α = factor, depending on stiffness and fixation pile head

f = shell factor (1.5 to 2.5)

q = uniform distributed load on the pile shaft

L_{pile} = pile length

E = modulus of elasticity of the pile

I = moment of inertia of the pile: $I = \frac{\pi.D^4}{64}$ (4.3)

σ_{xx} = lateral soil pressure on the pile shaft

β = depends on fixation of the pile ($\beta = 8 \div 10$)

4.3.3   Validation of the PLAXIS embedded pile by a comparison with the PLAXIS volume pile

In order to validate the embedded pile undergoing lateral soil movements by a comparison with the volume pile with a "soft" beam inside, the volume pile needs to be created with the same properties as the embedded pile (The way of making the volume pile with a "soft" beam inside was already elaborated in *part 4.2.3.1*). In this case, the volume pile is assumed to have a length of 15m & a diameter of 0.3m and have material properties of the *stiffness E=30.10^6 kN/m^2* & the *unit weight γ=25 kN/m^3*. Besides, it is necessary to ensure the similar mesh coarseness for a good comparison between the two pile models. Therefore *a cylinder* which has the same dimension with the volume pile is inserted around the embedded pile. In this test, the mesh in the cylinder is refined with *the fineness factor* of 0.3. As a result of mesh refinement, the generated meshes in the model with volume pile and in the model with embedded pile have 13190 elements and 13283 elements respectively.

Figure 4.24 shows a comparison of lateral displacements at the pile top as a function of time for both the 'near' pile and the 'far' pile. In general, the embedded pile is able to give lateral pile head displacements comparable to the volume pile. It can be seen that during the 100day-phase of increasing the embankment load, the behavior of the embedded pile matches with the behavior of the volume pile. However in the 900day-phase of creep behavior, the embedded pile predicts slightly higher displacements than the volume pile.

Figure 4.25 shows a distribution of bending moments along the pile at the end of 900 day-consolidation phase. It can be seen that the embedded pile is in good agreement with the volume pile. Nevertheless, there is a deviation between the embedded pile and the volume pile in both cases of

the 'near' pile and the 'far' pile, in which the embedded pile has a trend of underestimation of the bending moments.

In short, it can be concluded that the embedded pile is able to resemble the volume pile in the situation of being subjected to lateral soil movements induced by the construction of an embankment on soft soils.
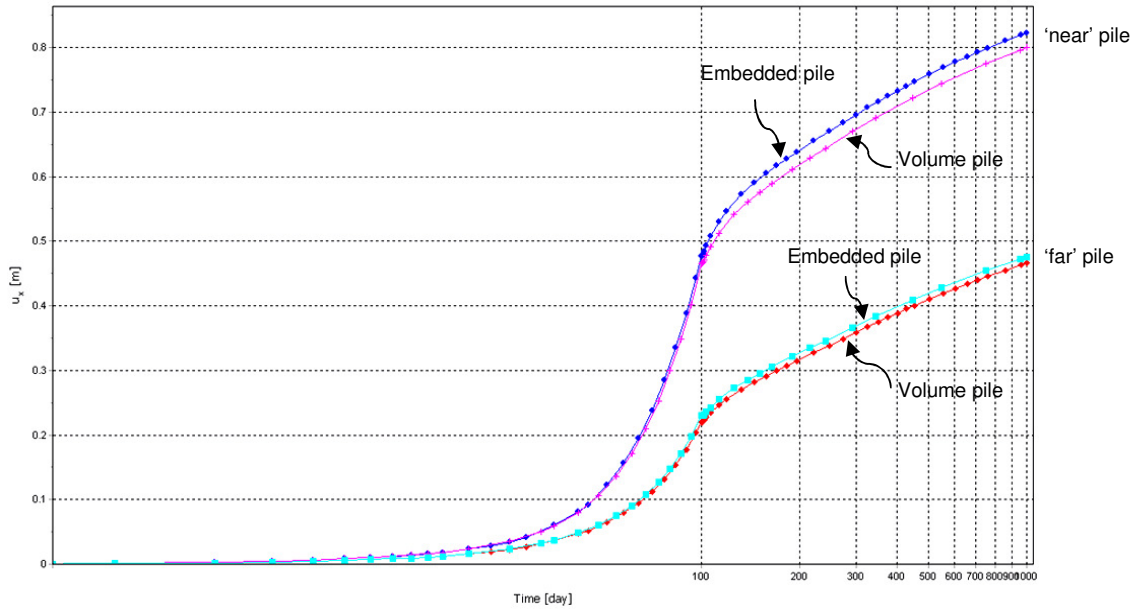
Figure 4.24 Lateral displacements at the pile top as a function of time
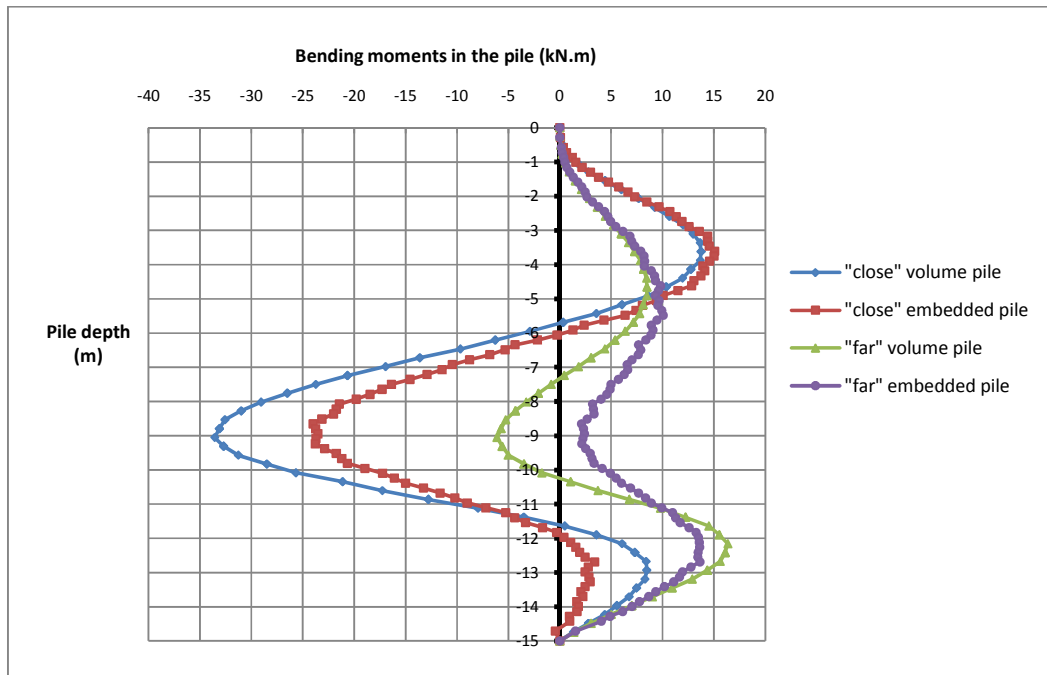
Figure 4.25 Distribution of bending moments in the pile

4.3.4 Summary

The embedded pile undergoing lateral soil movements was validated by evaluating the influences of pile properties and comparing with the volume pile.

➢ For the evaluation of the embedded pile properties, the following considerations were drawn:

- The lateral pile head displacement almost follows the lateral soil surface displacement and the "near" pile gives more displacements than the "far" pile;

- The "long" pile gives larger bending moments than the "short" pile. Furthermore, the increase of pile diameter results in the increase of maximum bending moments in the pile and the decrease of pile head displacements.

➢ For the comparison with the volume pile, in term of lateral pile head displacement the embedded pile completely matches with the volume pile during the loading phase and gives slightly higher predictions toward the later consolidation phase. On the other hand, the embedded pile has a trend to overestimate the bending moments in both cases of the 'near' pile and the 'far' pile. However it can be concluded that the embedded pile is able to resemble the volume pile.

In summary, the consistency which was found from the above results concludes that the embedded pile shows a good performance in the situation of being subjected to lateral soil movements induced by the construction of an embankment on soft soil. Such validation is very helpful for the interpretation of the results of further embankment applications shown in the following parts.

4.4   Conclusion

This chapter presented the validation of the embedded pile subjected to lateral loading caused by external forces as well as soil movements. Some conclusions were drawn as below:

➢ For external forces, the validation was made by evaluating the influence of mesh dependence as well as comparing with the volume pile. It can be seen that the finer mesh results in the more displacements and bending moments. Therefore, it can be concluded that the embedded pile is in good agreement regarding mesh dependence. Besides as a result of comparing with the volume pile, it is observed that the embedded pile is able to resemble the volume pile behavior. In addition, the value of the *strength reduction factor (R_{inter})* of the interface around the volume pile has a significant influence on both bending moments in the pile and pile head displacements

➢ For soil movements, the validation was made by evaluating the influence of pile properties and comparing with the volume pile. The following points were considered:

- In the part of evaluating the pile properties, it can be considered that the "near" pile gives more lateral displacements at the pile head than the "far" pile. Furthermore, the increases of maximum bending moments in the pile are caused by the increases of pile length or pile diameter.

- In the part of comparing with the volume pile, in term of lateral pile head displacement the embedded pile completely matches with the volume pile during the loading phase and gives slightly higher predictions toward the later consolidation phase. On the other hand, the embedded pile has a trend to overestimate the bending moments in both cases of the 'near' pile and the 'far' pile.

In brief, it is clearly observed that the embedded pile shows a good performance in situation of undergoing lateral loads. Furthermore, the validation of the embedded will be extended by a comparison with measurements as shown in the following chapter.

CHAPTER 5   VALIDATION OF THE PLAXIS EMBEDDED PILE BY COMPARISONS WITH MEASUREMENTS (CASE STUDY "CENTRIFUGEPROEF GEODELFT")

5.1   Introduction and Objectives

Before reaching the objectives of this chapter, it is useful to review the previous chapters. As mentioned in Chapter 2, the situation of the pile subjected to lateral soil movements has been conducted by different researchers and different methods, but many uncertainties still remain. Therefore, more experimental tests and in-situ tests should be worked out to get insight in the performance of the laterally loaded pile. Subsequently, Chapter 3 paid attention to the evaluation of the PLAXIS embedded pile undergoing lateral loading in a 'simplified' model. In this chapter, the evaluation was made by investigating the behavior of the surrounding soil as well as a comparison with a volume pile in terms of surrounding soil displacements and stress distributions. Based on the results obtained, it can be concluded that the embedded pile is not only good in simulating the laterally loaded pile, but also able to resemble the volume pile behavior. Chapter 4 showed the validation of the laterally loaded embedded pile caused by external forces as well as soil movements in 'advanced' models. In this chapter, the validation was made by investigating the pile displacements and bending moments in the pile. By the consistency in the results obtained from the PLAXIS model with the embedded pile, it can be concluded that the embedded pile shows a good performance in case of undergoing lateral load. Such a validation is very helpful for the interpretation for the results of a case study which will be shown in this chapter.

In brief, it can be recognized that the previous chapters only validated the PLAXIS embedded pile loaded laterally in imaginary models. Therefore in order to increase the reliability of the validation, this chapter mainly validates the PLAXIS embedded pile undergoing lateral soil movements by a comparison with measurements from a real test as well as with the PLAXIS volume pile. In addition to the validation of the embedded pile, an evaluation of the SSC model by a comparison of soil displacements with measured data is also considered as the secondary purpose of this chapter.

A real test named "Centrifugeproef GeoDelft" is chosen for the comparison between the *PLAXIS 3D model* using the embedded pile and a *real situation*. The centrifuge test involved a model pile adjacent to an embankment construction. The pile was strain gauged to record the bending moments acting in the pile. The construction of an embankment was carried out sequentially and the bending moments in the pile were measured at each stage. It's expected that the embedded pile will be able to resemble the real behavior.

It should be noted that this chapter is aimed to validate the PLAXIS embedded pile by a comparison with measured data, thus the details of the real centrifuge test will not be paid much attention. However, the general description of the centrifuge test will also be shown in order to help the reader to get the main points which will be used in the PLAXIS model. In short, the chapter is structured as below:

- *Section 5.2* gives a general description of the centrifuge test.
- *Section 5.3* describes the simulation of the centrifuge test in PLAXIS 3D using the embedded pile.
- *Section 5.4* describes the validation of the embedded pile by a comparison with the measurements.
- *Section 5.5* describes the evaluation of the SSC model by a comparison with the measurements.
- *Section 5.6* recalculates the PLAXIS model of the centrifuge test using the Soft Soil (SS) model.
- *Section 5.7* gives conclusions.

5.2   General description of the "Centrifuge test"

5.2.1   Geometry and Properties

In the centrifuge test, a "model box" with dimensions of 850mm long x 450mm wide x 200mm high was used. At the box bottom, a 50mm thick sand layer considered as Pleistocene sand was made. Subsequently, a 100mm thick clay layer composed of Speswhite clay was added above the sand. Because the centrifuge test was simulated with a scale of 1:100 it means that 1mm in the centrifuge test model corresponds to 100mm in "reality". Figure 5.1 shows the cross-section of the centrifuge model with a scale of 1:100.
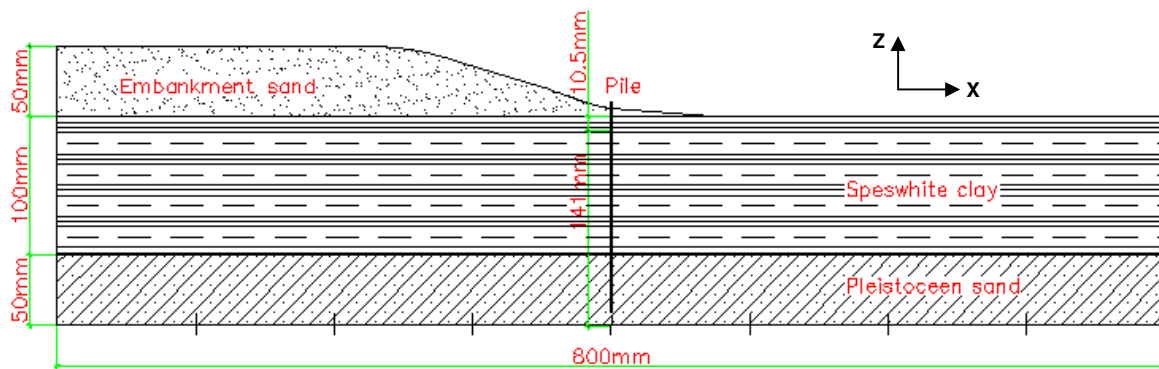
Figure 5.1 Cross section of centrifuge model with a scale of 1:100

The water level was at the ground surface. A pile was installed at the location of 400mm in X-direction. The pile had length of 151.5mm with 10.5mm above the ground surface. The model pile has a diameter of 5mm which was equivalent to a diameter of 500mm in "reality". The pile head was connected to a frame work. It should be reminded from the chapter of literature review that the condition of the pile head connection has a significant influence on the distribution of bending moments in the pile as well as on the pile head displacements. However in this test the detail of the connection at the pile head was not clearly described which makes it difficult to simulate the test in PLAXIS 3D later (more details of this connection in the PLAXIS model will be described in *part 5.3.1*). Furthermore, with reference to the properties of the model pile in the centrifuge test with a scale of

1:100, the parameters that will be applied for the pile in the PLAXIS model are summarized as in Table 5.1.

Table 5.1 Property of the pile in PLAXIS model

Parameter	Name	Value	Unit
Pile length	+ above ground surface L_a	1.05	m
	+ below ground surface L_b	14.1	m
Pile diameter	d	0.5	m
Elastic modulus	E	2.66×10^7	kN/m^2

In the centrifuge test, soil displacements and bending moments in the pile were measured at several locations where gauge instruments were applied. However this part isn't aimed to mention all of them, but some typical points whose measured results will be used to compare with the results from PLAXIS model are shown in the scheme below
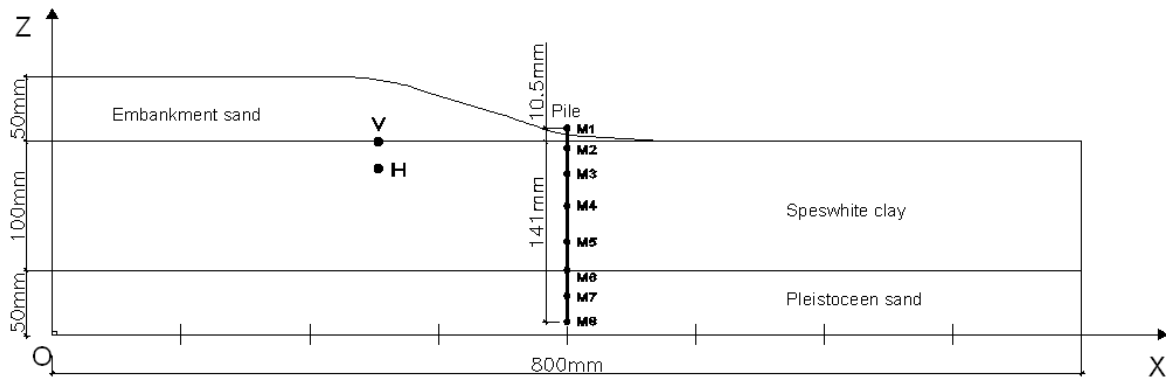
Figure 5.2 Scheme of measured points (XZ plane)

The locations of these points in XZ plane are as in Table 5.2

Table 5.2 Locations of measured points

Measurement	Point	X-direction (mm)	Z-direction (mm)
Vertical soil displacement	V	+250	+150
Horizontal soil displacement	H	+250	+135
Bending moments of pile	M1	+400	+160.5
	M2	+400	+145
	M3	+400	+125
	M4	+400	+100
	M5	+400	+72
	M6	+400	+50
	M7	+400	+35
	M8	+400	+9

5.2.2   Construction phases of the centrifuge test

Before creating the embankment, the model pile was installed at a location of X=400mm as in Figure 5.1. The sand embankment in the centrifuge test was constructed in five phases composed of "adding" and "consolidating". In the first phase, a 18mm thick sand layer was added and then consolidated in 7 days. Successively, 8mm thick sand layers were added to create the total thickness of 50mm. The construction phases are summarized in Table 5.3.

Table 5.3 Construction phases of the centrifuge test

Phase	Description	Increase of embankment thickness (mm)	Total embankment thickness (mm)	Time increment Δt (day)	Total time T (day)
1	- Install the pile	0	0	0	0
2	- 1st layer of sand: added	18	18	0	0
3	- 1st layer of sand: consolidated	0	18	7	7
4	- 2nd layer of sand: added	8	26	0	7
5	- 2nd layer of sand: consolidated	0	26	35	42
6	- 3rd layer of sand: added	8	34	0	42
7	- 3rd layer of sand: consolidated	0	34	84	126
8	- 4th layer of sand: added	8	42	0	126
9	- 4th layer of sand: consolidated	0	42	245	371
10	- 5th layer of sand: added	8	50	0	371
11	- 5th layer of sand: consolidated	0	50	210	581

5.2.3   Results of measurements

The centrifuge test provided the measured data for the pile as well as for the soil at the end of each consolidation phases. More details of measured data of bending moments in the pile as well as soil displacements are shown in *Appendix A*.

5.3   Simulation of the centrifuge test in PLAXIS 3D

5.3.1   Geometry and Properties

In PLAXIS 3D, the model geometry is made with the dimensions of 85m in X-direction, 45m in Y-direction and 20m in Z-direction. The soil has a thickness of 15m and consists of 5m sand layer below & 10 m clay layer above. The phreatic level is at the original ground surface. The embedded pile is located at the point (X=40m, Y=22.5m and Z=0m) which is adjacent to the embankment toe. The embedded pile has a length of 15.15m & a diameter of 0.5m and the pile top is at 1.05m above the ground surface. The overview of the model is shown in Figure 5.3.
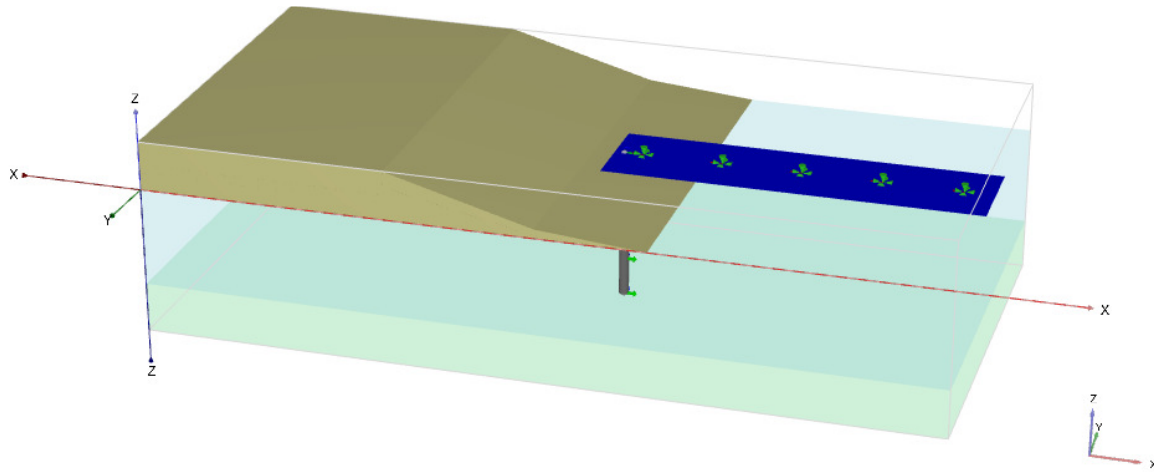
Figure 5.3 Visualization of the model in PLAXIS 3D

The connection at the pile head was not clearly described in the real centrifuge test, thus to create the same condition of this connection in PLAXIS 3D is difficult. Therefore different models of the pile head connection were tried to find out the best way in which the embedded pile is able to give the best approach of the real pile behavior in terms of the distribution of bending moments along the pile. Finally, the best approach could be obtained when the pile head is assumed to be fixed in X direction and Y direction and free to move in Z direction. To create this fixity in X and Y direction, the PLAXIS model is added with a very stiff plate with the *Young's modulus E=3.10^7 kN/m^2*, in which *the surface prescribed displacements* in X direction and Y direction have to be fixed. The plate has one side connecting to the pile head and the other side connecting to the model boundary in order to ensure that the pile head is totally fixed in these directions.

On the other hand, the clay layer is modelled with the SSC model which will later be evaluated (see Table 5.4) and the sand layer is modelled with the MC model (see Table 5.5). The sand embankment is modelled with the MC model which has the material properties as in Table 5.6. Furthermore, the material of the embedded pile is set up as in Table 5.7.

_Remark__:_ It should be noted that the parameters of the soils used in this model are taken to be the same as in the report of the real centrifuge test *"Centrifugeproeve GeoDelft"* without further evaluation.

Table 5.4 Properties of the clay layer

Parameter	Name	Value	Unit
Material model	Model	SSC	-
Drainage type	Type	Undrained	
Modified compression index (lamda*)	λ^*	0.085	-
Modified swelling index (kappa*)	k^*	0.022	-
Modified creep index	μ^*	0.00013	-
Poisson ratio for unloading/reloading	ν_{ur}	0.2	-
Cohesion	c'	0.5	kN/m^2
Friction angle	φ'	22	^{0}
Dilatancy angle	ψ	0	^{0}
Horizontal/Vertical stress ratio in normally consolidated 1D compression	K^0_{nc}	0.64	-
Horizontal permeability	k_h	0.0004	m/day
Vertical permeability	k_v	0.0002	m/day
Over-consolidation ratio	OCR	1.3	-
Pre-overburden pressure	POP	20	-
Unit weight	γ_{unsat}	16.2	kN/m^3
	γ_{sat}	16.2	kN/m^3

Table 5.5 Properties of the sand layer

Parameter	Name	Value	Unit
Material type	Type	MC	-
Drainage type	Type	Drained	-
Unit weight	γ_{unsat}	18	kN/m^3
	γ_{sat}	20	kN/m^3
Young's modulus	E'	7.5×10^4	kN/m^2
Poisson's ratio	ν'	0.3	-
Cohesion	c'	0.1	kN/m^2
Friction angle	φ'	35	^{0}
Dilatancy angle	ψ	0	^{0}
Horizontal permeability	k_h	1	m/day
Vertical permeability	k_v	1	m/day

Table 5.6 Properties of the embankment sand

Parameter	Name	Value	Unit
Material model	Model	MC	-
Drainage type	Type	Drained	-
Unit weight	γ_{unsat}	17	kN/m^3
	γ_{sat}	19	kN/m^3
Young's modulus	E'	10,000	kN/m^2
Poisson's ratio	ν'	0.3	-
Cohesion	c'	0.1	kN/m^2
Friction angle	φ'	42	^{0}
Dilatancy angle	ψ	3	^{0}
Horizontal permeability	k_h	1	m/day
Vertical permeability	k_v	1	m/day

Table 5.7 Properties of the embedded pile

Parameter	Name	Value	Unit
Predefined pile type	-	Massive circular pile	-
Young's modulus	E	2.66×10^7	kN/m^2
Unit weight	γ	0	kN/m^3
Pile diameter	d	0.5	m
Pile area	A	0.1963	m^2
Inertia moment	I	0.003068	m^4
Skin resistance type	Type	Linear	-
Maximum traction allowed at the pile top	$T_{top,max}$	200	kN/m
Maximum traction allowed at the pile bottom	$T_{bot,max}$	500	kN/m
Base resistance	F_{max}	10000	kN

5.3.2 PLAXIS calculation phases

The determination of calculation phases in PLAXIS 3D is based on the construction phases in the real centrifuge test which were already shown in Table 5.3. It should be noted that when the *SSC model* or a *Consolidation analysis* is used in PLAXIS, the time intervals set up for the *PLAXIS calculation phases* have to be larger than zero. However in the real centrifuge test, the *"adding"* phase is conducted with the time interval of 0 day that can't be worked in *PLAXIS calculations*. Therefore, in order to define the phases of *"adding"* embankment sand in the PLAXIS model, the time intervals are assumed to be equal to 0.5 day instead of 0 day as in the real test. For example, the PLAXIS simulation of the phases of *"adding"* and *"consolidating"* the first embankment sand layer is modified with the time intervals of 0.5 day for *"adding"* and 6.5 day for *"consolidating"* respectively. With this modification, the PLAXIS model has the same total time of calculation phases as the real centrifuge test. In addition, in order to make the overview of PLAXIS calculation phases, Figure 5.4 describes the relationship between the total thickness of embankment and the total calculation time.
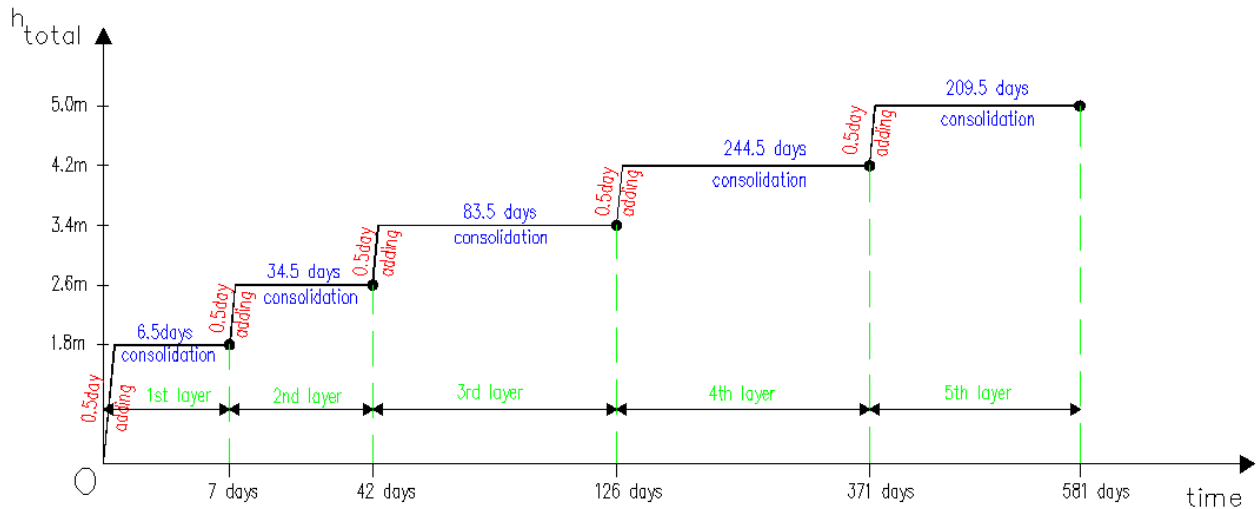
Figure 5.4 Scheme of the calculation time of the model

On the other hand, the *"adding"* phase is defined as *a plastic undrained analysis* and the *"consolidating"* phase is defined as *a consolidation analysis*. The details of the calculation phases in PLAXIS 3D are summarized in Table 5.8.

Table 5.8 Calculation phases of the model in Plaxis 3D

Phase No.	Description	Increase of embankment thickness (m)	Total embankment thickness (m)	Time increment Δt (day)	Total time T (day)	Calculation analysis type
0	Initial phase	0	0	0	0	K_0
1	Install the pile	0	0	0.5	0.5	Plastic undrained
2	- 1st layer of sand: added	1.8	1.8	0.5	1	Plastic undrained
3	- 1st layer of sand: consolidated	0	1.8	6.5	7.5	Consolidation
4	- 2nd layer of sand: added	0.8	2.6	0.5	8	Plastic undrained
5	- 2nd layer of sand: consolidated	0	2.6	34.5	42.5	Consolidation
6	- 3rd layer of sand: added	0.8	3.4	0.5	43	Plastic undrained
7	- 3rd layer of sand: consolidated	0	3.4	83.5	126.5	Consolidation
8	- 4th layer of sand: added	0.8	4.2	0.5	127	Plastic undrained
9	- 4th layer of sand: consolidated	0	4.2	244.5	371.5	Consolidation
10	- 5th layer of sand: added	0.8	5.0	0.5	372	Plastic undrained
11	- 5th layer of sand: consolidated	0	5.0	209.5	581.5	Consolidation

5.3.3   Results from PLAXIS 3D

Different from the real centrifuge test which only gives the measured data at the end of each *consolidation phase*, PLAXIS provides the estimations of the bending moments in the pile, the horizontal soil displacements and settlements as a function of time. Therefore, the full behavior of the piles as well as the soils can be investigated. *Appendix B* shows more details of the PLAXIS results.

**5.4	Validation of the PLAXIS embedded pile**

**5.4.1	Validation of the PLAXIS embedded pile by a comparison with measurements**

In this part, the validation of the embedded pile is made by a comparison of the bending moments in the pile with the measured data. Furthermore, it should be taken into account that the comparison is only examined at the end of each *consolidation phase.*

The results of the comparison are displayed as *"bending moment-depth"* graphs which are shown in Figure 5.5. In general, the similarity in shapes between *PLAXIS curves* and *measurement curves* shows that the PLAXIS embedded pile is able to give bending moments comparable to the results provided by the measurements. Nevertheless, there are remarkable deviations from the real test curves. In fact, it can be seen that the PLAXIS embedded pile has a trend to overestimate bending moments in the pile at the *early consolidation phases* and to underestimate them at the *later consolidation phases*. The best approximation can be found at the *"middle" phase* (corresponding to the 3rd *consolidation phase*) (see Figure 5.5c).

In addition to the general consideration, it's also noteworthy to compare between the PLAXIS embedded pile and the real test pile in more details at each *consolidation phase.* For this purpose, three points on the pile which show the maximum values of bending moments are investigated. They are at the pile head, at around the middle of clay layer and at around the interface between two different layers.

For the pile head, maximum difference in the bending moments is found especially at the *first and the second consolidation phase* (Figure 5.5a & Figure 5.5b), in which the PLAXIS embedded pile predicts the bending moments around *a factor 2* higher than the measured data. However, the approximation between the embedded pile and the real pile becomes better towards the *later consolidation phases.* In fact, at *the fourth and the fifth consolidation phase* the embedded pile is in very good agreement with the real pile behavior (Figure 5.5d & Figure 5.5e).

For the middle of the clay layer as well as the interface between two layers, the embedded pile gives a remarkable underestimation of bending moments towards *the later consolidation phases*. It can be seen at *the fifth consolidation phase* (Figure 5.5e) that, the embedded pile predicts the bending moments approximately 50% lower than the measurements. In addition, the same trend of predictions can be seen at *the fourth consolidation phase* (Figure 5.5d), where an underestimation of around 46% and 41% on the bending moments compared to the real test can be found at around the middle of the clay layer and around the interface between two layers respectively.
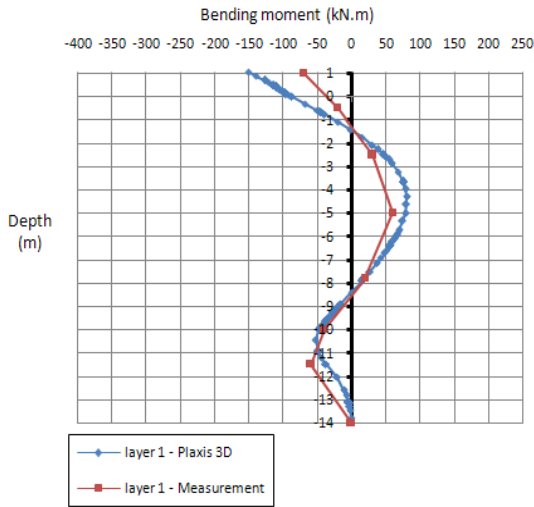
Figure 5.5a Bending moment-depth (layer 1)
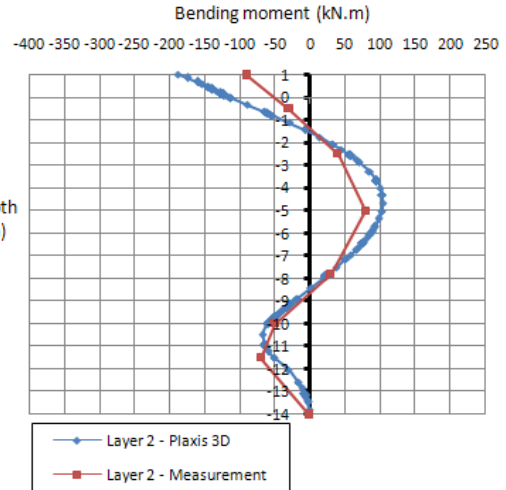
Figure 5.5b Bending moment-depth (layer 2)
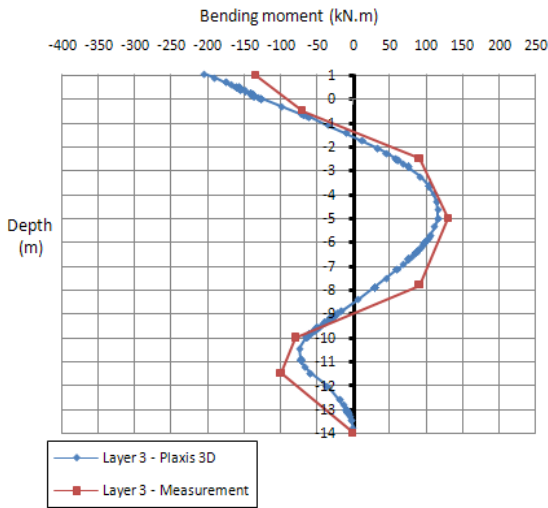
Figure 5.5c Bending moment-depth (layer 3)
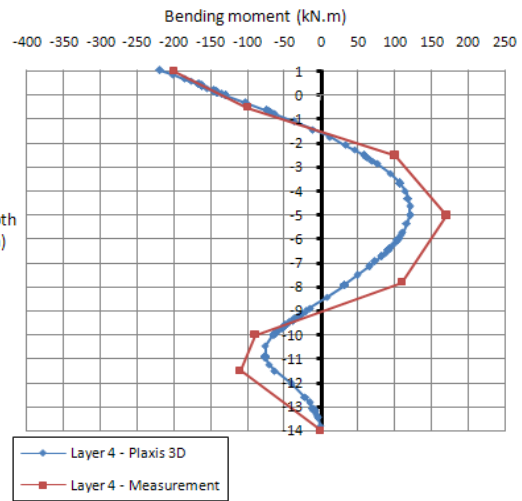
Figure 5.5d Bending moment-depth (layer 4)
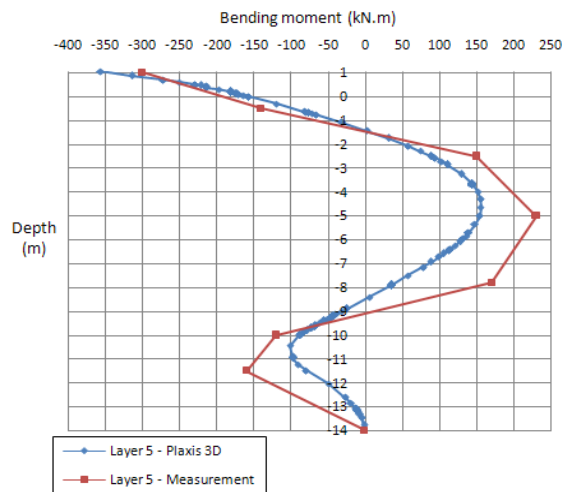
Figure 5.5e Bending moment-depth (layer 5)

Figure 5.5 Distribution of bending moments along the pile

5.4.2   Validation of the PLAXIS embedded pile by a comparison with the PLAXIS volume pile

In order to validate the embedded pile by a comparison with the volume pile, the volume pile needs to be created with the same properties as the embedded pile (the way of making the volume piles in PLAXIS 3D was already elaborated in *part 4.2.3.1*). For this purpose, the volume pile is set up with the material parameters as in Table 5.9. Besides, to make a realistic comparison it is necessary to ensure similar mesh coarseness between them. In fact, the generated mesh elements in the model with the volume pile and the model with the embedded pile are 15601 elements and 15495 elements respectively. With the same test conditions, it's expected that the embedded pile is able to resemble the volume pile behavior.

Table 5.9 Input parameters of the volume pile set up in Plaxis 3D

Parameter	Name	Value	Unit
Material model	-	Linear elastic	-
Drainage type	-	Non-porous	-
Young modulus	E	2.66×10^7	kN/m^2
Poisson's ratio	ν	0.15	-
Length	L	15.15	m
Diameter	D	0.5	m

Figure 5.6 shows the distribution of bending moments along the pile at the end of *each consolidation phase*. It can be seen that although the embedded pile predicts slightly lower bending moments than the volume pile, generally the embedded pile is in good agreement with the volume pile. The small difference between them regarding the bending moments in the piles may be caused from the small difference in the generated mesh.
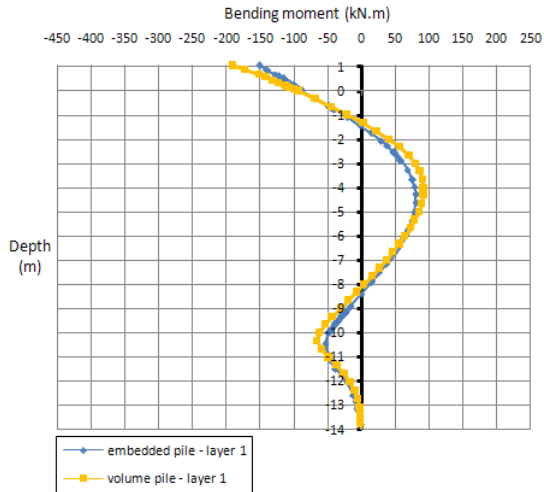
Figure 5.6a After 1st consolidation phase
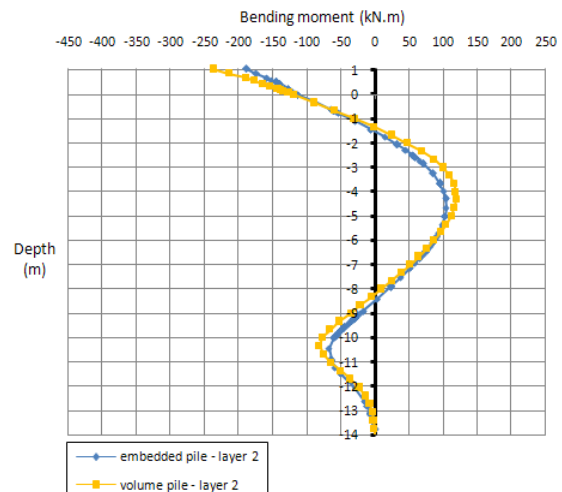
Figure 5.6b After 2nd consolidation phase
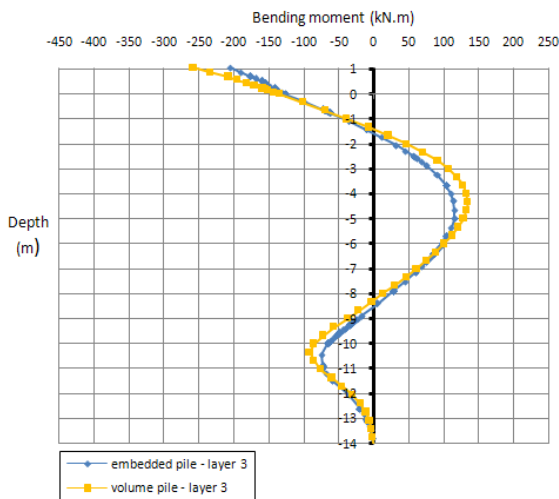
Figure 5.6c After 3rd consolidation phase
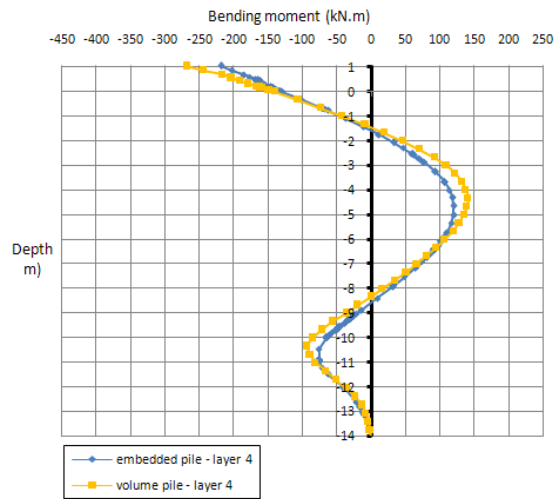
Figure 5.6d After 4th consolidation phase
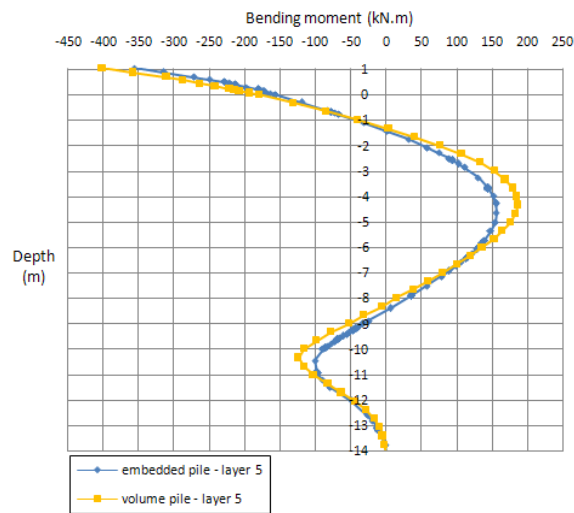
Figure 5.6e After 5th consolidation phase

Figure 5.6 Distribution of bending moments along the pile

5.5 Evaluation of the SSC model by a comparison with measurements

In this part, the evaluation of the SSC model applied for the clay layer is made by a comparison of the settlements and the horizontal soil displacements the measured data.

Remark: The centrifuge test only provided measured data of the soil displacements at the end of *each consolidation phase*, while Plaxis 3D presents the soil displacements as a function of time. Therefore, for the purpose of the comparison of the soil displacements between the *PLAXIS model* and the *real test*, the separate measured points obtained from the real test have to be connected to formulate the *Measurement curve* whose shape may be comparable to the *PLAXIS curve.*

Figure 5.7 shows the developments of surface settlements under the embankment at a point (X=25m) as a function of time (logarithmic). The similarity in the shapes of two curves shows that the SSC model is generally able to resemble the real soil behavior. However, there is a deviation of the surface settlements from the real soil. It can be seen that the SSC model has a trend of overestimating settlements before the end of *the third consolidation phase* and underestimating towards *the later consolidation phases*. The maximum difference between two curves can be found at the end of *the fourth consolidation phase*, in which the SSC model predicts the settlements approximately 20% lower than the real soil. However, a good agreement with the real soil behavior is revealed at the end of *the third and the fifth consolidation phase.*
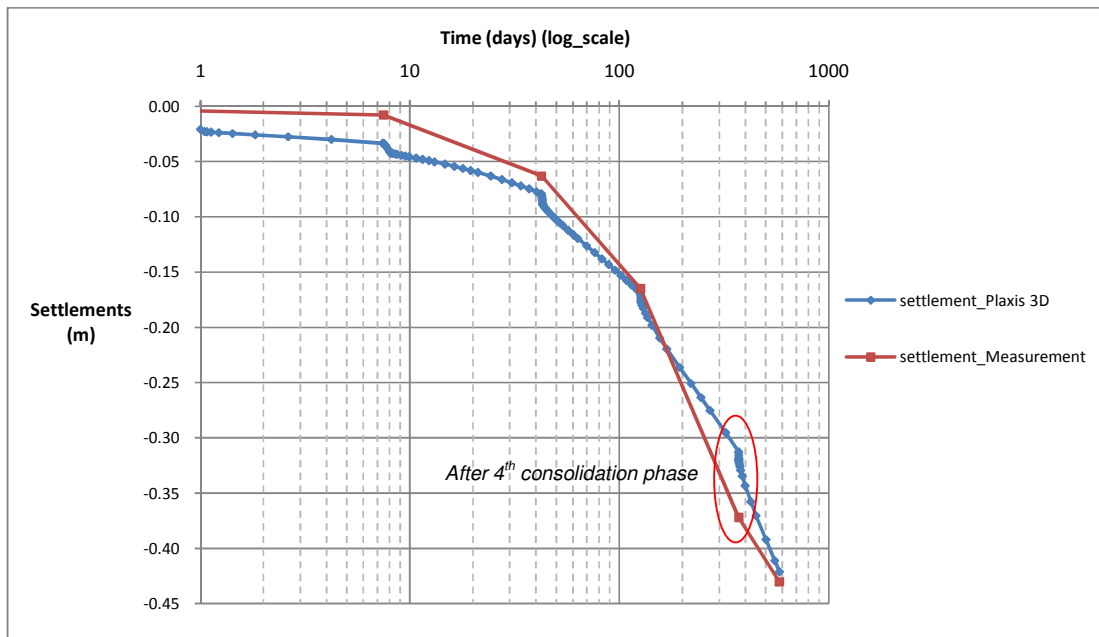
Figure 5.7 Surface settlement at X=25m

Figure 5.8 represents the developments of lateral soil displacements as a function of time (logarithmic). It should be noted again that the report of *"Centrifuge test"* just provided the measured data of the horizontal soil displacements at *the end of each consolidation phase*, whereas PLAXIS shows the full results of the horizontal displacements with time. Consequently, it can be seen that the shapes of *"Horiz. Disp.–Plaxis 3D" curve* and *"Horiz. Disp.-Measurement" curve* are remarkably

different such that makes it impossible to compare them. Therefore in order to make a reliable comparison, the *"Horiz. Disp.–Plaxis 3D" curve* is modified into the *"Modified Horiz. Disp.–Plaxis 3D" curve*, in which the horizontal soil displacements are only investigated at the end of the *consolidation phases*. In short, the *"Modified Horiz. Disp.–Plaxis 3D" curve* and the *"Horiz. Disp.-Measurement" curve* are examined for the purpose of the comparison of the horizontal soil displacements.

It can be seen that it's not really a good match between the two mentioned curves. The SSC model tends to overestimate the horizontal displacements before the end of *the third consolidation phase* and then gives an underestimation towards *the later consolidation phases*, complying with the trend as seen for the surface settlements displayed in Figure 5.7. In particular, at the end of *the final consolidation phase* the SSC model underestimates the horizontal soil displacements by 13%.

Besides, the finding of the similar trend between the surface settlements and the horizontal soil displacements may be interpreted based on the *horizontal/vertical stress ratio in normally consolidated 1D compression, K^0_{nc}*. It indicates that with the same value of K^0_{nc}, the higher vertical displacements (settlements) will lead to the higher horizontal displacements.
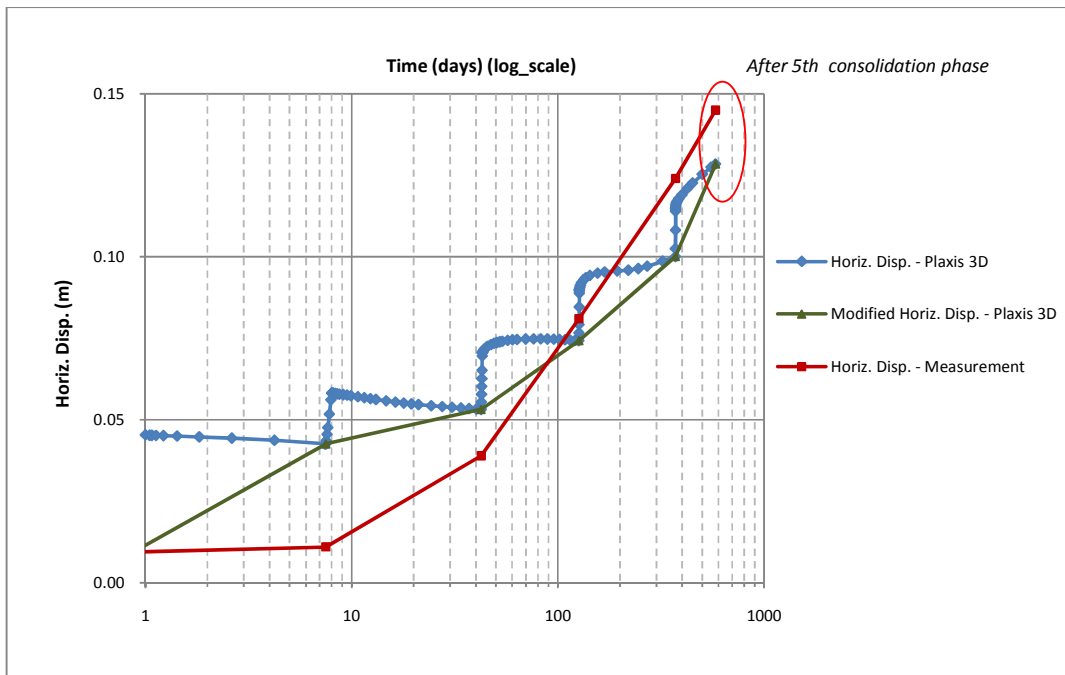
Figure 5.8 Horizontal soil displacements at X=25m and Z=1.5m

5.6 Recalculation of the PLAXIS model of the centrifuge test by using the Soft Soil (SS) model

5.6.1 Introduction

It should be noted that, for the purpose of validating the embedded pile as well as evaluating the soil displacements by a comparison with measured data, the PLAXIS simulation was performed by applying the SSC model for the clay layer. However the *SSC model* was set up with a very low *creep parameter* (which corresponds to *Modified creep index* $\mu^*=0.00013$) that seems to yield very little creep behavior. Therefore the PLAXIS simulation is recalculated using the *SS model* which has the same properties as the *SSC model*. The material data set of the *SS model* is described in Table 5.10. Furthermore in order to investigate creep behavior in the longer term, an *additional phase* is added after *the 5th consolidation phase* that extends the total calculation time to 10,000 days without further increase of embankment load. This recalculation is aimed to consider whether there is a difference between the *SSC model* with a very low *modified creep index* and the *SS model* in terms of bending moments in the pile as well as soil deformations.

Remark: This recalculation with the *SS model* is not related to the main objectives of the thesis which are mainly validating the embedded pile and secondarily evaluating the *SSC model*. This part is only considered as an additional part to compare between the *SS model* and the *SSC model* with a very low *creep parameter*.

Table 5.10 Material data set of the SS model

Parameter	Name	Value	Unit
Material model	Model	SSC	-
Drainage type	Type	Undrained	
Modified compression index (lamda*)	λ^*	0.085	-
Modified swelling index (kappa*)	k^*	0.022	-
Poisson ratio for unloading/reloading	ν_{ur}	0.2	-
Cohesion	c'	0.5	kN/m^2
Friction angle	φ'	22	^{0}
Dilatancy angle	ψ	0	^{0}
Horizontal/Vertical stress ratio in normally consolidated 1D compression	K^0_{nc}	0.64	-
Horizontal permeability	k_h	0.0004	m/day
Vertical permeability	k_v	0.0002	m/day
Over-consolidation ratio	OCR	1.3	-
Pre-overburden pressure	POP	20	-
Unit weight	γ_{unsat}	16.2	kN/m^3
	γ_{sat}	16.2	kN/m^3

5.6.2 Result and Discussion

Figure 5.9 shows comparisons of bending moments in the pile which are displayed as *"bending moment-depth"* graphs. In general, it can be seen that the SSC model and the SS model match completely at the *early consolidation phases.* Only a very small difference between them is revealed at the end of the 5th *consolidation phase and after the total calculation time of 10,000 days.* Therefore, it can be concluded that the SS model gives almost similar bending moments in the pile as the SSC model using a very low *creep parameter*. In the other words, the influence of creep cannot be clearly seen in terms of the investigation of bending moments in the pile.
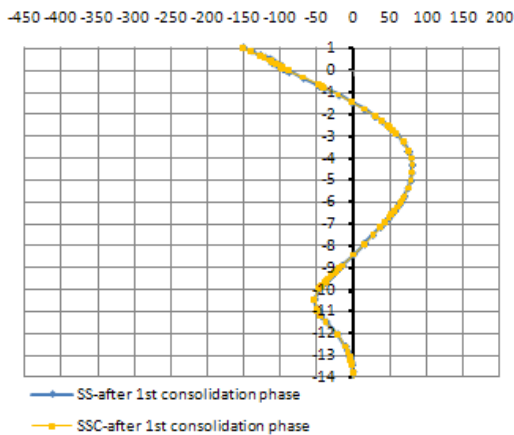
Figure 5.9a After 1st consolidation phase
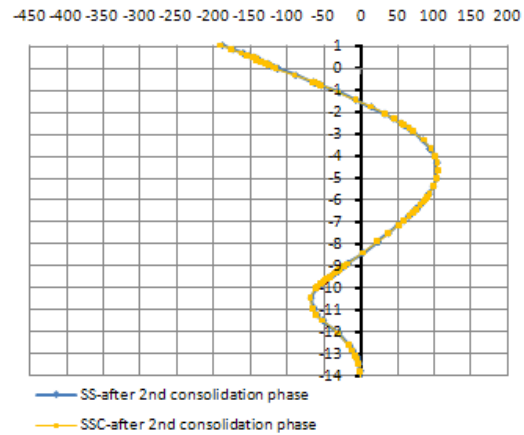
Figure 5.9b After 2nd consolidation phase
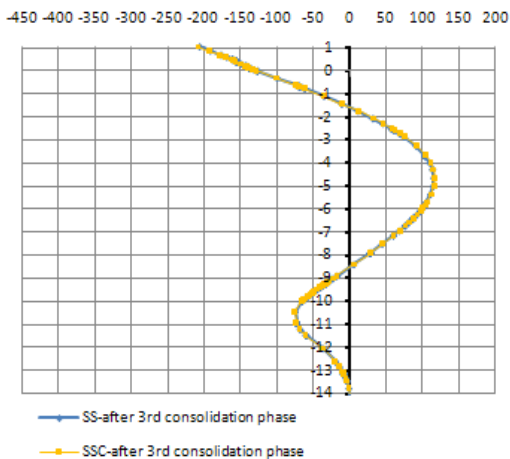
Figure 5.9c After 3rd consolidation phase
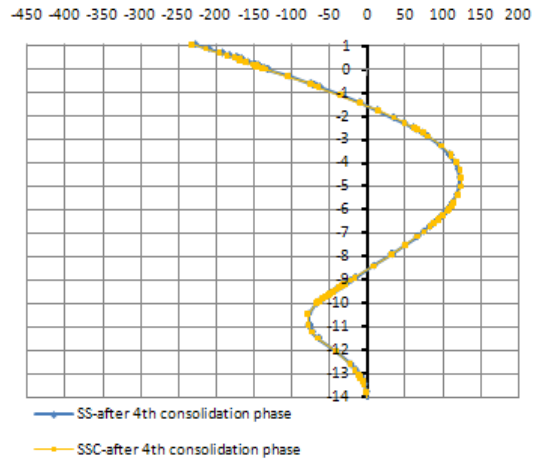
Figure 5.9d After 4th consolidation phase

SS-after 5th consolidation phase
SSC-after 5th consolidation phase

SS-after 10,000 days
SSC-after 10,000 days
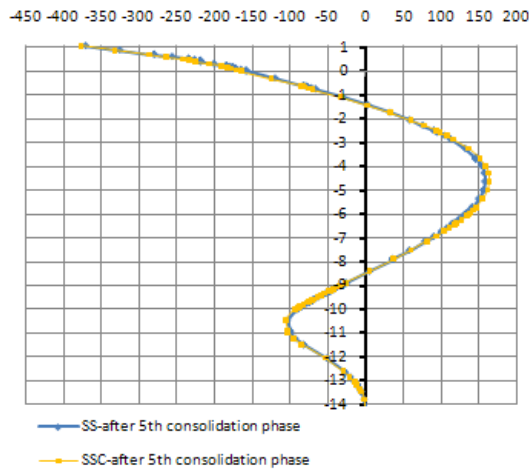
Figure 5.9e After 5ᵗʰ consolidation phase   *Figure 5.9f After 10,000 days*
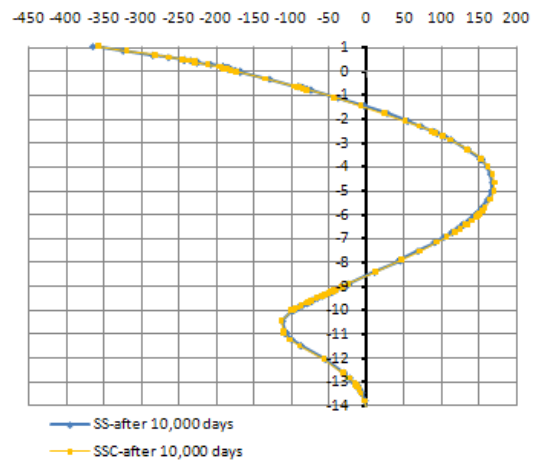
Figure 5.9 Bending moment-depth

Figure 5.10 shows the development of excess pore pressures as a function of time (logarithmic). It can be seen that during the loading phases the SSC model and the SS model gives the similar generated excess pore pressures. However towards *the later consolidation phases,* due to creep the excess pore pressures in the SSC model dissipate slightly slower than those in the SS model.

Furthermore, the influence of creep is also revealed in terms of volumetric strains as displayed in Figure 5.11. It can be seen that after full consolidation (around 4,000 days) where the excess pore pressures have fully dissipated, the volumetric strain comes to the end for the SS model, whereas for the SSC model the volumetric strain process continues due to creep. The strain rate depends on the value of μ^*. In this situation, the SSC model is set up with *a very low value of μ^*-parameter*, thus the strain rate does not differ much from the SS model. In fact at the reference time (10,000 days), the SSC model only predicts the volumetric strains approximately 5% higher than the SS model.
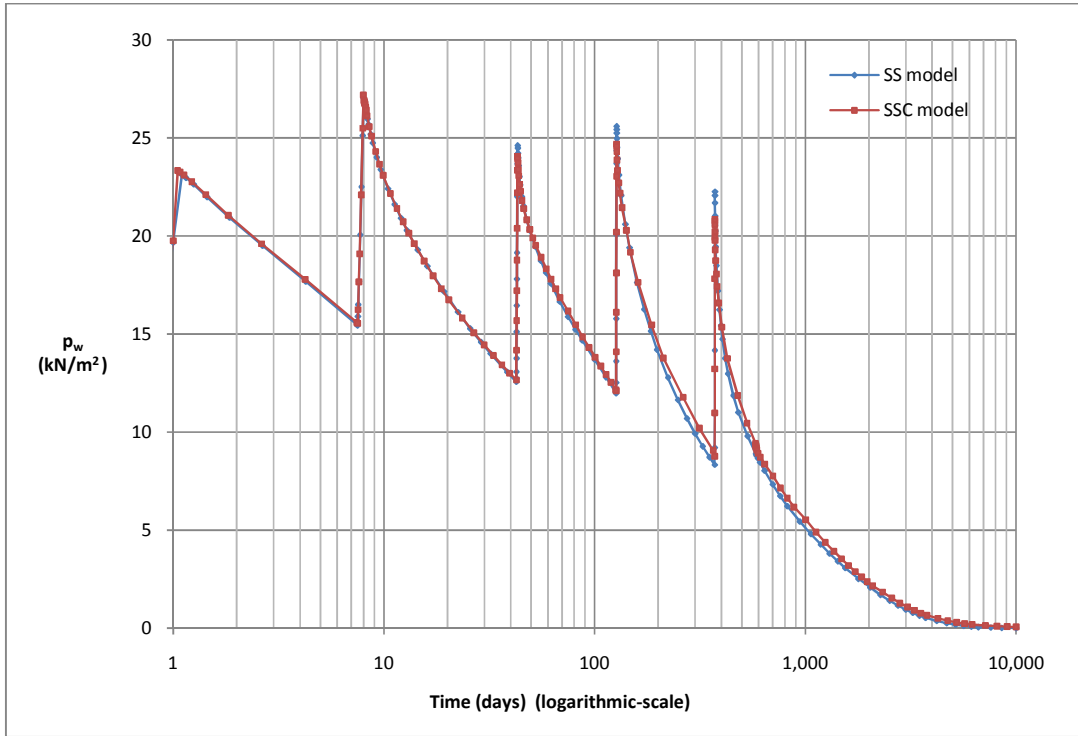
Figure 5.10 Development of excess pore pressure as a function of time
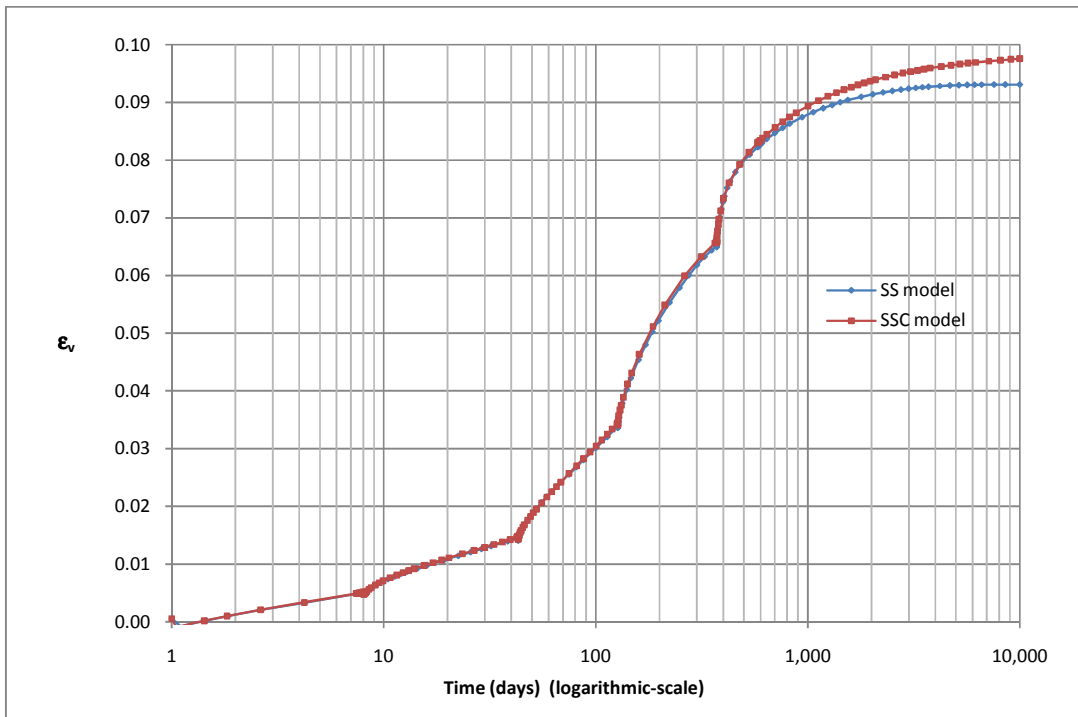
Figure 5.11 Development of volumetric strain as a function of time

5.7   Conclusion

This part mainly validated the embedded pile undergoing lateral soil movement induced by the construction of an embankment on soft soils and secondarily evaluated the SSC model.

➢ For the validation of embedded pile, comparisons of the bending moments in the pile with measurements and with the volume pile were made. Some conclusions were drawn:

- From the comparison with measurements, it is clearly considered that the condition of the pile head connection has a significant influence on the distribution of bending moments in the pile. In this test, a comparable distribution of bending moments between the PLAXIS model and the real test is only revealed when the pile head is fixed in X direction & Y direction and free to move in Z direction. In general, it can be concluded that the embedded pile is able to resemble the real behavior. Nevertheless, the embedded pile has a trend to overestimate the bending moments in the pile at *the early consolidation phases* and to underestimate towards *the later consolidation phases*. A good agreement with the measurement is revealed at *the "middle" phase (the third consolidation phase)*. Furthermore, in terms of investigating the bending moments at three typical points of the pile, it can be seen that the maximum difference of the bending moments at the pile head is found at *the early consolidation phases*, whereas the maximum difference of the bending moments at around the middle of the clay layer as well as at around the interface between two layers is revealed at *the later consolidation phases.*

- From the comparison with the volume pile, it can be seen that the embedded pile gives slightly lower predictions of the bending moments. However, in general the embedded pile is in good agreement with the volume pile behavior. This finding also indicates that the small difference between the two PLAXIS pile models may be caused from the small difference in the generated meshes.

➢ For the evaluation of the SSC model, comparisons of the settlements and the horizontal soil displacements with measurements were made. In general, it can be concluded that the SSC model is able to resemble the real soil behavior. However the SSC model shows a trend of overestimating the surface settlements before the end of *the third consolidation phase* and thereafter underestimating towards *the later consolidation phases*. This finding is consistent with the trend as seen for the horizontal soil displacements.

➢ For the recalculation with the SS model, it can be seen that the SS model and the *SSC model with a very low modified creep index* completely match in terms of bending moments in the pile. However, in terms of excess pore pressure development and volumetric strain development, the influence of creep is only revealed during *creep phases*. It is clearly seen that due to creep, the excess pore pressures dissipate slightly slower and the strain process continues after full consolidation (around 4,000 days). In addition, the strain rate depends on the parameter μ^*.

Therefore *for a very low value of μ^*,* the difference of volumetric strain between the two models at the end of total calculation time (10,000 days) is rather small.

It can be recognized that the comparisons between the *PLAXIS 3D model* and the *real test* are limited due to lack of measured data which are only provided at particular times. Therefore, the real behaviors as a function of time in the real test cannot be seen.

CHAPTER 6   CONCLUSION AND RECOMMENDATION

In this research, the embedded pile was validated for lateral loading caused by external forces as well as soil movements. Some aspects were required: investigating the surrounding soil, evaluating the pile properties, comparing with the volume pile and with measurements. The validation was firstly considered in imaginary PLAXIS models ('simplified' model and 'advanced' model) and secondly in a PLAXIS model of a real case study.

In the part of a 'simplified' model as considered in Chapter 3, the following conclusions were drawn:

➢ For an investigation of the surrounding soil (based on the assumption that a 'cylinder' with local mesh refinement is added around the embedded pile), the soil is fully elastic inside the 'cylinder' and becomes plastic outside that region. In addition, total strains of the soil elements in the plastic region mostly result from plastic strains. Besides, compressive stresses and tension stresses are found at the front and the back of the surface shaft of the elastic region, complying with the trend as seen for the distribution of strains.

➢ For a comparison with the volume pile (based on the assumption that the embedded pile model with a 'cylinder' around to have the same geometry with the volume pile model), the pile-soil interaction model was considered. The volume pile 'without' an interface implies for a 'rough' pile-soil interaction, and the volume pile 'with' an interface having $R_{inter}<1$ (0.5 in this case) implies for a 'smoother' pile-soil interaction. It can be concluded that the embedded pile is perfect in modelling the pile having 'rough' surface and overestimates the displacement-load behavior in modelling the pile having 'smoother' surface. This is because the embedded pile doesn't take into account the relative pile-soil displacements ('slide') in the lateral directions. Moreover, for a more realistic application (based on the assumption that the embedded pile 'without' any local mesh refinement around), the embedded pile overestimates the load-displacement behavior.

In the part of 'advanced' models as considered in Chapter 4, lateral loads were considered with both causes of external forces and soil movements. The main conclusions were drawn:

➢ For the cause of external forces, the main points were considered:
  • The embedded pile is also influenced by mesh coarseness which shows the finer mesh results in the larger pile deformations and bending moments in the pile.
  • When comparing with the volume pile in the same test conditions, it is clearly seen that the situation of the pile undergoing lateral load, in which the embedded pile gives good predictions, depends much on the roughness of the pile-soil interaction regarding R_{inter}.

➢ For the cause of soil movements, the main points were considered:
  • The bending moments in the pile and the pile deformations depend on the pile properties. The 'near' pile gives higher predictions than the 'far' pile. Furthermore, the increases of bending moments in the pile are caused by the increases of pile length and pile diameter.

- When comparing with the volume pile in the same test conditions, the embedded pile gives almost similar lateral pile head displacements as the volume pile. However, in terms of bending moments in the pile after the last consolidation phase, the embedded pile gives lower predictions.

In the part of PLAXIS model of a real case study as considered in Chapter 5, the validation of embedded pile was made by comparing with measurements and with the volume pile. Besides, the evaluation of the SSC model applied for the clay layer was also considered. Some conclusions were drawn:

➢ For the validation of the embedded pile by comparing with measured data, the following points were considered:
  - The condition of the pile head connection has a significant influence on the distribution of bending moments along the pile. In this case, a comparable distribution of bending moments between the PLAXIS model and the real test is only revealed when the pile head is fixed in X direction & Y direction and free to move in Z direction.
  - The embedded pile has a trend to overestimate the bending moments at the *early consolidation phases* and to underestimate towards the *later consolidation phases*. A good agreement with the real pile is found at the *'middle' consolidation phase.*
  - When investigating the bending moments at three typical points of the pile, the maximum difference from measurements at the pile head is found at the *early consolidation phases*, whereas the maximum difference at around the middle of the clay layer and at around the interface between two layers is revealed at the *later consolidation phases*.
➢ For the validation of the embedded pile by comparing with the volume pile in the same test conditions, the embedded pile gives slightly lower prediction of bending moments. This is due to the small difference in the generated mesh between the two pile models.
➢ For the evaluation of the SSC model, comparisons of the settlements and the lateral soil displacements with measured data were made. The SSC model shows the trend of overestimating the surface settlements at *the early consolidation phases* and underestimating towards *the later consolidation phases*. This finding is consistent with the trend as seen for the horizontal soil displacements. However because the SSC model is set up with a very low modified creep parameter μ^*, it seems to yield very little creep. Therefore, the recalculation with the SS model was also made in order to find the difference between the two models and to recognize creep in the longer term. Some main considerations were drawn:
  - In terms of bending moments in the pile, the SS model and the SSC model with *a very low creep parameter* completely match.
  - In terms of excess pore pressure development and volumetric strain development, the finding shows that there is no difference between the SS model and the SSC model during *loading and consolidation phases*, only a small difference during *creep phases* (due to creep, the excess pore pressures dissipate slightly slower and the strain process

continues after full consolidation). This small difference is because the SSC model is set up with *a very low modified creep index μ*.*

It is clearly observed in this research that the embedded pile shows a good performance in modeling the laterally loaded pile. However, currently the embedded pile does not take into account the "slide", which is used to model pile-soil interaction, in horizontal directions. This makes the embedded pile impossible to model the laterally loaded pile with "smooth" surface. Therefore, the "slide" in the horizontal directions should be developed for the improved embedded pile model in further research.

REFERENCES

[1] Adachi, T. and Oka, F. 1982. *Constitutive equation for normally consolidated clays based on elasto-viscoplastic*. Soil and Foundation, Vol. 22, pp. 57-76.

[2] Berry, P.L. and Poskitt, T.J. 1972. *The consideration of peat*. Geotechnique, Vol. 22, pp. 27-52.

[3] Biot, M.A. 1943. *Journal of Applications of Physical differential equations*. ASCE, Vol.15, pp.60-71.

[4] Bjerrum, L. 1967. *Rankine Lecture*. Geotechnique. Vol.17, pp. 81-118.

[5] Breedeveld, J., Feddema, A. and Havinga, H. 2008. *Door Grond Horizontaal Belaste Palen*. Deltares, The Netherlands.

[6] Brinkgreve, R.B.J. 2007. *Time-dependent behavior of soft soils during embankment construction-A numerical study*. Delft university of technology, Delft, The Netherlands.

[7] Brinkgreve, R.B.J., Engin, E. and Swolfs, W.M. 2010. *Plaxis 3D 2010 Manual*. Plaxis company, Delft, The Netherlands.

[8] Byrne et al. 1984. Response of piles and casings to horizontal free-field soil displacements. Geotechnical Journal, Vol. 21, pp. 720-725.

[9] Borja, R.I. and Kavaznjian, E. 1985. *A constitutive model for the stress-strain-time behavior of "wet" clays*. Geotechnique, Vol.25, pp. 283-298.

[10] Buisman, K. 1936. *Results of long duration settlement tests*. Proceedings 1st International conference on Soil mechanic and Foundation engineering, Mass. Vol. 1, pp. 103-107.

[11] Chen, L. 1994. *The effect of lateral soil movement on pile foundation*. PhD thesis. The university of Sydney.

[12] Christie, I.F. 1964. *A re-appraisal of Merchant's contribution to the theory of consolidation*. Géotechnique, Vol. 14, pp. 309-320.

[13] Cryer, C.W. 1962. *The evaluation of three-dimensional compression*. Pretoria, South Africa.

[14] Dartevelle, S. 2003. *Numerical and granulometric approaches to geophysical granular flows, Ph.D. thesis*. Department of Geological and Mining Engineering, Michigan Technological University, Michigan.

[15] Debbarh, A. 1988. *Consolidation of elastic saturated soil due to water withdrawal by numerical Laplace-Fourier inversion methods*. Ph.D Thesis. Dept. of Civil and Min. Eng., Univ. of Minneapolis.

[16] De Beer, E.E. & Wallays, M. 1972. *Forces induced in piles by unsymmetrical surcharges on the soil around the piles.* Proc. 5th European conference on Soil Mechanics and Foundation Engineering, Marid, Vol.1, pp. 325-332.

[17] De Beer, E.E. 1977. *Piles subjected to static lateral loads*. State of Art report. Proc. 9th ICSMFE, Specialty Session 10, Tokyo, pp. 1-14.

[18] El-Mossallamy Y. 1999. *Load-settlement behaviour of large diameter bored piles in over-consolidated clay*. Proc. 7th Int. Symp. on Numerical Models in Geotechnical Engineering – NUMOG VII, Graz, 1-3 September 1999, 443-450. Balkema. Rotterdam (The Netherlands).

[19] Esu, F. and D'Elia, B. 1974. *Laterally loaded piles*. International conf. on measurements of piles. Italia, Vol. 22, pp. 17-30.

[20] Engin H.K., Septanika E.G. and Brinkgreve R.B.J. 2007. *Improved embedded beam elements for the modelling of piles*. Proc. 10th Int. Symp. on Numerical Models in Geotechnical Engineering – NUMOG X, Rhodes (Greece). April 2007.

[21] Engin, H.K. 2007. *Report on tension pile testing using embedded piles*. Plaxis internal report. Delft (The Netherlands) Ismael N.F., Al-Sanad H.A. and Al-Otaibi F. 1994. Tension tests on bored piles in cemented desert sands. Canadian.

[22] Finno, R.J. al et. 1991. Analysis of pile groups adjacent to deep excavations. Journal of Geotechnical Engineering. ASCE, Vol. 117, pp. 934-955.

[23] Fukuoka, M. 1977. *The effects of horizontal loads on piles due to landslide*. Proc. 9th ICSMFE, Specialty Session 10, Tokyo, pp. 77-80.

[24] Gabr, M.A and Borden, R.H. 1990. *Lateral analysis of Piers constructed on Slopes*. *Journal of Geotechnical engineering*. ASCE, Vol. 116, No. 12, pp. 1835-1850.

[25] Gibson, R.E. 1967. *The theory of one dimensional consolidation of saturated clays*. Geotechnique, Vol.17, pp. 261-273.

[26] Hagerty, D.J. and Peck, R.B. 1971. *Heave and lateral movements due to pile driving.* Journal of Soil mechanic and Foundation. ASCE, No. 11, pp. 1513-1532.

[27] Heyman, L. 1965. *Measurements of the influence of lateral earth pressure on pile foundation*. Proc. 6th ISCMFE, Montreal, Vol. 2, pp. 257-260.

[28] Heyman, L. and Boersma, F. 1962. *Bending moments in the piles due to lateral earth pressure*. Proc 5th ICSMFE, Paris, Vol.2, p.425-429.

[29] Hull, et. al. 1991. *Mechanics of piles reinforcement for unstable slope*. Research Report No. R636, The university of Sydney.

[30] Hull, T.S. and McDonald, P. 1992. *Lateral soil movements loading in bridge foundation piles*. Proc. 6th, ANZ Conf. Geomech., Christchurch, pp. 146-150.

[31] Ingold, T.S. 1977. *A field study of laterally loaded piles*, Proc. 9th ICSMFE, Spec. Sess. 10, Tokyo, pp. 77-80.

[32] Ismael N.F., Al-Sanad H.A. and Al-Otaibi F. 1994. *Tension tests on bored piles in cemented desert sands*. Canadian Geotechnical Journal, pp. 597-603.

[33] Ito, T. and Matsui, T. 1975. *Methods of estimating lateral force acting on stabilizing piles*. Soils and Foundations. Vol. 15, p. 43-59.

[34] Kalteziotis, N. 1993. *Experimental studies of landslide stabilization by large diameter piles*. Geotechnical Engineering of Hard soil and soft rock. Rotterdam, pp. 1115-1125.

[35] Kelesoglu, M. K. & Cinicioglu, S.F. 2009. *Soil stiffness degradation in the design of passive piles.* 2nd International Conference on New Developments in Soil Mechanics and Geotechnical Engineering, 28-30 May 2009. Pp. 194-197. North Cyprus.

[36] Ladd, C.C. *et al.* 1994. Stress-deformation behaviour of an embankment on Boston Blue Clay. Vertical and horizontal deformations of foundations and embankments. Geotechnical Special Publication No. 40, ASCE, pp. 1730-1759.

[37] Landva, A.O. and La Rochelle, P. 1982). *Compressibility and shear characteristics of Radforth peats*. Testing of Peats and Organic Soils, ASTM, pp. 157-191.

[38] Larsson, R. et al. 1997. *Predictions of settlement of embankments on soft, fine grain soils.* Swedish Geotechnical Institute, Report No. 63, Linkoping.

[39] Leonards, G.A. and Girault, P. 1961. *Proc. Fifth Int. Conf. Soil mechanics.* Spec. Sess. 1, Paris.

[40] Leussink, H. & Wenz, K.P. 1969. *Storage yard foundation on soft cohesive soil.* Proc. 7th, Vol. 2, pp. 149-155.

[41] Leroueil, S. et al. 1990. *Embankment on soft clays (English translation).* Ellis Horwood, London.

[42] Leroueil, S. et al. 1985. *Stress-strain rate relation for the compressibility of sensitive natural clays.* Geotechnique, Vol. 35, pp. 159-180.

[43] Magnan, J. P. 1983. *Etude d'un remblai sur sols compressibles: Le remblai B du site experimental de Cubzac-lesPonts*, Laboratoire Central Des Ponts Et Chaussees Rapport de recherche, LPC No.127.

[44] Massou, M. and Kawomura, K. 1977. *Diagram for construction control of embankment on soft ground.* Soils and Foundations, Vol. 17, pp. 37-52.

[45] Matsui, T. 1982. *Earth pressure on the piles due to lateral soil movements.* Soils and Foundations, Vol.22, pp.71-81.

[46] Matsuo, M. and Kawamura, K. 1977. *Diagram for construction control of embankment on soft ground.* Soils and Foundations, Vol. 17, pp. 37-52.

[47] Mesri, G. and Choi, Y. K. 1985. *Settlement analysis of embankments on soft clays.* Journal of Geotechnical Engineering, ASCE, pp. 441-464.

[48] Nicu, N.D 1971. Field measurement on instrumented piles under an overpass abutment. Highway research record, Vol. 354, pp. 90-99.

[49] Peters, M.G.J.M. and Steenbrink, R. 2008. *Berekening van door grond zijdelings belaste palen, conservatief of niet.* Geotechniek, April, pp. 30-37.

[50] Popescu, M.E. 1991. *Landslide control by means of a row of piles.* Int. Conf on Stability Engineering. Isle of Wight, p. 389-394.

[51] Poulos, H.G. 1973. *Analysis of piles in soil undergoing lateral movement.* Journal of Soil Mechanics and Foundation Engineering, ASCE, Vol. 99, pp. 391-406.

[52] Schmidt, H.G. 1977. *Large diameter bored piles for abutments.* Proc. 9th ICSMFE, Specialty Session 10, Tokyo, pp. 107-112.

[53] Schofield, A. and Wroth, P. 1968. *Critical state soil mechanics.* Cambridge University Press, Cambridge.

[54] Silva, N. 2009. *Presentation "Shear strength of soil".* University of Moratuwa, Sri Lanka.

[55] Skempton, A.W. 1984. *Effective stress in soils, concrete and rocks.* Selected papper on Soil mechanics, Thomas Telford, Londan.

[56] Springman, S.M. 1989. *Lateral loading of piles due to simulated embankment construction*, PhD thesis, Engineering Department, Cambridge University.

[57] Sterling, R.H. and Strohbeck, E.E. 1973. *Failure of south pass 70 'B' platform in Hurricane Camille.* 5th annual offshore conference. Tex., pp. 719-730.

[58] Stewart, D.P. 1992. *Lateral loadings of pile bridge due to embankment construction.* PhD thesis, University of Western Australia.

[59] Tavenas, F. *et al.* (1979). *Lateral displacements in clay foundations under embankments*. Canadian Geotechnical Journal, Vol. 16, pp. 532-550.

[60] Tavenas, F. and Leroueil, S. 1980. *The behavior of embankment on clay foundations*. Canadian Geotechnical Journal, Vol. 17, pp. 236-260.

[61] Taylor, D.W. and Merchant, J. 1940. *Mathematical soil formulation*. Vol. 10, pp. 167.

[62] Terzaghi, K. 1943. *Soil mechanics in engineering practice, 3rd edition*. John Wiley & Sons, New York.

[63] Tschebotarioff, G.P. 1973. *Foundations, Retaining, and Earth Structures.* McGraw-Hill, New York.

[64] Valliappan, S. 1981. *Continuum mechanics fundamentals*. Balkema, Rotterdam.

[65] Vermeer, P.A. & Neher, H.P. 1999. A soft soil model that accounts for creep. In R.B.J. Brinkgreve (ed), *Beyond 2000 in Computational Geotechnics - Ten Years of Plaxis International*: 249-261. Rotterdam: Balkema.

[66] White, R. 1979. *Foundation Engneering*. Geotechnical Journal, pp. 309-331.

[67] Whitlow, R. 1983. *Basic soil mechanics*. Construction Press, London.

[68] Wood, D. M. 1990. *Soil behavior and critical state soil mechanics*. Cambridge Uni. Press, Cambridge.

[69] Zdravkovic, L. et al. 2002. *The effect of strength anisotropy on the behavior of embankment on soft ground*. Geotechnique, Vol. 52, pp.447-457.

APPENDIX

Appendix A – Measured data of centrifuge test

Table A-1 Maximum bending moments in the pile at the end of each consolidation phase

Pile depth	Maximum bending moments in the pile				
	Layer 1	Layer 2	Layer 3	Layer 4	Layer 5
1.05	-70	-90	-135	-200	-300
-0.5	-20	-30	-70	-100	-140
-2.5	30	40	90	100	150
-5.0	60	80	130	170	230
-7.8	20	30	90	110	170
-10.0	-40	-50	-80	-90	-120
-11.5	-60	-70	-100	-110	-160
-14.1	-1	-1	-1	-1	-1

Table A-2 Settlements at ground surface (X=25m)

Phase	Time	Settlement
Layer 1	7	0.008
Layer 2	42	0.063
Layer 3	126	0.165
Layer 4	371	0.372
Layer 5	581	0.430

Table A-3 Horizontal soil displacements at point (X=25m and Z=-1.5m)

Phase	Time	Settlement
Layer 1	7	0.011
Layer 2	42	0.039
Layer 3	126	0.081
Layer 4	371	0.124
Layer 5	581	0.145

Appendix B – Graphical PLAXIS 3D Output for the centrifuge test

- The graphical output of bending moments in the embedded pile at the end of each consolidation phase is shown from Figure B-1 to Figure B-5.

- Figure B-6 shows the graphical output of the settlements at the end of the 5th consolidation phase.

- Figure B-7 shows the graphical output of the horizontal deformations at the end of 5th consolidation phase.
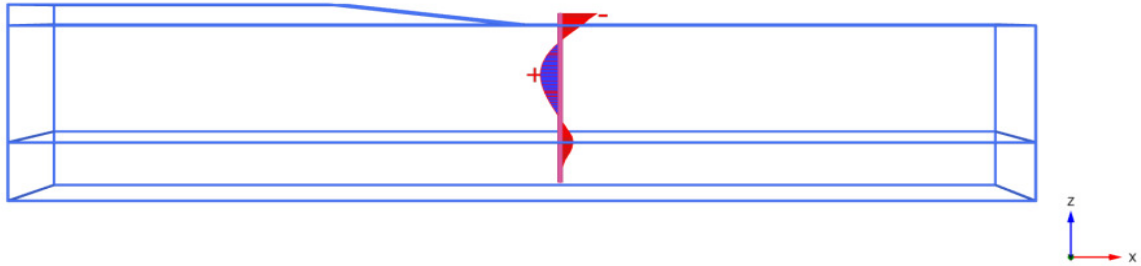
Bending moments M$_3$ (scaled up 0.0200 times)
Maximum value = 80.18 kNm (Element 33 at Node 22431)
Minimum value = -151.3 kNm (Element 1 at Node 22367)

Figure B-1 Bending moment in pile at the end of consolidating layer 1
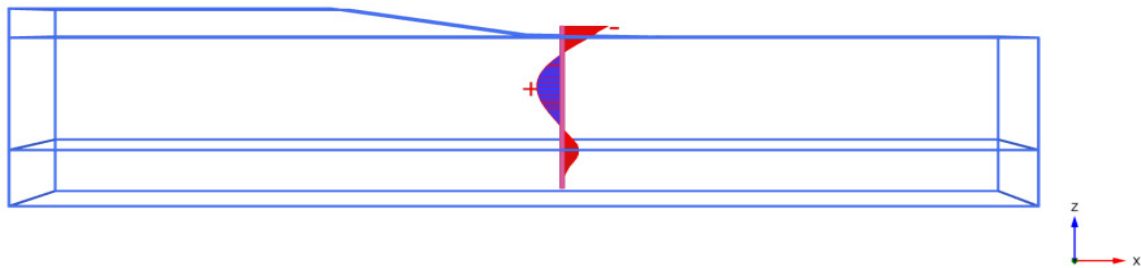
Bending moments M$_3$ (scaled up 0.0200 times)
Maximum value = 103.8 kNm (Element 33 at Node 22432)
Minimum value = -188.7 kNm (Element 1 at Node 22367)

Figure B-2 Bending moment in pile at the end of consolidating layer 2

Figure B-3 Bending moment in pile at the end of consolidating layer 3

Figure B-4 Bending moment in pile at the end of consolidating layer 4

Figure B-5 Bending moment in pile at the end of consolidating layer 5
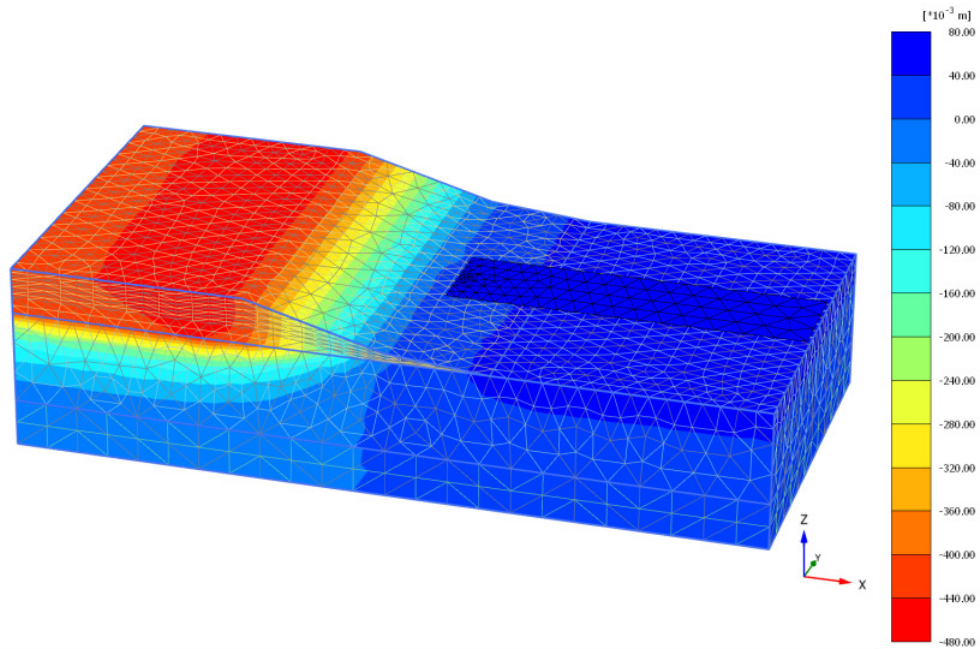
Total displacements u_z

Maximum value = 0.06456 m (Element 11378 at Node 18979)

Minimum value = -0.4642 m (Element 5 at Node 1325)

Figure B-6 Total settlements at the end of the 5th consolidation phase
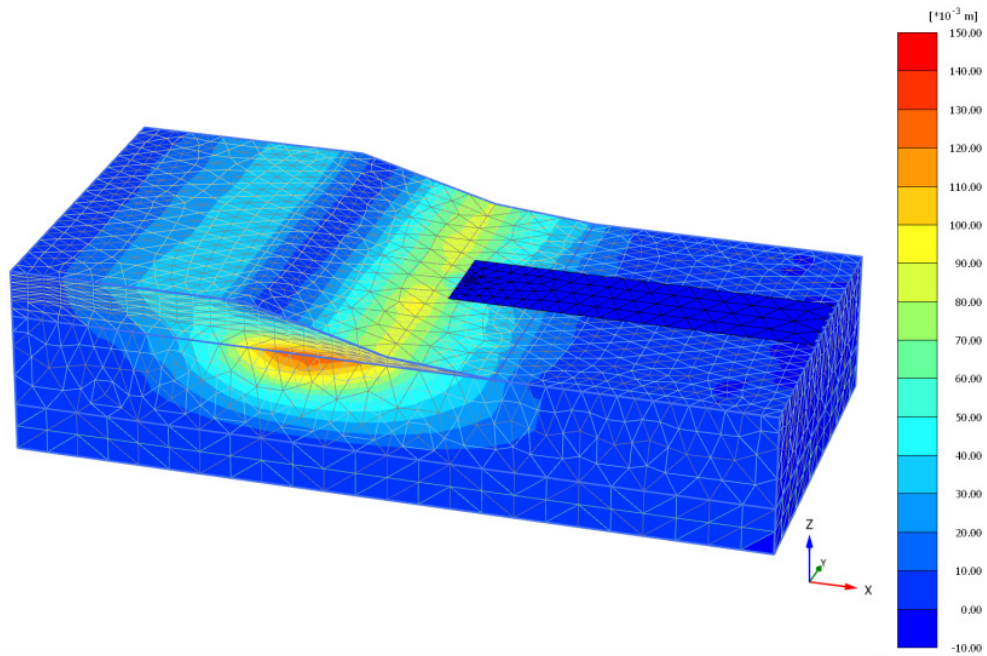
Total displacements u_x

Maximum value = 0.1456 m (Element 3289 at Node 6651)

Minimum value = -3.183*10^{-3} m (Element 5736 at Node 5567)

Figure B-7 Total horizontal displacements at the end of the 5th consolidation phase